

TOWARDS DEVELOPING STANDARDIZED PRECISION AGRICULTURE BOOM SPRAYER VIA HYBRID COMMUNICATION NETWORK FOR REAL-TIME SPOT APPLICATION

by
Mozammel Bin Motalab

Submitted in partial fulfillment of the requirements
for the degree of Doctor of Philosophy

at
Dalhousie University
Halifax, Nova Scotia

April 2025

Dalhousie University is located in Mi'kma'ki, the
ancestral and unceded territory of the Mi'kmaq.
We are all Treaty people.

© Copyright by Mozammel Bin Motalab, 2025

DEDICATION

All praises be to Allah SWT for His infinite guidance, blessings, and wisdom that have enabled me to embark on and complete this journey. My salutations to Prophet Muhammad (SM.), whose life and teachings inspire the pursuit of knowledge, resilience in hardship, and the betterment of humanity.

This PhD dissertation is dedicated to my beloved family. My wife, who has always been my strength, stood by me with unwavering patience, support, and encouragement. My children, whose precious time and moments I had to compromise in pursuit of this academic journey. I also dedicate this work to my father, who has always been my source of enthusiasm, and to my mother, who instilled in me the values of respect and kindness toward others. To all my sensei, mentors, and teachers, who have guided me and shaped me into who I am today, this journey would not have been possible without you.

*Author,
Mozammel Bin Motalab*

TABLE OF CONTENTS

LIST OF TABLES	vi
LIST OF FIGURES	vii
ABSTRACT.....	ix
LIST OF ABBREVIATIONS AND SYMBOLS	x
ACKNOWLEDGEMENTS.....	xii
Chapter 1: INTRODUCTION	1
1.1 STATUS OF SPRAYING IN PRECISION AGRICULTURE	1
1.2 AGRICULTURAL SPRAYERS AND THEIR APPLICATION.....	3
1.3 RESEARCH GAP.....	8
1.4 RESEARCH OBJECTIVES	10
Chapter 2: LITERATURE REVIEW: COMMUNICATION	12
2.1 OVERVIEW	12
2.2 ETHERNET AND ITS ROLE IN TCP/IP COMMUNICATION.....	13
2.2.1 OSI Model for Ethernet-based TCP/IP	13
2.2.2 Client-Server communication in TCP/IP	15
2.2.3 DHCP Network Protocol	16
2.3 CAN BUS AS EMBEDDED COMMUNICATION PROTOCOL	17
2.3.1 OSI Model for CAN.....	18
2.3.2 CAN Network Architecture	18
2.3.3 CAN Bus Speed and Physical Layer	20
2.4 CAN MESSAGES	21
2.5 ISOBUS FOR AGRICULTURAL IMPLEMENTS.....	22
2.5.1 ISOBUS Standard	23
2.5.2 ISOBUS message decoding	24
2.5.3 ISOBUS and AEF	25
2.6 ISOBUS EXPLOITATION IN RESEARCH.....	27
2.7 COMPARISON OF CAN, ISOBUS COMPLIANT, AND ISOBUS STANDARDIZED	28
Chapter 3: CASE STUDY - CASE IH PATRIOT 3240	30
3.1 OVERVIEW	30
3.2 OUTLINE THE BOOM SPRAYER.....	30
3.3 KEY FEATURES AND SPECIFICATIONS	31
3.4 COMMUNICATION ARCHITECTURE.....	32

3.5	POWER FOR IMPLEMENT BUS.....	35
Chapter 4: DEVELOPMENT OF AN ECU TO ENABLE MACHINE VISION SYSTEM INTEGRATION WITH THE BOOM SPRAYER.....		
4.1	OVERVIEW.....	37
4.2	ECU DESIGN AND IMPLEMENTATION.....	37
4.2.1	Defining Protocol Message.....	37
4.2.2	Hardware of ECU.....	40
4.2.3	Software of ECU.....	43
4.2.4	Apparatus and Test Scenarios.....	46
4.3	RESULT AND DISCUSSION.....	50
4.3.1	Lab Test Scenarios.....	50
4.3.2	Field Test Scenario.....	54
4.4	CONCLUSION.....	57
Chapter 5: DEVELOPMENT OF ISOBUS-COMPLIANT MVN FOR HYBRID COMMUNICATION.....		
5.1	OVERVIEW.....	59
5.2	ISOBUS ECU DESIGN AND IMPLEMENTATION.....	59
5.2.1	Hardware of MVN.....	59
5.2.2	Software of ECU.....	61
5.2.3	Lab Apparatus and Scenarios.....	67
5.2.4	Field Apparatus and Scenarios.....	68
5.3	RESULT AND DISCUSSION.....	74
5.3.1	ECU Algorithm Performance.....	74
5.3.2	Busload Analysis.....	76
5.3.3	Field Implementation Analysis.....	79
5.4	CONCLUSION.....	80
Chapter 6: DEVELOPMENT AND INTEGRATION OF A PARALLEL CONTROLLER AREA NETWORK BUS FOR SPOT SPRAYING.....		
6.1	OVERVIEW.....	82
6.2	CAN FILTER AND DATA LOGGER ECU DEVELOPMENT.....	82
6.2.1	Hardware of the ECUs.....	83
6.2.2	Software for the ECUs.....	85
6.2.3	Evaluation and Discussion.....	86

6.3	COMPREHENSIVE COMMUNICATION ARCHITECTURE TOWARDS MACHINE VISION BASED SPOT APPLICATION	89
6.4	INVESTIGATION OF ELECTRICAL REQUIREMENTS ASSOCIATED WITH MOUNTING SPOT APPLICATION SYSTEM	91
6.4.1	Power Requirements of ISOBUS system	92
6.4.2	Power Requirements for Machine Vision and Hydraulics Components	94
6.4.3	Power Source and Modifications	97
6.5	CONCLUSION.....	99
Chapter 7:	FUTURE WORKS AND CONCLUSION.....	100
7.1	OVERVIEW	100
7.2	Methodology for Machine Vision-Based Spot Application Evaluation of Liquid Spraying	100
7.2.1	System Components and Configuration	101
7.2.2	Test Environment and Anomaly Layout.....	101
7.2.3	Evaluation of Latency and Spatial Accuracy	102
7.3	POTENTIAL DEVELOPMENTS IN ISOBUS TECHNOLOGY	104
7.4	ENHANCED ISOBUS SECURITY USING OPC UA AND OPEN62541	105
7.5	SUMMARY AND CONCLUDING REMARKS	109
	REFERENCES	111

LIST OF TABLES

Table 2.1: Relationship between bitrate and other physical characteristics of CAN network	21
Table 2.2: Overview of ISOBUS functionalities and corresponding ISO 11783 documents.....	24
Table 2.3: SPNs for PGN 0xFE49 specify speed, distance, and direction data parameters	25
Table 2.4: AEF specified ISOBUS functionalities align with ISO 11783 standards.....	27
Table 3.1: The PGN distribution of the boom sprayer in parentage.....	33
Table 4.1: Different ECU testing scenarios for integration flexibility and spraying accuracy.....	48
Table 4.2: Detection and spray performance in different camera-nozzle ratios in a 6-nozzle sprayer.....	53
Table 4.3: Different distributions and speeds, with the spray ground coverage.....	55
Table 5.1: Time taken for MVN to display on various VT/UT across different setups.....	76
Table 5.2: Unified spraying areas at different distributions of objects and different speeds.....	79
Table 6.1: Maximum current and power consumption for key components of the Pentair system	93
Table 6.2: Peak current and power requirements for machine vision components and pumps....	96

LIST OF FIGURES

Figure 2.1: OSI model mapped with TCP/IP sublayers and their relationship.....	14
Figure 2.2: TCP/IP client-server communication establishment	16
Figure 2.3: OSI model mapped with CAN sublayers and their relationship to real-time implementation	18
Figure 2.4: CAN bus network showing interconnected ECUs with protocol layers for data transmission	19
Figure 2.5: Comparison of CAN 2.0A and CAN 2.0B message frames with size and structure .	22
Figure 2.6: 29-Bit extended CAN ID structure showing source and destination addressing in J1939.....	25
Figure 3.1: boom sprayer field operation (a) side view (b) rear view showing full boom coverage	31
Figure 3.2: The boom sprayer side view with distances between key elements.....	32
Figure 3.3: The boom sprayer ECU mapping through CAN messages.....	34
Figure 3.4: Power connection of the boom sprayer implement bus	35
Figure 4.1: UART protocol message to communicate with machine vision system based on UART. Yellow boxes indicate data used by ECU to determine insect location across the boom 38	
Figure 4.2: (a) Camera and nozzle setup on a boom sprayer showing FOV and spray, (b) Top view from a camera sectionizing FOV according to number of nozzles, (c) Example of protocol messages leaving the machine vision system to ECU	40
Figure 4.3: ECU hardware consisting of nozzle section converter and CAN message converter with two interfaces with machine vision system and implement bus. Keypad serves as interface for the operator when initializing the ECU.....	42
Figure 4.4: CAN 2.0 frame with 29-bit arbitration field, 8-byte data field.	43
Figure 4.5: Flow diagram of the ECU, two separate algorithms are presented (a) Nozzle Section Converter and (b) CAN Message Converter.....	45
Figure 4.6: Generalized CAN-compatible spraying system communicating with machine vision systems through the ECU.....	47
Figure 4.7: ECU deployed on UTV equipped with Pentair spraying system controlling 12 nozzles by machine vision of 6 cameras.....	49
Figure 4.8: (a) Multicolor targets (b) target distribution on the ground, showing distances in mm, for the ECU field test	50
Figure 4.9: Spraying pattern of the first, second and third scenarios for four different pest distributions when (a) one target is detected, (b) two close targets are detected, (c) two far targets are detected, and (d) three targets are detected	52
Figure 5.1: MVN hardware consisting of SBC (Raspberry Pi) and two-channel CAN HAT, CAN 1 communicates with parallel implement bus, CAN 0 receives speed data from the sprayer	61

Figure 5.2: Flow diagram of the MVN including the thread control for protocol messages and CAN messages	63
Figure 5.3: Custom user interface for VT designed to enter the number of nozzles controlled by one camera	64
Figure 5.4: MVN queue generation for protocol messages received for machine vision computer, following FIFO	65
Figure 5.5: Screen view while MVN connected with three VT across different manufacturers: (a) RAVEN CR7 UT, (b) Raven AFS-Pro 700 VT, and (c) John Deere 4640 UT	68
Figure 5.6: Drawing of the CAN-compatible spraying system for the Patriot 3240, MVN mounted and integrated into a Pentair spraying system, controlling 60 nozzles individually.....	70
Figure 5.7: MVN mounted on UTV, equipped with Pentair spraying system, controlling 12 nozzles through a machine vision system comprising 6 cameras.....	71
Figure 5.8: Three different images of Hair Fescue for field experimental detection with UTV setup	72
Figure 5.9: Target distribution on the ground, showing distances in cm, for the MVN field test	73
Figure 5.10: MVN timeline performance showing Ethernet communication, message processing, and CAN frame transmission.....	74
Figure 5.11: Oscilloscope signals of CAN frame transmission the MVN.....	76
Figure 5.12: MVN busload performance comparison at different numbers of CAN frames and their frequency	77
Figure 5.13: ISOBUS load performance during a 10-min evaluation of the two different spray systems, on Patriot 3240, and the UTV	78
Figure 6.1: Two ECUs CAN filter and data logger, both using RPi4 and 2 channel CAN expansion hat. CAN filter connected with both busses to exchange information between them. Data logger acquiring all the CAN data from the Pentair system.....	83
Figure 6.2: BUS connection of the ECUs on the Case IH Patriot 3240 CAN network for spot spraying.....	87
Figure 6.3: ISOBUS compatible ECU including a router (marked MVN), CAN filter and data logger deployed in the cabin of Patriot 3240	88
Figure 6.4: Overall network architecture for machine vision-based spot spraying	90
Figure 6.5: Integration of new alternator and battery pack with boom sprayer for enhanced power supply	98
Figure 7.1: Hypothetical management map considering real pest density with artificial pest on water-sensitive paper	102
Figure 7.2: Future integration of ISOBUS and cloud through OPC UA for secure and scalable agricultural data management.....	107

ABSTRACT

The transition of boom spraying towards spot application under precision agriculture schemes faces challenges due to the large volume of data generated by a large number of sensing and actuation devices. This research focuses on developing a universal communication network for real-time spot application, using Controller Area Network (CAN) at its core, offering the advantages of potentially error-free communication and seamless integration of machine vision systems into different boom sprayers. To handle the narrow bandwidth characteristic of CAN, a novel electronic control unit (ECU) was developed to encapsulate pest detection results into CAN data frames based on detected pest locations in images received from one machine vision system consisting of multiple cameras. The machine vision data were transmitted through UART to identify the number of nozzles to be actuated via CAN. The ECU was designed to accommodate different machine vision systems with varying camera counts and image resolutions. For real-time control, the ECU extracted data every 40 ms and constructed CAN frames in two separate threads simultaneously. Field tests demonstrated that the ECU managed nozzle actuation for targets distributed across diverse scenarios, including spatial and temporal successions.

Since the conditions on wide boom sprayers require multiple machine vision systems to actuate dozens of nozzles, an upgraded communication protocol was built at the interface of the machine vision with the ECU based on Ethernet. An application layer based on ISO 11783 was added to the CAN interface, widely used in agricultural machinery including sprayers. These upgrades allowed handling nozzle actuation at variable sprayer speeds up to 9.66 kph with a minimum spray length of 345 mm per detection, processing over 30 data frames every 40 ms. Finally, a new ISO 11783-compliant CAN bus with 60 nozzles was installed on a 36 m boom sprayer, used as a case study. This new bus featured two additional ECUs: one to communicate with other buses in the sprayer to import data like speed, and another to store pest detection and nozzle actuation data for further analysis. The case study demonstrated that a complete real-time spot application mechanism, including 30 cameras, would require an additional 4034 W for full functionality.

LIST OF ABBREVIATIONS AND SYMBOLS

Abbreviation*	Meaning
μs	Microseconds
A	Binary array of size N
A	Amps
AEF	Agricultural Industry Electronics Foundation
B	Byte in CAN data
CAN	Controller Area Network
CAN BUS	Controller Area Network BUS
CAN ID	Controller Area Network Identifier
ECU	Electronic Control Unit
FOV	Field of View
HEX	Hexadecimal
HLP	Higher Layer Protocol
I	Order of camera on boom
IP	Internet Protocol
ISO	International Organization for Standardization
J	Order of nozzle on boom (Section number)
K	Byte index of CAN data
Kbps	Kilobytes per second
LiDAR	Light Detection and Ranging
M	Number of cameras
Mega	Arduino Mega board
ms	Milliseconds
MVN	Machine Vision Node
N	Number of nozzles on the boom.
P	Number of x-axis intermediate object points
PGN	Parameter Group Number
PWM	Pulse Width Modulation
R	Ratio of cameras (M) and nozzles (N).
RGB	Red, Green, and Blue
RPi	Raspberry Pi
S	Subset of x-axis intermediate points
SC	Section Control Function
UART	Universal Asynchronous Receiver Transmitter
USB	Universal Serial Bus
UTV	Utility Task Vehicle
V	Volts
VT	Virtual Terminal
W	Watts
x_{max}	Maximum x -value of an object in a FOV

x_{min}	Minimum x -value of an object in a FOV
x_{obj}	x -axis object points relative to the FOV
x_{total}	Width of image
Z	Total set of x -values

ACKNOWLEDGEMENTS

I extend my deepest appreciation to the numerous individuals who have provided unwavering support throughout my graduate studies at Dalhousie University. First and foremost, I am profoundly grateful to my supervisor, Ahmad Al-Mallahi, PhD, for his exceptional guidance and profound knowledge, which have played a pivotal role in the successful completion of my PhD. I sincerely appreciate Alex Martynenko, PhD, and Karama Al-Tamimi, PhD, members of my supervisory committee, for generously devoting their time and sharing their valuable expertise throughout the various stages of my research.

I am grateful to my motherland, Bangladesh, where I grew up and gained the expertise that shaped my academic and professional journey. I would like to express my heartfelt gratitude to the wonderful and hospitable country of Canada for providing me with this invaluable opportunity.

I would also like to acknowledge McCain Foods Company for granting me access to the fields at the Farm of the Future in New Brunswick, where I deployed and tested my prototypes. Furthermore, I extend my gratitude to Potatoes New Brunswick for their additional support. My sincere appreciation goes to the Natural Sciences and Engineering Research Council of Canada (NSERC) for supporting this research through the Collaborative Research and Development Program. Special recognition is also due to the Mitacs Globalink Research Award for generously funding my internship at Hochschule Geisenheim University, Germany, which contributed significantly to the successful completion of major project deliverables.

Additionally, I extend my heartfelt thanks to my lab members, whose support and collaboration have been invaluable in making the spot application deployment a success. I am also

grateful to my dearest friends for their unwavering motivation, which has propelled me toward achieving my academic goals.

I extend my deepest appreciation to my father (Abdul Motalab), mother (Saifunnesa), brother (Muktadir), sister (Salsabil), my in-laws (Badrul Kamal, Sogra Sultana), and all other family members for their unwavering support and care throughout this transformative journey. Their love and encouragement have been indispensable in shaping my success today.

A special dedication goes to my wife, Shabnam Sharmeen, for her unwavering support, constant encouragement, and endless sacrifices. Her presence has been a source of strength and stability throughout this journey. I am profoundly grateful to my son, Muddassir, whose resilience and unwavering spirit, despite his special needs, have been my greatest source of inspiration. His strength has taught me perseverance and given me the motivation to push forward even in the most challenging times.

Lastly, my wonderful sweetheart, my daughter, Sidratul Muntaha, whose laughter and playful moments have been a constant source of joy during this demanding journey. Her innocence and joy have reminded me to cherish the small moments in life and have kept me grounded throughout this process.

CHAPTER 1: INTRODUCTION

1.1 STATUS OF SPRAYING IN PRECISION AGRICULTURE

Precision Agriculture (PA) is an advanced, methodical farm management approach that uses technology to account for spatial and temporal variability in agricultural fields, intending to enhance productivity, reduce farming costs and input usage, increase profitability, and minimize environmental impacts (Hester, 2012; Pandeya et al., 2025). At its core, PA follows the 4R principle; applying the right material, in the right amount, at the right location, and at the right time to optimize input efficiency and sustainability (Gulaiya et al., 2025). Since its emergence in the 1990s, PA has been widely regarded as a key strategy for improving the efficiency of agricultural operations, particularly in commercial farming, where concerns over potential yield loss have historically led to excessive chemical applications (Krill, 1994). While crop yield monitoring has been practiced for nearly two decades, recent advancements in intelligent farm machinery, crop sensors, and data analytics have revolutionized decision making processes, leading to more precise input applications and better yield outcomes (Pandit et al., 2025). Unlike conventional, i.e. mechanically dependent agricultural practices, the agricultural sector today leverages a range of modern technologies to implement PA. In recent years, these modern technologies include Artificial Intelligence (AI) and big data for predictive analytics, sensors, and broadband networks for real-time monitoring, and Internet of Things (IoT) technologies for automated data collection (Al-Mallahi, 2024). Geographic Information Systems (GIS), Global Navigation Satellite System (GNSS), and aerial imagery enrich the spatial analysis of agricultural data, exact mapping, and decision making (Jin, 2025; Neményi et al., 2003). According to the Food and Agriculture

Organization (FAO), automated and connected agricultural machinery improves efficiency by optimizing field operations, drudgery and health risks (Valle & Kienzle, 2020). The concept of PA has been gaining traction in recent years as researchers remain engaged, focused, and continuously improving technologies, while farmers recognize the benefits of managing variations in soil conditions (Yin et al., 2021), pest distribution (Tang et al., 2023), and crop health status (Radočaj et al., 2023). However, the implementation yet lacks specifically tailored actions or applications to effectively address these differences across the field. Growing concerns about sustainable resource use have made PA a priority for both the agricultural industry and researchers (Stafford, 2000). A central feature of PA is real-time spot application, which customizes treatments based on within field variability, contrasting with the conventional “one-size-fits-all” method that applies the same treatment uniformly across an entire field (McBride & Daberkow, 2003).

To achieve PA, sensors and actuators are integrated with ECUs in tractors and implements to automate adjustments based on site specific field conditions, optimizing input application and resource utilization for improved efficiency (Fountas et al., 2015). One aspect of PA is remote sensing systems, which include GNSS guided tractors and GIS. These systems rely on post processed data rather than real-time analysis, as captured imagery requires processing and interpretation before actionable insights can be derived (Jung et al., 2020). Recent advancements in cloud based Farm Management Information Systems (FMIS) analytics are improving predictive capabilities in certain agricultural scenarios, such as yield prediction, irrigation management, etc. The latest advancements in machine vision, which uses cameras as sensors to capture visual data processed by AI algorithms, identification and analysis of weeds, pests, or crop characteristics individually

(Cavallo et al., 2019; Ye et al., 2025). This technology is used for targeted applications like variable rate spraying, selective weeding, and nutrient application. It helps optimize resources, reducing water waste, fertilizer runoff, and pesticide resistance (Paustian & Theuvsen, 2017).

Sprayers play a crucial role in PA, particularly in applying pesticides and fertilizers. In Canada, technologies used in custom PA applications such as sprayer boom sections and nozzle control are the most widely adopted, with 76% of the total custom sprayed area using these tools. Variable Rate Application is also growing as it accounts for 10% of custom applications of pesticides as well as 36% of fertilizer and 28% of lime applications. This shows a clear move toward more precise and efficient input management in Canadian agriculture (Mitchell et al., 2020). A major innovation in automated boom sprayers is spot spraying, which uses AI driven machine vision to detect and apply pesticides or fertilizers only where needed, possibly reducing herbicide use by up to 90%, cutting costs, and minimizing environmental impact (López-Correa et al., 2024; Olds College, 2024).

1.2 AGRICULTURAL SPRAYERS AND THEIR APPLICATION

Agricultural sprayers vary in size and complexity, ranging from handheld models for localized applications to large, automated systems designed for high capacity field operations. They are categorized by application mode into horizontal and vertical sprayers, each designed to suit specific crops, structures, and application needs while ensuring targeted coverage and minimal spray drift (Asaei et al., 2016; Tian et al., 1999).

Vertical sprayers are used primarily in orchards, vineyards, and target crops grown in a vertical canopy structure. Equipped with fans or air blast systems, they propel spray upwards and sideways to reach all foliage layers. This ensures thorough coverage in tall, dense canopies, crucial for pest and disease control in trees and vines (Campos et al., 2019). The airflow helps the spray penetrate dense foliage, adhering to both upper and lower leaf surfaces, which enhances pest management while minimizing chemical waste (Palleja & Landers, 2015). Xiao et al. (2017) described a spraying system using two RGB cameras, each controlling six nozzles, where a single detection activates three nozzles per camera. This sectionized single camera view simplifies spraying by enabling simultaneous nozzle activation. However, these systems face communication limitations, as many rely on UART for camera-to-vision processing and lack CAN based nozzle control, restricting integration, scalability, and future upgrades. However, these systems face communication limitations, as many rely on UART for camera-to-vision processing and lack CAN based nozzle control, restricting integration, scalability, and future upgrades.

Horizontal sprayers are designed for row crops like corn, wheat, and potatoes, where the spray is applied parallel to the ground at low to medium heights across wide crop rows. These sprayers typically feature long horizontal booms equipped with multiple nozzles, ensuring uniform coverage over large areas (Deveau, 2015). Boom sprayers, a type of horizontal sprayer, are commonly mounted on tractors or self-propelled vehicles and are widely used due to their ability to provide even liquid distribution while reducing treatment time and minimizing over-application risks (Dou et al., 2021; Asaei et al., 2016; Jia et al., 2013). However, conventional boom sprayers have limitations, such as over-application in low-need areas and under-application in high-need areas, leading to chemical wastage and

potential environmental risks (Nicolopoulou-Stamati et al., 2016). To address this, modern PA techniques integrate geospatial technologies like GNSS, sensors, and Pulse Width Modulation (PWM) into boom sprayers, enabling variable rate application to adjust spray rates dynamically based on the speed and trajectory of the vehicle and field conditions (Rahman & Zhang, 2018; Van Loon et al., 2018). Additionally, GNSS-based spraying using prescription maps allow boom sprayers to spray differently in different field zones according to soil composition, weed presence, and pest distribution, although creating these maps can be time-consuming and resource-intensive (Zhang et al., 2010).

In relation to real-time horizontal spraying, solutions for machine vision-based spot spraying have just started to emerge in the market (Münzenmay et al., 2020; Staff, 2022). These are typically presented in new self-propelled sprayers that require factory installation and are tailored to specific crops and pests, mainly weeds. Several commercial systems have been introduced by leading agricultural equipment manufacturers, including See & Spray (John Deere, Illinois, US), Smart Spraying Solution (Amazonen-Werke H. Dreyer SE & Co. KG, Hasbergen, Germany), SenseSpray (CNH Industrial N.V., Amsterdam, Netherlands) (CASE IH, 2023), One Smart Sprayer (Fendt, AGCO, Marktoberdorf, Germany), and AiCPlus (Agrifac Machinery BV, Steenwijk, Netherlands). These solutions operate exclusively with specific machine vision system providers. For instance, See & Spray is powered by Blue River Technology (Santa Clara, California, US), Smart Spraying Solution integrates systems by Bosch (Robert Bosch GmbH, Baden-Württemberg, Germany) and xarvio (BASF Digital Farming GmbH, Münster, Germany) (Bob Blakely, 2023). While other systems rely on providers like Agtecnic (Tingalpa, Australia) and WEED-IT (Rometron, Steenderen, Netherlands). These technologies are proprietary and

often confidential, typically requiring full sprayer replacement (Taylor, 2017), which poses significant financial and operational challenges for farmers (Vogt, 2021). Furthermore, no existing solution combines essential capabilities such as individual nozzle control, multi-nozzle coordination with a single camera, multi-purpose detection (weeds, pests, nutrient deficiencies), and retrofitting across diverse boom sprayer sizes (Sharipov et al., 2021). When considering retrofitting, two major challenges arise: (a) integrating machine vision technology onto an existing sprayer, and (b) adapting spot spraying systems to different makers (Backman et al., 2019). Another critical limitation in commercial spot spraying systems would be their lack of adaptability to varying field conditions (Kool et al., 2023). Agricultural terrains are diverse, and sprayers do not always operate at constant speeds, yet most current solutions fail to adjust spraying accordingly, leading to inefficiencies in chemical application (Serrano et al., 2024).

Various research efforts have developed prototype models where a single camera controls individual nozzles or spray sections to detect weeds in specific crops (Alam et al., 2020; Dange et al., 2023; Farooque et al., 2023; Raj, 2018; Sanchez & Zhang, 2023). While single-camera configurations may suffice for certain crops, scaling them for larger fields and diverse pest types is challenging. Boom sprayers may control dozens of nozzles simultaneously, and implementing machine vision for this task introduces significant challenges in data management and communication (Esau et al., 2018; Terra et al., 2021). Al-Mallahi et al.(2023) and Terra et al. (2021) focused on developing modular designs that allow machine vision and sensors to be integrated into existing boom sprayers those already owned by farmers, preparing them for machine vision–based spot spraying while retaining the option for traditional spraying to suit specific needs. A major limitation of machine

vision-based spot spraying systems in academia is their communication architecture, as research focus tends to lean towards machine vision capabilities with inadequate investigation of the communication requirements of wide boom sprayers, which tend to be complex. Additionally, most prototypes lack CAN-based nozzle control, limiting integration capabilities and scalability towards different types of sprayers.

Many modern sprayers use ISO 11783 (ISOBUS), a standardized CAN-based protocol that facilitates seamless communication between components like GNSS modules, nozzle valves, and rate controllers, ensuring compatibility across equipment from different manufacturers (Paraforos et al., 2017). While ISOBUS provides a structured communication framework for agricultural equipment, it does not support machine vision integration. Its primary role is to enable an ECU to utilize the VT for configuration, simplify user interaction, and reduce the need for multiple interfaces (Shannon et al., 2018; Stoll et al., 2021). Therefore, additional development is required to bridge the gap between ISOBUS and machine vision systems, ensuring data exchange for real-time spot spraying applications.

To address the current gap in ISOBUS support for machine vision, this research proposes an enhanced ECU architecture that integrates real-time image processing with standardized communication protocols. The solution features a hybrid communication grid capable of managing multiple vision nodes for synchronized spot spraying, requiring precise coordination between cameras and nozzles. Building on prior developments in individual nozzle control, the study introduces an ISOBUS-compliant Machine Vision Node (MVN) designed to scale machine vision systems for large-scale applications. By

consolidating data from multiple cameras into a unified control interface, the MVN enables real-time coordination between vision inputs and nozzle actuation. This modular, scalable approach allows existing boom sprayers to be retrofitted for adaptable, precision spot spraying across diverse field conditions. In doing so, the system advances the goals of precision agriculture—enhancing operational efficiency, reducing chemical inputs, and minimizing environmental impacts.

1.3 RESEARCH GAP

Despite significant advances in boom sprayers, technological gaps remain in fully adaptable machine vision-based spot spraying systems for horizontal boom sprayers. Anastasiou et al. (2023) analyzed 172 scientific articles and found that most solutions either lack full-width boom coverage or are limited to specific applications like self-propelled sprayers for weed control. The integration of machine vision with nozzle setups remains rigid, with a one-to-one relationship between specific machine vision systems and sprayers. This restricts flexibility, requiring dedicated calibration, communication protocols, and control logic for each sprayer-nozzle setup, limiting scalability and widespread deployment (Pallottino et al., 2019). Scaling up machine vision-based spot spraying for larger boom sprayers requires integrating multiple machine vision sensors, computing units, and nozzle controllers. The research gap is the communication bottleneck, which presents a critical challenge in integrating multiple machine vision sensors, computing units, and sprayer components for spot spraying.

The absence of a complete, scalable solution highlights the need for flexible, real-time spraying technologies that can work with different camera-to-nozzle setups without

losing detection accuracy or slowing down response time (Nils Herterich, 2025). The lack of robust communication protocols further complicates machine vision integration with existing sprayers, especially when retrofitting older models. Without standardized communication interfaces, integration requires complex manufacturer-specific modifications, reducing scalability. Al-Mallahi et al. (2023) addressed this issue by developing a protocol for basic communication between machine vision outputs and CAN-compatible spraying systems. However, their protocol supported only equal camera-to-nozzle configurations, limiting flexibility across boom sprayer models. The underutilization of existing CAN-based sensors in agricultural machinery may present an opportunity to optimize resource utilization and improve adaptability without requiring entirely new infrastructure.

ISOBUS compatibility is a beneficial but not essential feature for spot application, as the absence of a unified communication architecture hampers integration and complicates the deployment of large-scale, high-speed spraying solutions across diverse field conditions (Wei et al., 2022). Paraforos et al. (2019) reviewed 154 articles, out of which 76 articles directly focused on studies and sources related to ISOBUS and identified three main areas of ISOBUS-related research: (a) guidance and control, (b) data acquisition and transfer, and (c) data management and analytics. Under guidance and control, they discussed ISOBUS-compatible applications like sprayers, which incorporate advanced sensor and control systems to align with ISOBUS. A key limitation noted was that ISOBUS development work is concentrated in commercial companies, with limited research focused on developing ISOBUS-compatible ECUs for spot application, detection, and spraying tasks in academia.

Patents related to spot spraying technology highlight advancements in image-based agricultural spraying but leave key gaps unaddressed, particularly in real-time nozzle control, ISOBUS integration, and adaptive spraying based on sprayer speed. The patent by Wu & Deutsch (2019) focuses on mounting image sensors (e.g., cameras or video systems) on agricultural vehicles, allowing for real-time image capture, correction, and analysis to support crop monitoring and yield assessment without extending to controlling individual nozzles based on machine vision detection. In addition, the patent introduced a separate control box for managing sensors instead of leveraging ISOBUS for direct integration with sprayers, making retrofitting complex. Also, the patent lacks a mechanism to convert FOV data into real-time nozzle control. The patent by Feldhaus et al. (2022) focused on spray distribution mechanics, considering factors such as vehicle speed, travel direction, and nozzle height adjustments. However, it does not incorporate image sensors for real-time weed, pest, or nutrient deficiency detection, nor does it provide a framework for individual nozzle control or speed-based application variation, both of which are crucial for optimizing chemical use in variable field conditions. This thesis addresses these limitations by developing a real-time, ISOBUS-compatible, machine vision-based spot spraying system, capable of translating camera detections into individual nozzle activation.

1.4 RESEARCH OBJECTIVES

The primary aim of this research is to upgrade boom sprayers to perform machine vision-based spot spraying on the go, targeting only the detected areas. This study focuses on developing a scalable communication solution for targeted pest and weed control in field crops by designing an advanced ECU. The ECU is intended to retrofit existing boom

sprayers with machine vision capabilities and standardized communication protocols, enabling real-time, site-specific applications that help reduce chemical use and operational costs. As such, the objectives of this research are as follows:

1. Development of an ECU to enable machine vision system integration with the boom sprayer.
2. Development of ISOBUS-compliant MVN for hybrid communication.
3. Development and integration of a parallel Controller Area Network bus for spot spraying.
4. Investigation of electrical requirements associated with the transition towards spot application for precision agriculture.

CHAPTER 2: LITERATURE REVIEW: COMMUNICATION

2.1 OVERVIEW

This chapter provides an overview of the two primary serial communication protocols used in this research, Ethernet and CAN. Among the common communication topologies such as star, bus, and mesh, in a star topology, all devices connect to a central hub; commonly used for centralized and scalable communication, such as in Ethernet-based networks. In a bus topology, all devices share one communication line, making it suitable for systems that need a simple setup and low wiring cost, like CAN-based networks. Ethernet supports high-speed data exchange and is ideal for server-based networks. Ethernet operates at the physical and data link layers and is governed by the TCP/IP protocol stack, which enables scalable communication across networks. The inclusion of Dynamic Host Configuration Protocol (DHCP) automates IP address allocation, simplifying network management. CAN is a message-based protocol that provides reliable communication in noisy environments, making it the backbone of ECU and sensor interaction in agricultural machinery. ISOBUS, built upon CAN, standardizes communication between tractors and implements, ensuring compatibility and interoperability across different manufacturers. This plug-and-play functionality eliminates manual setup, improving operational efficiency and flexibility in the field. The chapter also examines the technical structure, benefits, and limitations of both protocols within industrial and agricultural contexts.

2.2 ETHERNET AND ITS ROLE IN TCP/IP COMMUNICATION

Ethernet is one of the most widely used networking technologies. It is commonly used to create Local Area Network (LAN), connecting individual computers to a network in settings ranging from offices to industrial automation systems, where stable and high-speed data transmission is essential (Decotignie, 2005). The Ethernet star topology simplifies network management, enhances fault isolation, and supports high-speed communication, making it suitable for machine vision computers to communicate reliably (Sommer et al., 2010). At the core of Ethernet-based communication, there is the TCP/IP protocol suite, which governs how data is transmitted, routed, and reassembled. TCP/IP operates as a packet-switched protocol, breaking data into packets that Ethernet transports across the network (Kay et al., 2014). TCP/IP is widely implemented also in Wi-Fi and fibre-optic networks, ensuring reliable data exchange and scalability in global communication systems (Comer, 2004). In this research, Ethernet is used as the primary medium for TCP/IP communication to receive detection results from multiple machine vision computers sent to a centralized node to enable fast and reliable communication.

2.2.1 OSI Model for Ethernet-based TCP/IP

Open Systems Interconnection (OSI) is a framework that organizes general electronics communication into seven layers: Application, Presentation, Session, Transport, Network, Data Link, and Physical. Among these layers, the application, data link, and physical layers are fundamental for communication networks. Unlike the seven-layer OSI framework, TCP/IP follows a four-layer framework, consisting of the Application, Transport, Internet, and Network Link layers (Tomsho, 2011), as depicted in

Figure 2.1. The Application Layer provides standardized communication between applications through protocols like Hypertext Transfer Protocol (HTTP), File Transfer Protocol (FTP), Simple Mail Transfer Protocol (SMTP), Domain Name System (DNS), and DHCP. The Transport Layer ensures end-to-end communication between hosts, with TCP providing reliable, connection-oriented communication, while User Datagram Protocol (UDP) offers faster, connectionless communication (Murkomen, 2024). The Internet Layer manages packet transmission across networks using IP and handles error reporting through Internet Control Message Protocol (ICMP). The Network Link Layer, also known as the Data Link Layer, facilitates data transfer over physical network media (Hasan & Mohd Hanapi, 2023).

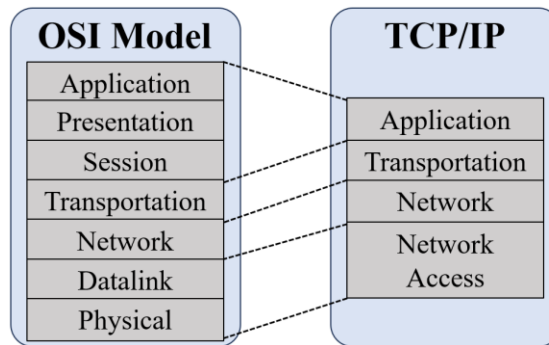


Figure 2.1: OSI model mapped with TCP/IP sublayers and their relationship

TCP operates at Layer 4 (Transport Layer) of the OSI model to ensure data delivery by establishing connections, managing packet flow, and retransmitting lost packets. IP functioning at Layer 3 (Network Layer) is a connectionless protocol responsible for packet addressing and routing. Together, TCP and IP provide end-to-end data transmission, breaking information into packets and ensuring they reach the correct destination (Cowley, 2013). TCP also acts as an abstraction layer between internet applications and the

underlying network infrastructure, allowing communication between computers, web servers, and applications. Its error-checking and congestion control mechanisms for network reliability ensure automatic recovery from failures (Insam, 2003).

2.2.2 Client-Server communication in TCP/IP

The client-server architecture is a fundamental networking model where devices, known as clients, request services or resources from a centralized server. The server functions as a powerful processing unit, managing multiple client requests simultaneously, storing and distributing data, and maintaining network resources (Priyadarshi, 2024). Clients act as endpoints that access these resources without directly storing them. The server can be either a local machine or a remote system, depending on the network infrastructure (Ibrahim et al., 2021).

In a TCP/IP-based client-server network (Figure 2.2), communication is established through a dedicated port. Once a connection is initiated, data can be transmitted bidirectionally between the client and the server. The connection remains active until explicitly closed by either the client or the server, and the continuous exchange of data during this period is referred to as a session (Nowakowski et al., 2021). Creating sessions allows for efficient allocation of resources and continuous data exchange, which is necessary for applications such as cloud computing, remote desktop access, and real-time monitoring systems. A significant advantage of the client-server model is the centralized resource management, where files, databases, and applications are stored together on the server rather than on individual client devices. However, the major drawback of this setup would be its total reliance on the status of the server (Felix, 2024).

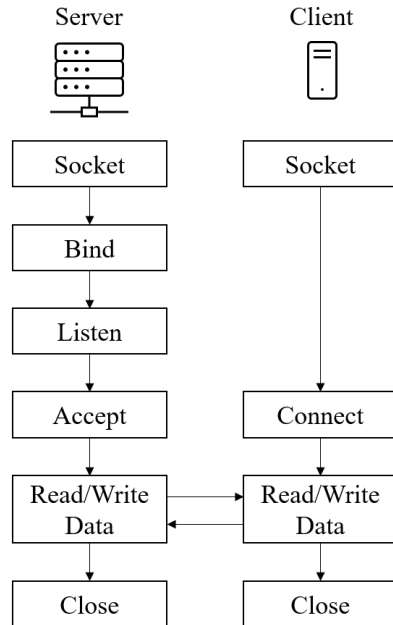


Figure 2.2: TCP/IP client-server communication establishment

The client-server model relies on sockets for establishing network communication. A socket is a software-defined endpoint that enables data exchange between processes running on different devices over a network (Kolluru & Reddy, 2021). The TCP ensures the sequencing, error checking, and retransmission of lost packets to ensure high reliability for data synchronization. Unlike DHCP, which dynamically assigns IP addresses to devices, TCP guarantees reliable delivery by maintaining a structured handshake process for data transmission (Rooney & Dooley, 2021). The client-server model, combined with TCP/IP socket communication, serves as the foundation of modern networked applications.

2.2.3 DHCP Network Protocol

The DHCP is a network protocol that automates the assignment of IP addresses and configuration settings to devices on a TCP/IP-based network. Every networked device requires a unique unicast IP address to communicate and access resources (Soepeno, 2023).

Without DHCP, network administrators must manually configure IP addresses, leading to errors, conflicts, and inefficiencies (Patadia et al., 2024). DHCP automates this process by dynamically assigning IP addresses, optimizing utilization, preventing conflicts, and supporting scalable network growth. Unlike static IP configurations, DHCP enables subnet transitions, benefiting portable devices like laptops. It also enhances network management efficiency by allowing administrators to define additional TCP/IP settings (Cochran, 2024), such as including default gateways (router), DNS servers, and DNS domain name, which allows clients to automatically get integrated into the network (Fontein, 2023). Additionally, the DHCP relay agents forward DHCP messages across different network segments, eliminating the need for a DHCP server on every subnet (Sheikh, 2024). In this research, DHCP-enabled clients were used to ensure seamless device registration and connectivity in scalable network infrastructures (discussed in Chapter 5).

2.3 CAN BUS AS EMBEDDED COMMUNICATION PROTOCOL

CAN is a robust, high-speed serial communication protocol designed for real-time data exchange between ECUs in embedded systems. It operates as a multi-master, message-based protocol, allowing multiple devices to communicate without a central host. CAN was standardized by the International Organization for Standardization (ISO) as ISO 11898, commonly known as CAN 2.0A and was expanded to CAN 2.0B to support longer device identifiers (Reuss, 1993). CAN typically connects networked ECUs through twisted-pair cables to ensure uninterrupted communication among components (Voss, 2008).

2.3.1 OSI Model for CAN

As shown in Figure 2.3, CAN operates within three layers of the OSI model forming CAN sublayers, the foundation of its communication framework (Cena et al., 2019). The physical layer includes hardware components such as cables, connectors, transceivers, and electrical signalling parameters. Standard CAN implementations typically operate at baud rates ranging from 125 kbps to 1 Mbps.

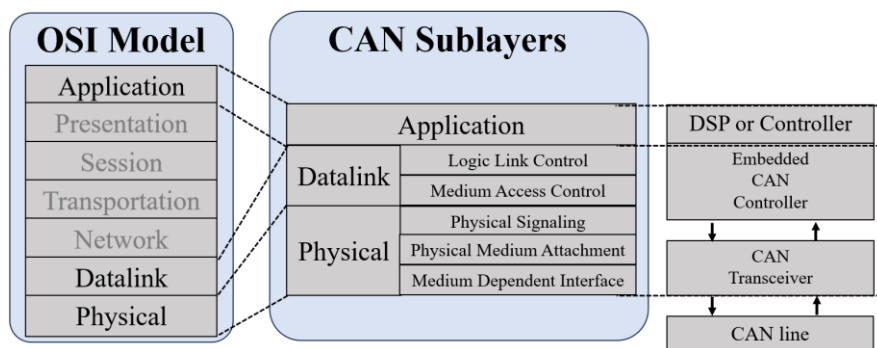


Figure 2.3: OSI model mapped with CAN sublayers and their relationship to real-time implementation

The application layer in CAN varies depending on the specific high-level protocol used. For instance, ISOBUS defines standardized communication interfaces for agricultural machinery, enabling integration between different equipment brands (Chincholi, 2009).

2.3.2 CAN Network Architecture

In CAN architecture, the physical and data link layers are combined with an application layer to enable higher-level functions like actuator or machinery control (Kozik & Choraś, 2016). This layered interaction creates a structured framework (Figure 2.4) for communication and control within the CAN network (Zhou et al., 2013). The data link

layer is responsible for Media Access Control (MAC), message framing, arbitration, and error handling (Zeltwanger, 2000).

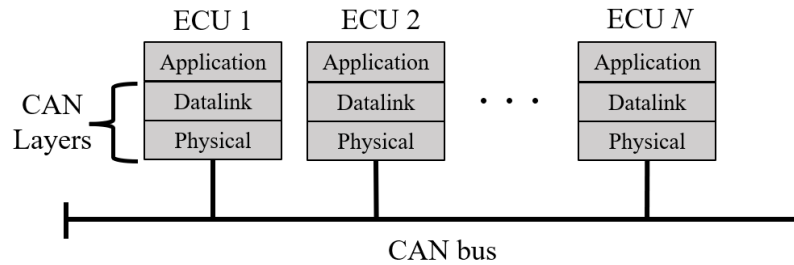


Figure 2.4: CAN bus network showing interconnected ECUs with protocol layers for data transmission

In CAN communication, each message is assigned an identifier that determines its priority on the network. CAN employs a priority-based arbitration mechanism, where messages with the highest priority (lowest identifier value) gain bus access first, ensuring that time-critical data is transmitted without delay. Additionally, error detection techniques such as Cyclic Redundancy Check (CRC) and acknowledgment protocols enhance the robustness of the network (Cena & Valenzano, 2000).

CAN networks are designed for high reliability and fault tolerance. Even if one ECU fails, the others can continue to communicate. CAN also supports unified expansion, allowing new devices to be integrated without modifications to the existing network. When a device transmits data, it is broadcast to all nodes, but only the intended recipient processes and utilizes it (Lafata & Vodrazka, 2011). Beyond its fundamental architecture, Higher Layer Protocols (HLPs) build on the basic CAN system to meet the needs of different industries. They add standard message formats, device profiles, and network management features to help devices from different manufacturers work better together. For example,

in addition to ISOBUS, SAE J1939 is widely used in heavy-duty vehicles (Walter & Walter, 2016), CANopen facilitates embedded control (Plotnikov et al., 2023), also ARINC825, CANaerospace, CAN fieldbus, and NMEA2000 are used for airborne systems (Darif et al., 2022), aerospace (Janu, 2014), and automotive (Wang et al., 2024), and marine systems (Kim & Lee, 2015), respectively. In agricultural sprayers, multiple CAN-based HLPs operate simultaneously. NMEA2000 is used for GNSS data integration, SAE J1939 handles tractor-related communication, whereas ISOBUS manages the implement functions such as nozzle and boom control. Despite their differences, all these protocols are fundamentally based on CAN (ISO 11898), demonstrating the protocol's adaptability across industries (Rogers et al., 2022).

2.3.3 CAN Bus Speed and Physical Layer

The CAN bus physical layer operates at different bit rates depending on the machine type and required reliability levels, typically ranging from 125 to 1000 kbps (BSI, 2016). Higher speed CAN supports higher data volumes and is commonly used where faster data rates improve system performance, although it comes with a higher risk of faults. Alternatively, low-speed CAN is specifically designed to offer greater fault tolerance (Steve Corrigan, 2008). Table 2.1 below outlines the recommended maximum cable lengths for each bus speed.

Table 2.1: Relationship between bitrate and other physical characteristics of CAN network

Bus Speed (kbps)	Max. Bus Length (m)	Cable Stub Length (m)	Highest ECU Distances (m)
1000	40	0.3	40
500	100	0.3	100
250	250	0.3	250
100	500	0.3	500
50	1000	0.3	1000

A common CAN bus speed used in agricultural and other heavy-duty machinery is 250 kbps with a recommended maximum cable length of about 250 m, and a cable stub of no more than 0.3 m is suggested for connecting ECUs. This rate makes sure that the transmitted signals remain clear and synchronized across all devices on the network across the relative wide dimensions of these type of vehicles and machinery.

2.4 CAN MESSAGES

CAN communication relies on CAN messages which are the basic units of data transmission also called CAN frames. CAN messages are typically broadcast across the network, so that all ECUs can receive them but only the designated ECUs may act on the messages (Lafata & Vodrazka, 2011). Each CAN message has two main parts: the CAN ID, which is a unique identifier, and the data section, which holds the actual information payload. While CAN 2.0A used an 11-bit identifier, CAN 2.0B used a 29-bit identifier. The extra bits in CAN 2.0B are used to target specific ECUs and support private communication between devices. Figure 2.5 shows a comparison between the structures of CAN 2.0A and CAN 2.0B message frames, detailing components such as the Start of

to-point connection standards, DIN 9684/1 and ISO 11786, which defined how tractor sensor signals should be provided to implement control to eliminate additional sensors, establishing an open, interconnected system for onboard electronics (Auernhammer & Demmel, 2015). ISOBUS adopted CAN 2.0B to support up to 254 ECUs in a network (ISO 11783-9, 2012). ISOBUS is also compatible with truck and bus manufacturers by integrating the SAE J1939 protocol (ISO 11898-1:2024, 2017).

2.5.1 ISOBUS Standard

The ISOBUS standard is documented under ISO 11783, which is organized into several parts each focusing on specific aspects of the communication protocol as shown in Table 2.2. These standards cover various OSI layers, device discovery, network management, and other essential modules, providing a robust framework for achieving control of agricultural equipment (ISO 11783-2, 2019). The physical layer, as specified in ISO 11783-2, functions as the CAN backbone with a standard bus speed of 250 kbps. This layer allows around 1,800 messages per second, though traffic should not exceed 45-50% of the busload to reduce network congestion (kvaser, 2023; Salim et al., 2016). Over time, further additions like ISO 11783-3 and ISO 11783-5 improved network management and communications, tailoring ISOBUS to meet the evolving needs of the agricultural industry

Table 2.2: Overview of ISOBUS functionalities and corresponding ISO 11783 documents

ISO Document	Functionality	Latest update
ISO 11783-1	Framework and basic concepts	2017
ISO 11783-2	Physical layer	2019
ISO 11783-3	Data link layer	2018
ISO 11783-4	Network layer	2011
ISO 11783-5	Network management	2019
ISO 11783-6	Virtual terminal	2018
ISO 11783-7	Implement messages application layer	2022
ISO 11783-8	Power train messages	2006
ISO 11783-9	Tractor ECU	2012
ISO 11783-10	Task controller	2015
ISO 11783-11	Mobile data element dictionary	2011
ISO 11783-12	Diagnostics	2019
ISO 11783-13	File server	2022
ISO 11783-14	Sequence control	2013

2.5.2 ISOBUS message decoding

Key features of ISOBUS include dynamic address claiming for automatic device identification (ISO 11783-5, 2022) and the integration of J1939 components like Parameter Group Numbers (PGN) and Suspect Parameter Numbers (SPN) (ISO 11783-3, 2018). The CAN 2.0B identifiers use PGNs and SPNs (Figure 2.6) to categorize and prioritize messages. PGNs define message types, allowing ECUs to group and interpret data, while SPNs represent specific parameters like sensor readings (SAE, 2020). This structured approach helps the ECUs to retrieve information by isolating specific data points within each category (Doopalam et al., 2014). For example, an extended CAN ID like 0x0CFE4926, which includes PGN 0xFE49, is used to broadcast speed and distance data to all devices on the network.

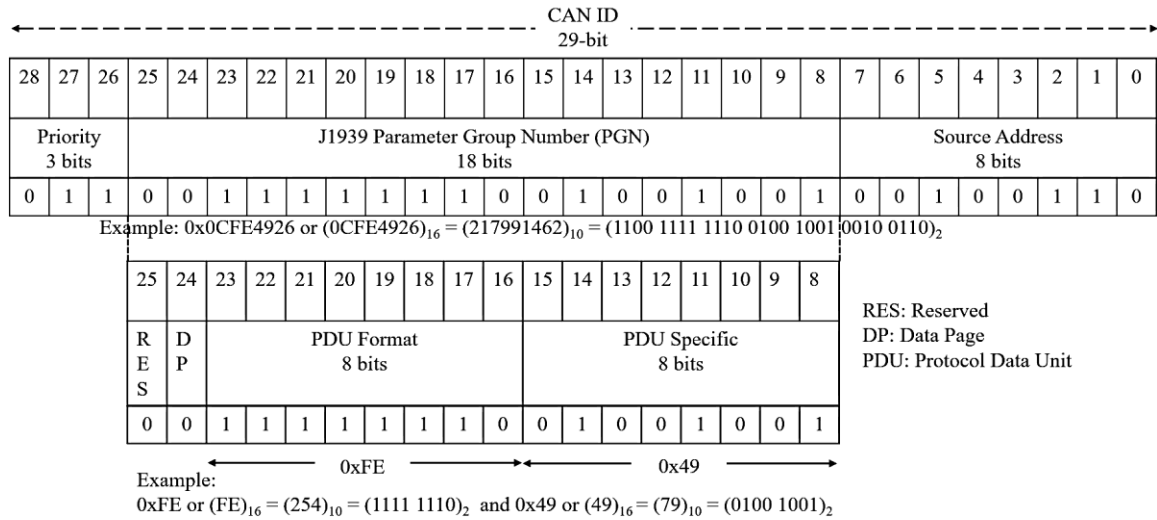


Figure 2.6: 29-Bit extended CAN ID structure showing source and destination addressing in J1939

Within this PGN, specific SPNs define detailed parameters such as speed, distance, and direction. The SPNs associated with PGN 0xFE49 are outlined in Table 2.3, providing a standardized reference for data interpretation and communication among ECUs. In ISO 11783-7, 2022, this hierarchical structure standardizes data identification, ensuring accurate processing in agricultural CAN networks.

Table 2.3: SPNs for PGN 0xFE49 specify speed, distance, and direction data parameters

SPN	SP Name	SP Position in CAN Data	SP Length (bit)	Scaling
1859	Ground-based machine speed	1-2	16	0.001 m/s per bit
1860	Ground-based machine distance	3-6	32	0.001 m per bit
1861	Ground-based machine direction	8.1	2	4 states per 2 bits

2.5.3 ISOBUS and AEF

Although the purpose of ISOBUS is to establish universal communication for agricultural machinery, variations in implementation among manufacturers have led to

compatibility challenges. To address these inconsistencies, the Agricultural Industry Electronics Foundation (AEF) introduced additional guidelines for ISOBUS compliance. These guidelines, endorsed by 104 members as of March 2025 (AEF, 2024), incorporate different manufacturers and ensure consistent functionality within ISOBUS systems (Case, 2019; Harris, 2018).

As defined in ISO 11783-6, a VT centralizes control of multiple implements from different manufacturers, enabling cross-brand implement management into a single display. The VT allows for graphical visualization and unified control of each implement (ISO 11783-6, 2018). The Tractor ECU (TECU) connects the internal CAN network of a tractor (J1939) with ISOBUS, enabling data exchange and access to parameters like speed, RPM, fuel consumption, and load to optimize implement performance (Harris, 2018). ISOBUS functionalities include Task Controller (TC) for automated task execution, Auxiliary Control (AUX) for implement handling, and Tractor Implement Management (TIM) for bi-directional control, enhancing efficiency (Pampattiwar et al., 2025). Additional features include the LOG function for data recording and the ISOBUS Shortcut Button (ISB) for quick implement function deactivation (AEF, 2015). Together, these functions improve field operations and integration in modern farming which are summarized in Table 2.4.

Table 2.4: AEF specified ISOBUS functionalities align with ISO 11783 standards

Functionality	Description
VT / UT	Centralizes control and operates implements across brands via one display.
TECU	Bridges tractor CAN bus with ISOBUS, enables advanced control between tractor and implement.
TC	Records, plans, and executes operations, facilitating automated and fine-grained implement control.
AUX	Provides finer implement control, available in non-cross-compatible old (AUX-O) and new (AUX-N) versions.
TIM	Aims for bi-directional control between tractor and implement, enhancing productivity and reducing operator fatigue.
LOG	Independently logs tractor/implement data in ISO XML format for improved compatibility and analysis.
ISB	Enables swift deactivation of specific implement functions, ideal for managing multiple implements through one terminal.

2.6 ISOBUS EXPLOITATION IN RESEARCH

The integration of CAN and ISOBUS in agricultural machinery has led to significant advancements in PA and automation. While the comparison of these communication protocols highlights their technical distinctions, their real-world implementations demonstrate their impact on efficiency, accuracy, and operational flexibility. CAN has become the core communication protocol in modern tractors, boom sprayers, and autonomous agricultural vehicles. It enables real-time sensor data exchange, which is critical for automated implement adjustments, power management, and diagnostics.

One notable example of CAN application in agriculture is a tractor-controlled boom sprayer developed by Yuki et al. (2013), which demonstrated using CAN improved spray rate accuracy and reduced operation time by 47% compared to conventional control

methods. Similarly, Dou et al. (2021) developed an automated sprayer height-adjustment system based on CAN-integrated GNSS and ultrasonic sensors, improving field adaptability for varying crop heights and terrain conditions. As digital farming platforms and cloud-based farm management systems gain prominence, ISOBUS is integrated with IoT, AI-based decision support, and real-time analytics (Stein & Boysen, 2025). Furthermore, ongoing research explores enhancing ISOBUS with edge computing and 5G connectivity, allowing real-time data synchronization between field equipment and remote monitoring platforms (Vurchio et al., 2024).

2.7 COMPARISON OF CAN, ISOBUS COMPLIANT, AND ISOBUS STANDARDIZED

The communication architecture in agricultural machinery primarily involves three approaches: CAN-based communication, ISOBUS-compliant systems, and fully standardized ISOBUS implementations. While all are built on the CAN protocol (ISO 11898), they differ in interoperability, functionality, and standardization. CAN-based communication refers to the use of raw CAN for direct ECU-to-ECU data exchange without following any HLP standard. Manufacturers define their own message structures, resulting in vendor-specific systems that are often incompatible with other brands. In agricultural sprayers, this approach is commonly used for machine-specific functions such as nozzle control, boom height adjustment, and sensor monitoring, but it lacks interoperability with external implements unless additional adaptations are made. ISOBUS-compliant systems adopt selected elements of ISOBUS but do not fully implement the standard. These systems may support features like VT or TC integration while retaining proprietary components, which can limit compatibility. For example, a

sprayer may offer VT support but not work with third-party TCs. ISOBUS-standardized systems are fully compliant with ISOBUS and follow AEF guidelines. Components such as the VT, TC, ECU, and IBBC operate according to standardized specifications, ensuring compatibility and eliminating proprietary limitations. This research extends to enabling ISOBUS compatibility in a boom sprayer while utilizing CAN-based control for internal machine operations. The developed ECU in Chapter 4 is a CAN-based solution designed to integrate the machine vision system with the boom sprayer, whereas the developed MVN in Chapter 5 is an ISOBUS-compliant solution capable of integrating a large number of machine vision systems for large-scale boom sprayers with hybrid network.

CHAPTER 3: CASE STUDY - CASE IH PATRIOT 3240

3.1 OVERVIEW

This chapter presents a boom sprayer (Patriot 3240, Case IH, Wisconsin, US), which was used as the main apparatus in this research project to develop and integrate communication components for spot application. This sprayer represents modern agricultural machinery that relies primarily on CAN communication for sensing and control. The sprayer included a factory-installed high-output alternator designed to efficiently support all electric and electronic components. However, mounting additional components to enable spot applications including cameras, computers, and additional actuators required considerations to upgrade the electric power scheme in the tractor as discussed in this chapter and Chapter 6.

3.2 OUTLINE THE BOOM SPRAYER

Equipped with ISOBUS and a foldable boom, the boom sprayer provides a working width of approximately 36 m, which allows for a wide spray swath to reduce passes and minimize soil compaction. The design supports 60 nozzles to enable adjustable application rates for different farm operational conditions such as forward speed and uneven terrain. The sprayer is equipped with a VT (Viper 4, Raven Industries, Inc., South Dakota, US) and a GNSS guidance system (Trimble NavController III, Trimble Inc., Colorado, US) as well as PWM nozzle valves (1-063-0173-674, Hawkeye Control Valve, Raven Industries Inc., South Dakota, US), which are designed to compensate for changes in forward and angular speeds during application of pesticide. The VT and ISOBUS combination also support

spraying based on prescription maps, generated from manual scouting or remote sensing, to enable variable-rate zone application based on pest density.

3.3 KEY FEATURES AND SPECIFICATIONS

The sprayer is considered a large and fast agricultural machine, measuring approximately 8.8 m in length and about 4.5 m in width when the boom is folded (Raven Industries, 2014, 2016). The boom provides extensive field coverage when fully extended (Figure 3.1). It is capable of operating at high speeds, with a maximum travel speed of 48 kph, allowing efficient spraying over large fields (CNH Industrial N.V., 2014).



Figure 3.1: boom sprayer field operation (a) side view (b) rear view showing full boom coverage

The operator can mix several compatible pesticides in the 800-gallon tank and spray them simultaneously. However, mixing everything together presents a challenge for precision or spot spraying, because there is currently no machine vision system capable of detecting all possible spray targets simultaneously. One major issue in adapting the sprayer for precision agriculture is the need to rapidly process images to make real-time spray decisions. While mounting cameras at the front of the sprayer could help, it would require a completely new design, which is impractical and unfeasible for existing machines. The dimensions of the sprayer are shown in Figure 3.2.

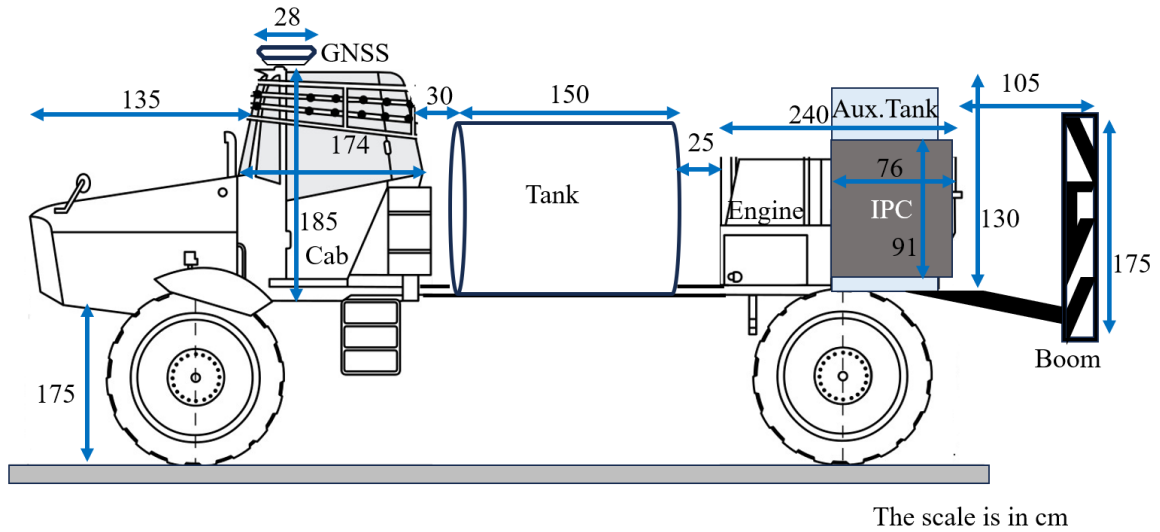


Figure 3.2: The boom sprayer side view with distances between key elements

3.4 COMMUNICATION ARCHITECTURE

The communication architecture of the boom sprayer is designed to integrate multiple ECUs and subsystems which uses three primary CAN communication networks: the tractor bus (J1939), the implement bus (ISOBUS), and the nozzle bus. As depicted in Figure 3.3, the tractor bus manages essential ECUs related to core machine functions, including the electronic engine controller (0x00), the retarder engine (0x0F) for braking, intermediate speed control (0x17), etc. The Tractor ECU (TECU, 0xF0) acts as a gateway between the tractor bus and the implement bus, allowing data exchange of vehicle speed, engine load, and other operational parameters (Fountas et al., 2015).

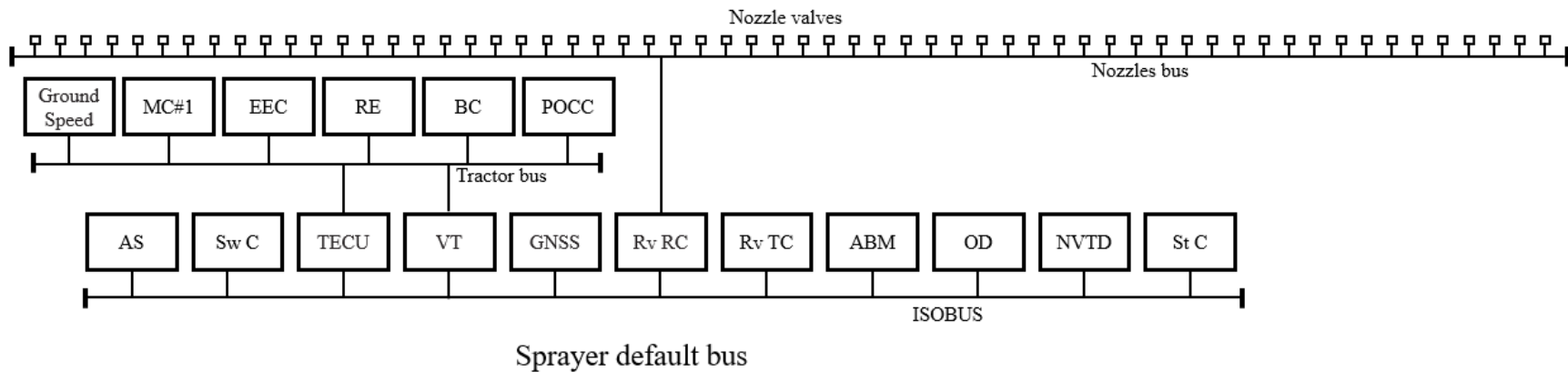
The implement bus integrates ECUs including the VT (0x26), TC (0xF7), product ECU (0x81), GNSS data management (0x1C), etc. The boom sprayer supports two in-cabin, and one out-cabin Implement BUS Breakaway Connector (IBBC) connection points, to facilitate the attachments of additional ECUs if needed. This flexibility optimizes

operations like fertilization, and crop protection in a single pass (Harris, 2018). The sprayer utilizes section control through the VT, with each section containing multiple nozzles. Multiple sections can be controlled simultaneously, allowing for individual control of PWM-controlled nozzles. This enables precise adjustments to application rates based on terrain, speed, and prescription maps.

A further analysis of the PGN distribution of the CAN messages on the boom sprayer is shown in below Table 3.1, which indicates that ISOBUS messages are the largest share . Although J1939 has more PGNs than NMEA 2000, NMEA holds a higher percentage of data compared to J1939 due to the large overhead needed when delivering GNSS data to the sprayer. Proprietary messages likely support specialized, manufacturer-specific functions.

Table 3.1: The PGN distribution of the boom sprayer in parentage

Protocol	Number of PGNs	Percentage (%)
ISOBUS	15	46
NMEA 2000	9	24
J1939	10	18
Proprietary	4	12



Legends:

 CAN bus
 ECU

Abbreviation:

MC#1	Management computer #1	TECU	Tractor ECU
EEC	Electronics engine controller	VT	Default sprayer virtual terminal
RE	Retarder engine	GNSS	Global navigation satellite system
BC	Body controller	Rv RC	Default sprayer rate controller
POCC	Passenger operator climate control	Rv TC	Default sprayer task controller
AS	Angle sensor	ABM	Auto boom control
Sw C	Switch controller	OD	Onboard diagnostic
ECU	Electronics control unit	NVTD	Non-virtual terminal display
		St C	Steering controller

Figure 3.3: The boom sprayer ECU mapping through CAN messages

3.5 POWER FOR IMPLEMENT BUS

The boom sprayer requires a substantial power supply to operate its components, especially when equipped with 60 Hawkeye nozzle valves, a VT, a rate controller, and a GNSS receiver for exact navigation. The alternator of the boom sprayer delivers around 160-200 A at 13.8 V equivalent to a maximum of 2.76 kW to meet these demands (Raven, 2019). In Figure 3.4, the power connection of the boom sprayer implement bus is shown.

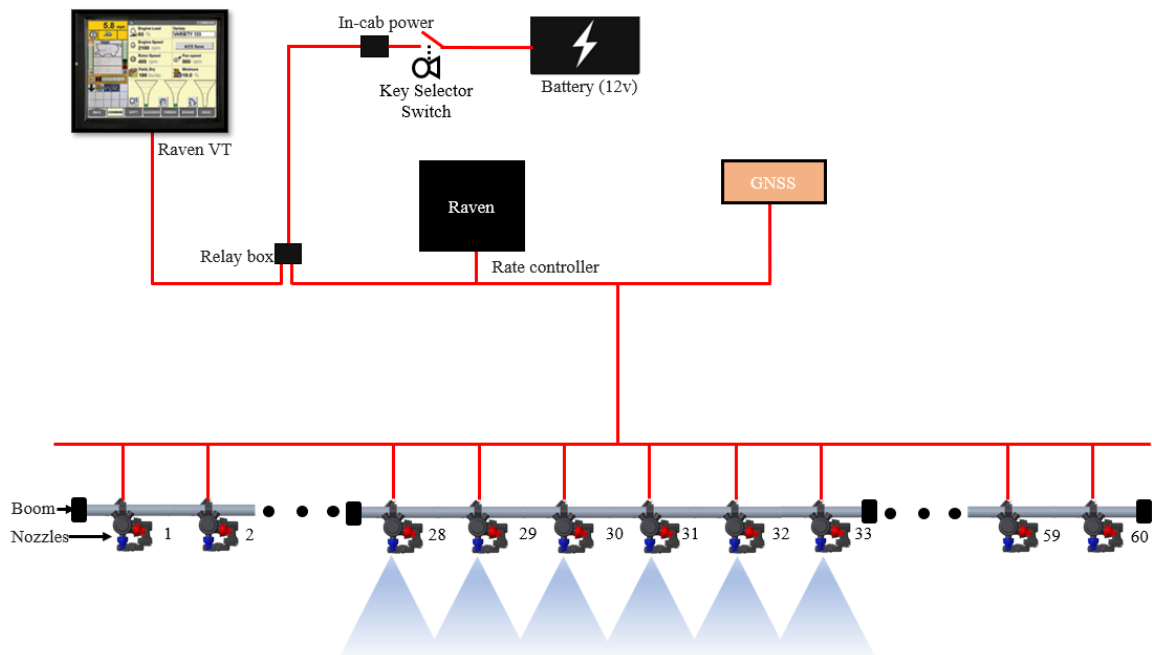


Figure 3.4: Power connection of the boom sprayer implement bus

Each nozzle valve generally consumes about 1-2 A at 12 V when active. Assuming an average consumption of 1.5 A per valve, each valve uses approximately 18 W. With all 60 valves active, they collectively consume a significant amount of power, totalling around 1,080 W. The VT typically requires around 15 W, while the Raven rate controller, which manages the spray application rates, averages around 40 W and the GNSS receiver adds approximately 10 W to the total power requirement. Combining these requirements, the

total power needed to operate the 60 nozzle valves, VT, Raven rate controller, and GNSS receiver is approximately 1,145 W. While this estimated power demand is relatively high, it remains well within the capacity of the alternator and battery system, ensuring reliable field performance.

To achieve spot spraying compatibility, multiple computers, cameras, and pumps are essential for a machine vision-based spot spraying system. These additions may exceed the default power capacity of the boom sprayer, requiring a detailed power calculation which are discussed in Chapter 6.

CHAPTER 4: DEVELOPMENT OF AN ECU TO ENABLE MACHINE VISION SYSTEM INTEGRATION WITH THE BOOM SPRAYER

4.1 OVERVIEW

This chapter presents the development of an ECU for flexible and scalable integration of machine vision systems with horizontal boom sprayers. The ECU introduces a novel approach to communication and control, supporting multiple cameras with overlapping FOVs and varying nozzle configurations. Laboratory and field tests demonstrate the ability of the ECU to process spatial data from machine vision systems, convert it into CAN frames, and control nozzle activation in real-time, enhancing spot spraying accuracy and efficiency. The results highlight its potential to overcome barriers to machine vision integration, offering a cost-effective and adaptable solution for precision spraying. By addressing both hardware and communication protocol requirements, the proposed ECU lays the groundwork for scalable spot spraying systems across diverse agricultural settings. These findings advance precision agriculture by promoting resource efficiency, reducing environmental impact, and improving the adaptability of spraying technologies.

4.2 ECU DESIGN AND IMPLEMENTATION

4.2.1 Defining Protocol Message

The communication between the machine vision and ECU was developed based on the Universal Asynchronous Receiver Transmitter (UART) protocol suitable for communication between two electronic entities. UART limits the system to a single interfacing point, enabling communication with only two computers simultaneously through a single UART interface. The architecture of the protocol message frame (Figure

4.1) includes the camera information within the machine vision system that detects a pest (Camera ID), the type of pest (Pest ID), spatial information to locate the pest within the FOV the camera, and the time of detection. The spatial information in the frame was reduced to the location of the first (Minimum x -value) and last (Maximum x -value) pixels of the pest along the x -axis of the FOV as well as the total width – i.e. the number of pixels across the x -axis – of the image (x_{total}). Including x_{total} in the message frame as a variable allows the ECU to identify the correct physical location of the pest relative to the location of the nozzle to be controlled regardless of the size of the image because different machine vision systems would use different image sizes to detect pests. The y -axis of the FOV was not considered because the spray from the nozzles would cover the y -axis as it aligns with the direction of boom travel as explained in Figure 4.2.

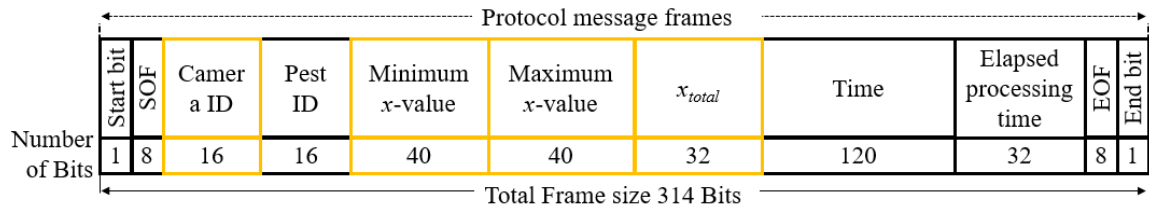


Figure 4.1: UART protocol message to communicate with machine vision system based on UART. Yellow boxes indicate data used by ECU to determine insect location across the boom

Figure 4.2 (a) demonstrates a sketch of the rear view of the camera and nozzle arrangement on a section of a boom, whereas Figure 4.2 (b) shows an example of the FOV of two adjacent cameras. In this example, where one camera covers an area of the boom of three nozzles, the machine vision system would send two message frames (one from each camera) to the ECU as shown in Figure 4.2 (c). The ECU, in turn, divides each frame into three regions (based on initial user input as explained in 4.2.2) and determines which

nozzles to open (based on the ECU algorithm as explained in 4.2.3). Assuming equal spacing between all nozzles and cameras across the boom (which is the common design in boom sprayers), this protocol message would enable a unified communication protocol for diverse machine vision systems despite their differences in terms of the number of cameras within the vision system and the physical width of the FOV.

In Figure 4.2 (b), for instance, an insect was detected near the left point within a specific section whose x-values range between -160 and -162 in a FOV whose x-total is 1000 pixels. Simultaneously, in an adjacent FOV, two insects were detected whose x-values range between -0080 and -0083 as well as +0200 to +0201. In this situation, the protocol message communicated a pest spread ranging from -0080 to +0201. With these detections, two protocol messages (Figure 4.2 (c)) from the machine vision are sent to the ECU – one from each FOV that detects any insect.

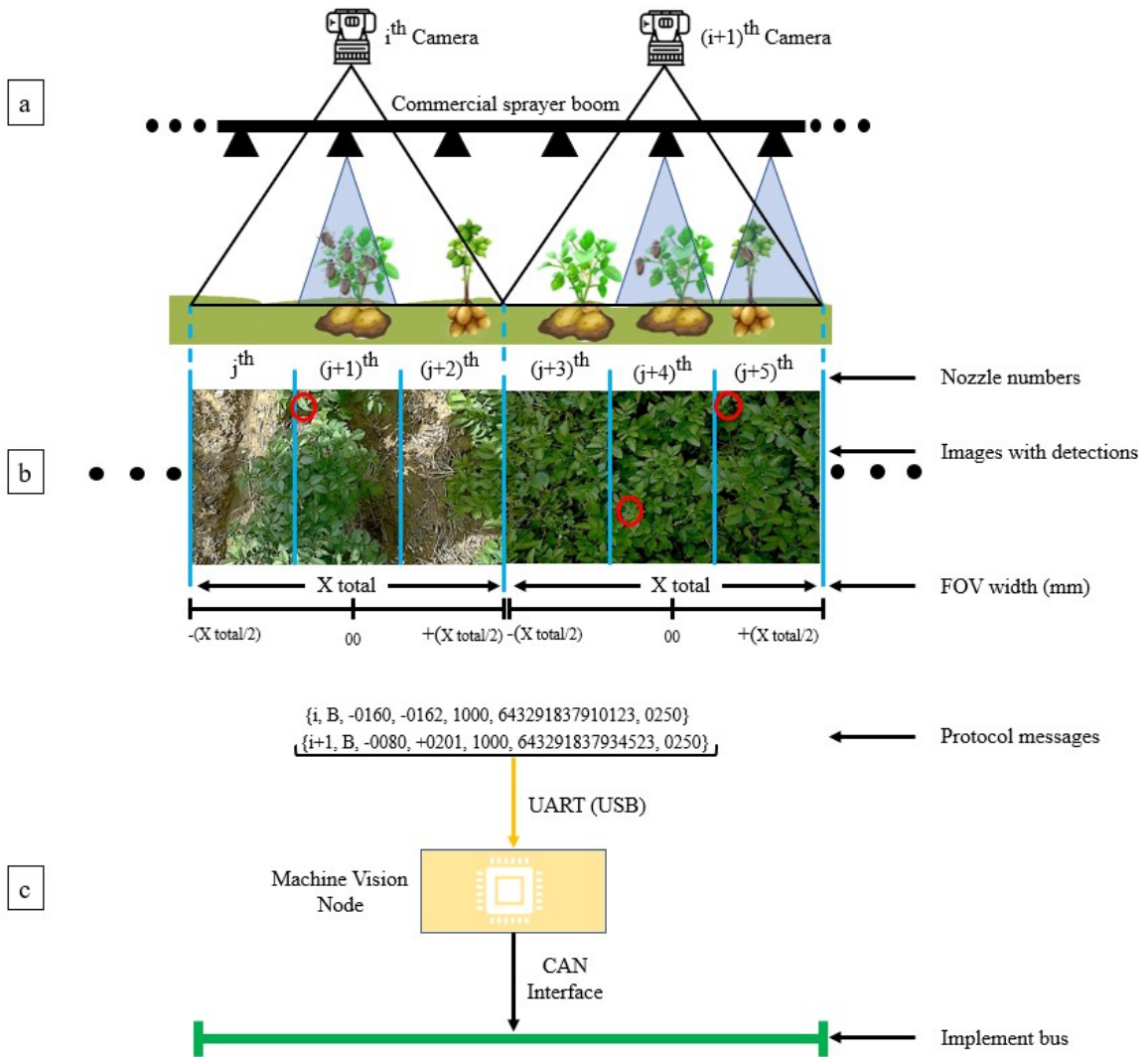


Figure 4.2: (a) Camera and nozzle setup on a boom sprayer showing FOV and spray, (b) Top view from a camera sectionizing FOV according to number of nozzles, (c) Example of protocol messages leaving the machine vision system to ECU

4.2.2 Hardware of ECU

The ECU depicted in Figure 4.3 consists of two electronic entities for synchronized and simultaneous management of two different communication protocols, UART and CAN. The first entity referred to as the ‘Nozzle Section Converter’ is implemented using an Arduino MEGA 2650 board (Arduino, Ivrea, Italy), while the second entity known as

the ‘CAN Message Converter’ utilizes an Arduino UNO board (Arduino, Ivrea, Italy), equipped with a CAN transceiver (CAN-BUS Shield V2.0, Seeed Technology, Shenzhen, China).

In the nozzle section converter, besides the UART port which receives the protocol messages from the machine vision, a second UART port is used to send the results of which nozzle to open to the CAN message converter. Also, a general-purpose input/output port is used to provide communication with a keypad. Upon turning on the ECU, it remains in an idle mode in terms of processing any data arriving from the machine vision system until the operator presses a number on the keypad equivalent to the ratio (r) between the number of cameras (M) and nozzles (N) on the boom as shown in Equation 4.1:

$$r = M / N \quad (\text{Eq. 4.1})$$

Once the value of r is set, the ECU enters a continuous mode of reading protocol messages, if received from the machine vision, and broadcasting CAN frames on the implement bus.

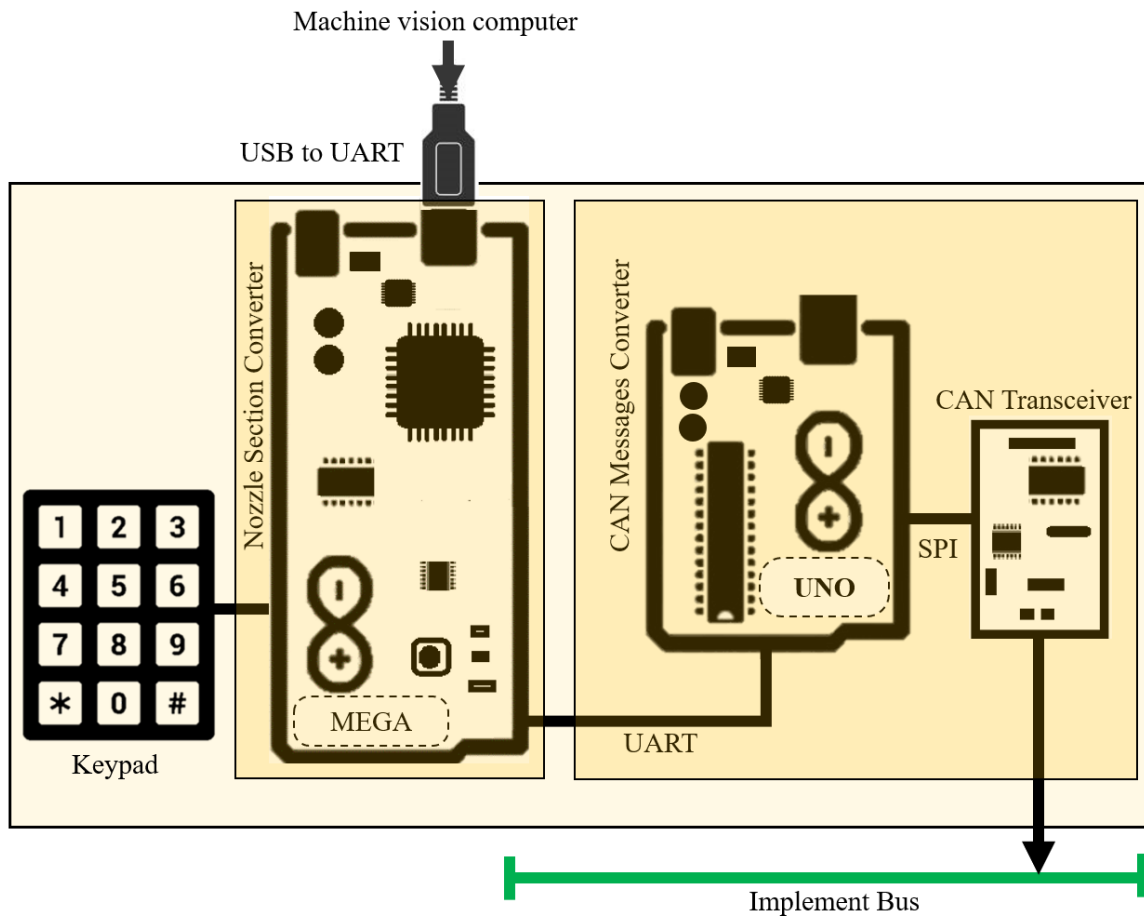


Figure 4.3: ECU hardware consisting of nozzle section converter and CAN message converter with two interfaces with machine vision system and implement bus. Keypad serves as interface for the operator when initializing the ECU

The nozzle section converter sends and receives data at both UART ports at a baud rate of 115200 bps creating a binary array A of size N , so that nozzles open and close will have the values of 1 and 0, respectively. A gets updated within a fixed period e.g. 10 ms, based on the protocol messages.

On the other hand, the CAN message converter creates CAN frames (Figure 4.4) based on the information carried by A to the implement bus. The CAN frames using a 29-bit identifier, and 64-bit data frame are commonly called CAN 2.0B. These frames are

transmitted through the CAN transceiver, which functions as the interface connecting to the implement bus as shown in Figure 4.3. The CAN message converter transmits CAN frames to the implement bus at 10 ms intervals by default; however, this can be extended to a deliberate actuation time based on system requirements determined through visual inspection of spray length.

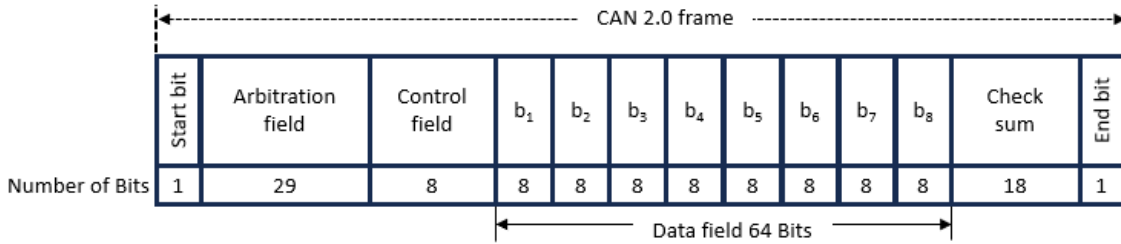


Figure 4.4: CAN 2.0 frame with 29-bit arbitration field, 8-byte data field.

4.2.3 Software of ECU

Figure 4.5 shows the flowcharts of the two software modules embedded in the section nozzle converter and CAN message converter. Figure 4.5 (a) describes how A gets constructed. Firstly, a default all-zero array is created. Once a protocol message was read, a subset of x -values (S) that represents intermediate object points between x_{min} and x_{max} is calculated, using Equation 4.2, to get one or more extra identification points of an object in the cases of large pests such as weeds or multiple scattered objects such as insects.

$$S_p = \begin{cases} x_{min} + i \times \left(\frac{x_{max} - x_{min}}{r-1} \right), & r \geq 3, \forall p \in \{1, 2, \dots, r-2\} \\ \emptyset, & r < 3 \end{cases}, r \in \mathbb{N} \quad (\text{Eq. 4.2})$$

If a single FOV contains multiple individual detections, consolidate the data by taking the leftmost x_{min} from the farthest left detection and the rightmost x_{max} from the

farthest right detection. This approach allows us to represent all detections within the frame as a single, larger detection in the protocol message. Consequently, this reduces the number of messages transmitted while still ensuring that the nozzle remains open to cover the entire detected area anyway.

The total set of x -values Z generated from one image includes x_{min} , x_{max} , as well as all the values in S , if any. Next, to find the location of each x -value relative to the size of the image, Equation 4.3 applies,

$$x_{obj} = \left(\frac{x_{total}}{2} \right) + x, \forall x \in Z \quad (\text{Eq. 4.3})$$

By utilizing x_{obj} , the section nozzle converter determines the section number (j) to be opened using Equation 4.4.

$$j = \left(\frac{x_{obj}}{(x_{total}/r)} + 1 \right) + (r \times (i - 1)), \forall j \in \{1, 2, \dots, r\} \quad (\text{Eq. 4.4})$$

Finally, the section nozzle converter converts the values of the ordinal of the calculated j s in A to 1 before reading another protocol message. This operation repeats for 10 ms after which A is sent to the CAN message converter before it gets reset as shown in Figure 4.5 (a). This 10 ms delay is deliberately chosen to observe the quickest possible response time of the ECU and the algorithm. However, further inspection is required to determine the actual delay needed for reliable operation. During this interval, all protocol messages arriving within that frequency must be read. The optimal delay time is influenced by the sprayer's speed, as different nozzle coverage lengths and varying delay times will result in different detection patterns. Therefore, measurements must be taken at different

speeds and delay intervals to determine a suitable delay that ensures legitimate coverage and accurate detection.

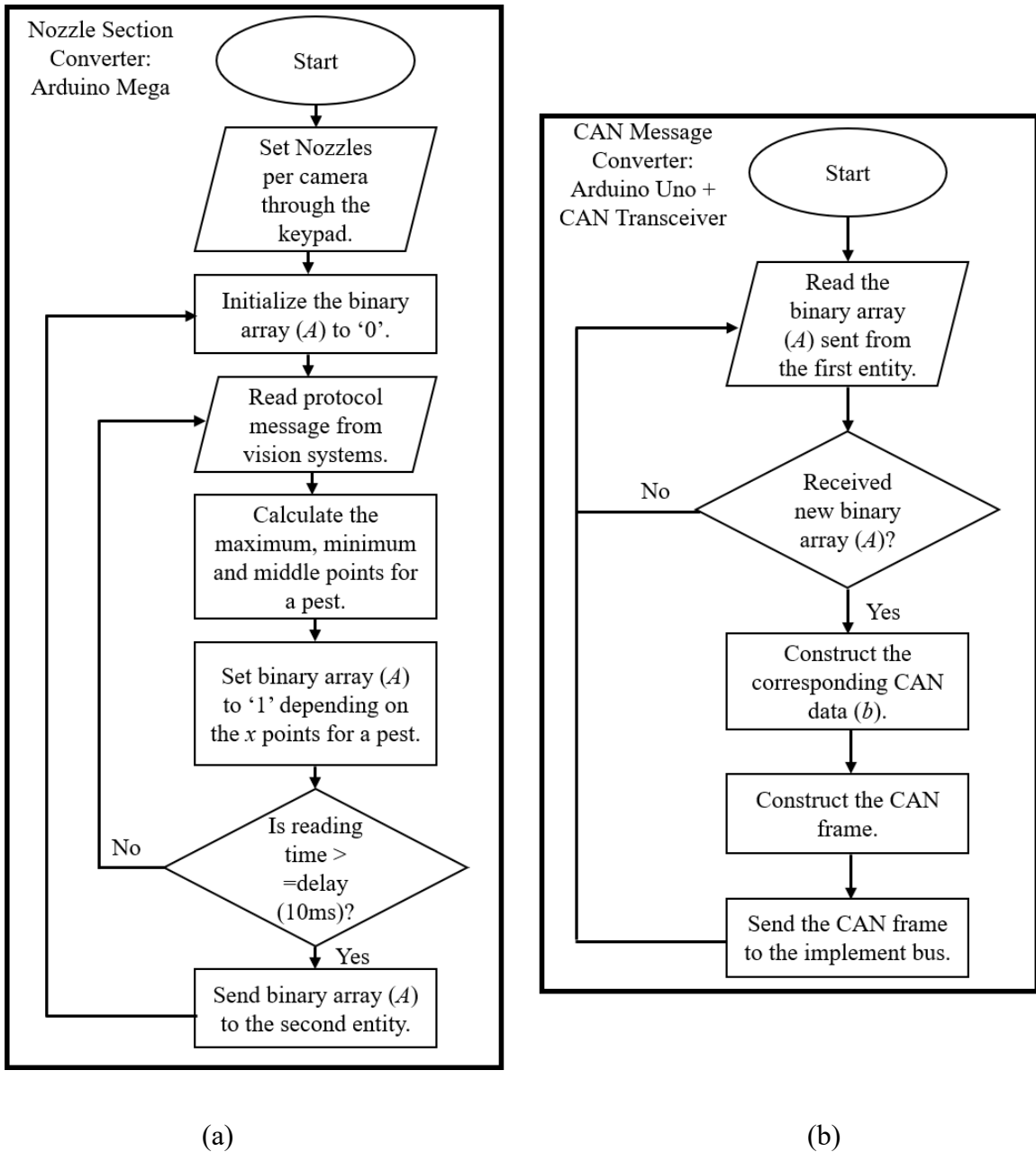


Figure 4.5: Flow diagram of the ECU, two separate algorithms are presented (a) Nozzle Section Converter and (b) CAN Message Converter.

After receiving the binary array as an input, the CAN message converter constructs CAN data and frame specific to the nozzle rate controller used for spraying. For instance, for a Raven rate controller (ISO product controller II, Raven Industries Inc., South Dakota, US) that can control up to 6 nozzles, the CAN frame construction method described by Al-Mallahi et al.(2023), was applied. On the other hand, for Pentair rate controller (Hypro ProStop-E ISOBUS System, Pentair plc, London, UK), which can control up to 16 nozzles, Equation 4.5 was developed and applied based on Pentair HYPRO (2019),

$$b_k = (A[2k] \times 10) + (A[2k - 1] \times 160), \text{ Where } k = \{1, 2, \dots, 8\} \text{ (Eq. 4.5)}$$

Equation 4.5 returns CAN data b in decimal which is then converted to hexadecimal format during the construction of the CAN data. These converted values are then merged with a specific CAN ID (18BB9680) to form a complete CAN frame.

4.2.4 Apparatus and Test Scenarios

The testing methodology of the ECU encompasses two distinct setups, each representing a different testing environment. The first setup involves a custom-made static sprayer comprising a Raven rate controller, toggle switches (ISO 6 Section Switch Box, Raven Industries Inc., South Dakota, US), a VT (AFS-Pro 700, Raven Industries Inc., South Dakota, US), and a one-inch boom pipe housing 6 nozzles with PWM control valves (1-063-0173-674, Hawkeye Control Valve, Raven Industries Inc., South Dakota, US). The second setup involves field testing utilizing a utility train vehicle (Gator™ XUV 4x4 825i, John Deere, Illinois, USA) on which a functional spraying system including a tank, and a fuel-based pump is mounted along with the VT, the Pentair rate controller and 12 Pentair rotating valves (Hypro ProStop-E Single, Pentair plc, London, UK) mechanically attached

with nozzle tips (3D90, Syngenta, Cambridge, UK). Figure 4.6 is a generalized visualization of the components of all the setups in terms of their connections on the communication buses. In addition, the figure shows how the different machine vision systems and the ECU get integrated into the communication bus of the different systems.

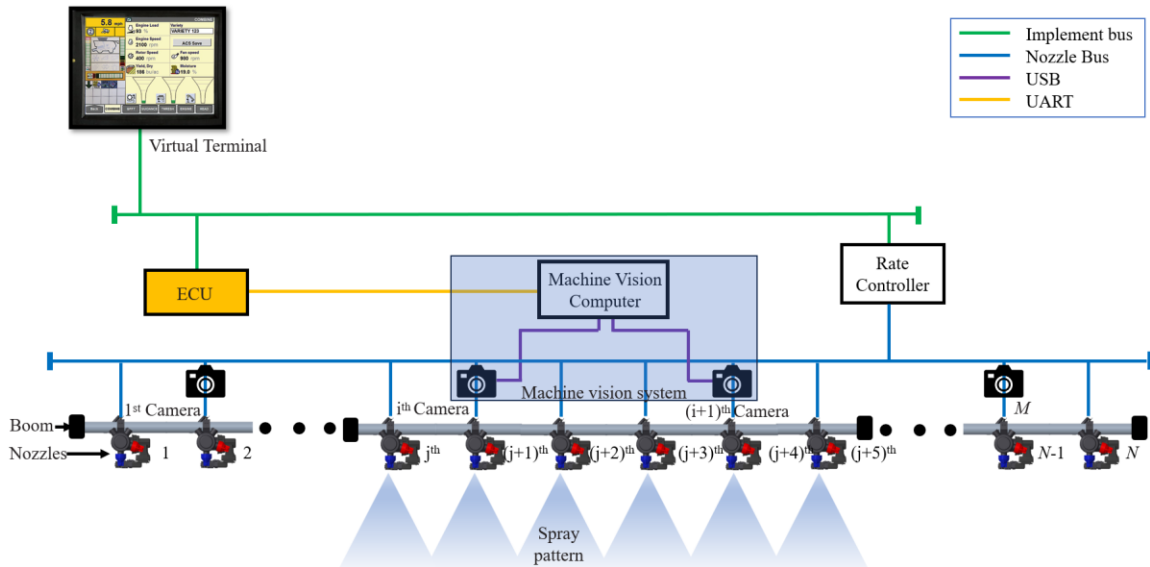


Figure 4.6: Generalized CAN-compatible spraying system communicating with machine vision systems through the ECU

Using these setups, the ECU was tested in four different scenarios leading to a scenario of field deployment as shown in Table 4.1. In the first scenario, an Arduino UNO board was programmed to emulate protocol messages for a single-camera machine vision system controlling 6 nozzles. On the other hand, in the second scenario, a machine vision system that consists of two RPi cameras (Raspberry Pi, Milton, Cambridge, UK) that simply detects red-colored targets was built to test the communication with actual machine vision. The third scenario was conducted with a machine vision system consisting of three

RX0II cameras (RX0II, Sony, Tokyo, Japan) suitable for on-the-go field operations (Campbell et al., 2022).

Table 4.1: Different ECU testing scenarios for integration flexibility and spraying accuracy

Scenario	Setup	Machine vision system	Camera model	Rate Controller	No. of cameras (m)	No. of nozzles (n)	Target
1		Emulator	-	Raven	1*	6	-
2	Static sprayer	2-camera	RPi	Raven	2	6	-
3		3-camera	RX0II	Raven	3	6	Red color
4	UTV	6-camera	OAK-D	Pentair	6	12	Multi-color object

* Mark indicates the camera number is emulation

In the last scenario, a bigger machine vision system consisting of 6 OAK-D cameras (OAK-D, OpenCV, Cyprus) mounted 0.5 m above the ground covering a narrower area. This setup was employed to control individual nozzles mounted on a Utility Task Vehicle (UTV), equipped with a Pentair spraying system featuring 12 nozzles shown in Figure 4.7. The angled Syngenta nozzles, which sprayed at a 55° angle, were mounted so that they sprayed backwards opposite to the travel direction of the vehicle. This arrangement was decided to give the machine vision-based spraying system the ability to detect and spray on the target even when the cameras and nozzles were mounted in proximity at the boom. This machine vision had the ability to detect multicolored targets in real-time while operating in the field.



Figure 4.7: ECU deployed on UTV equipped with Pentair spraying system controlling 12 nozzles by machine vision of 6 cameras

Utilizing this setup, an experiment designed to investigate various target distribution types that simulate weed distribution scenarios in agricultural fields: individual, intersection, sequential, wide/bulk, and long, as illustrated in Figure 4.8. The objectives for each type are as follows: activate a single nozzle at a time for the individual distribution (only one object within the field of view of each camera); activate both nozzles for the intersection distribution (one object falling between the FOV of two different cameras); sequentially activate a nozzle or more while another or more are already in a spraying mode (demonstrating the capability of simultaneous detection and spraying); activate multiple nozzles as needed for a cluster of targets for the wide/bulk distribution; and activate nozzles for elongate time when a target is in line with the direction of the UTV.

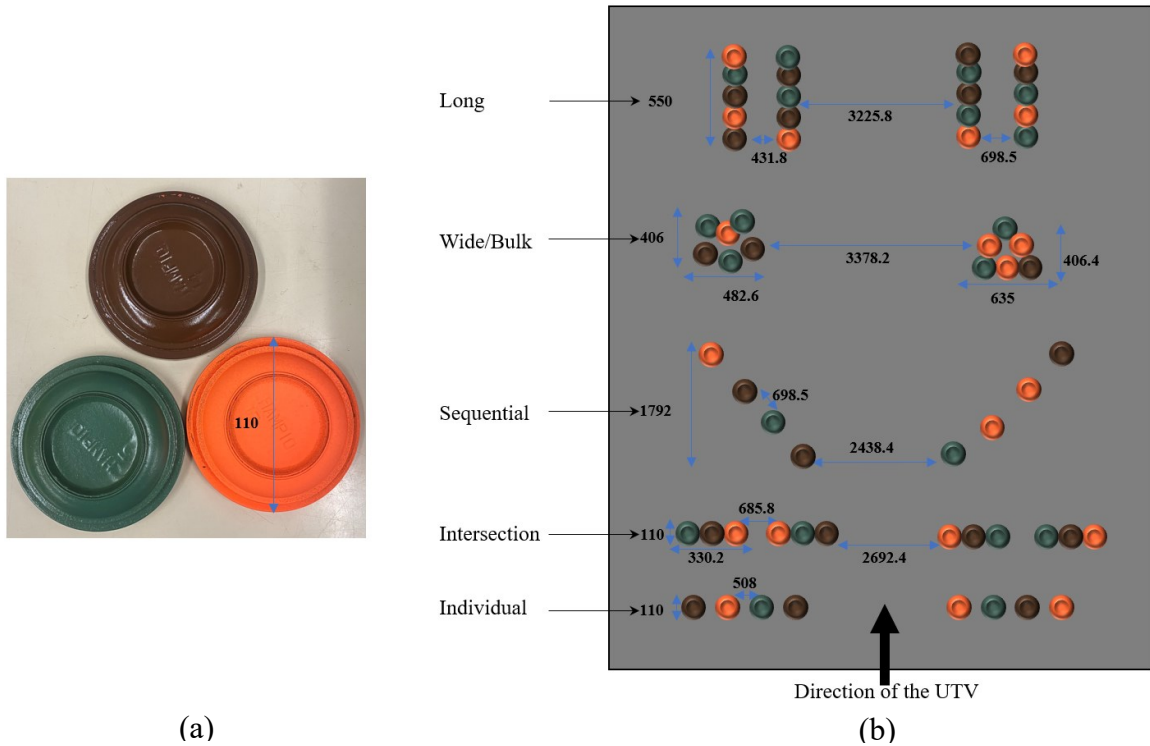


Figure 4.8: (a) Multicolor targets (b) target distribution on the ground, showing distances in mm, for the ECU field test

The experiment was conducted at an open space for vehicle testing in the Dalhousie Agricultural Campus (Truro, Nova Scotia, Canada) at three speeds, speed 1 (3.22 kph), speed 2 (6.44 kph), and speed 3 (9.66 kph), which are typical operational speeds of sprayers for a variety of crops by which the functionality and effectiveness of the ECU could determine in terms of its ability to establish successful communication between machine vision and nozzles to hit the target.

4.3 RESULT AND DISCUSSION

4.3.1 Lab Test Scenarios

In the first scenario, the emulator generated single-camera protocol messages to control six nozzles individually, dividing the FOV of the camera into 6 areas by the nozzle

section converter of the ECU for the individual nozzle control. In the second scenario, the protocol messages were generated for two cameras, dividing the FOV for one camera into three areas. In the third scenario, the protocol messages were generated by three cameras, with each camera splitting its FOV into two areas. In all three scenarios, the protocol messages were received by the nozzle section converter every 1.3 ms to 1.5 ms via the UART interface and produced the binary array (A) of size 6 every 10 ms as expected by the algorithm (Figure 4.5 (a)). On the other hand, the CAN message converter generated CAN data based on A as described in Figure 4.5 (b). Since the Raven rate controller was the one used in the laboratory test scenarios, the equation described in Al-Mallahi et al. (2023) applied to construct the corresponding CAN frame before broadcasting on the implement bus.

A comparison between the three scenarios, in terms of the response to detected targets, is shown in Figure 4.9. While all scenarios were able to partition the FOVs of the cameras to match the number of nozzles, there were differences in performance in terms of matching nozzle openings with the distribution of pests within the FOV. When one object was present within the region of the six sections, the required nozzle was opened as shown in Figure 4.9 (a). On the other hand, when two objects were present as shown in Figure 4.9 (b), the nozzle was opened not only in Sections 1 and 3 where objects were present but also in Section 2 in both the first and second scenarios. This occurred because Equation 4.2 computes a subset of x-axis intermediate points (S) for every section between the first and last objects within the FOV of each camera. In the first scenario (Figure 4.9 (c)), all 6 nozzles were opened because the first and last objects were within the FOV of the same camera, generating x_{obj} for all sections using Equation 4.3. In the second and third

scenarios, the nozzles were opened in two sections, aligning with the distribution of objects on the ground. Figure 4.9 (d) whose object distributions were a combination of Figure 4.9 (b) and (c) shows that spraying at each object was guaranteed regardless of the machine vision system in terms of cameras used to cover the boom. While in the three scenarios, all the pests were targeted which is the minimum expected from any sensor-based spot spraying, the third scenario excelled by ensuring that excessive spraying did not take place.

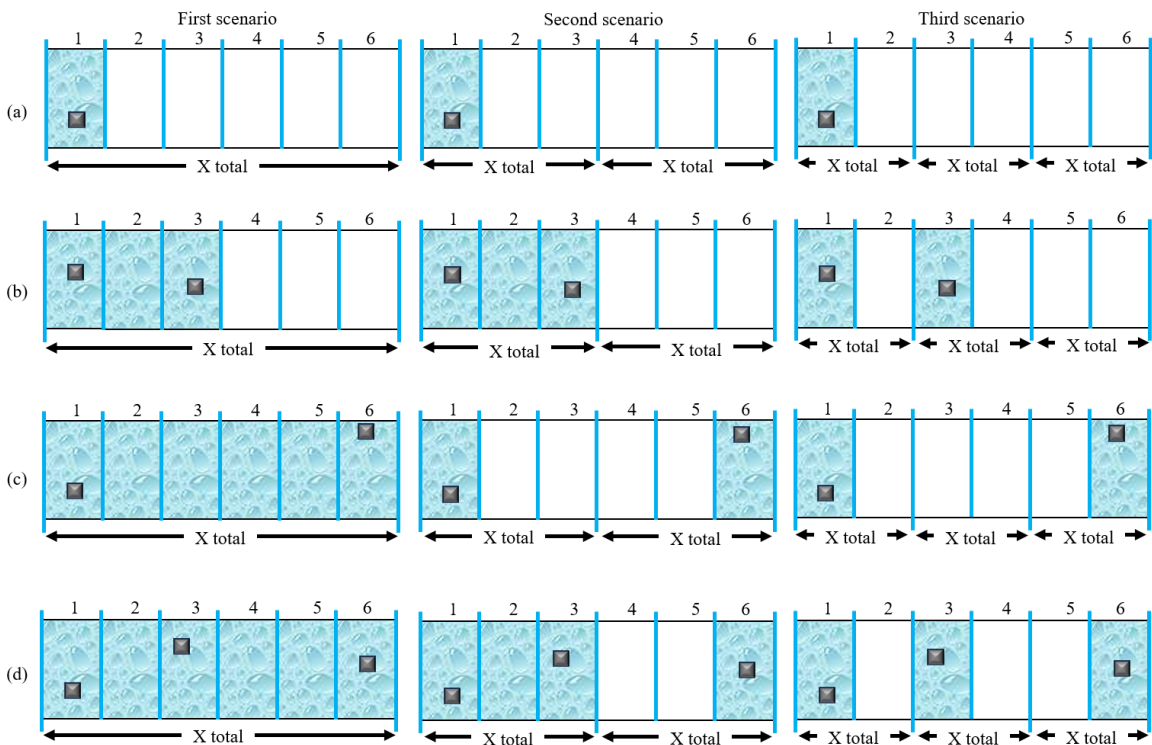


Figure 4.9: Spraying pattern of the first, second and third scenarios for four different pest distributions when (a) one target is detected, (b) two close targets are detected, (c) two far targets are detected, and (d) three targets are detected

While the decision to open extra nozzles might initially appear as a drawback, it represents a deliberate trade-off aimed at preserving the concise UART messaging between the machine vision system and ECU, ensuring timely nozzle response within the designated timeframe as well as giving the option to reduce the number of cameras of the machine

vision to reduce cost. Table 4.2 presents the results of using the ECU to control the interaction between machine vision and nozzles in a 6-nozzle sprayer system resulting in 64 unique nozzle configurations. Each of these 64 configurations was evaluated across 6 nozzle spray systems for individual nozzles on/off scenarios, leading to 384 different possible results. For all ratios (1:1, 1:2, 1:3, and 1:6), the system successfully sprayed all detected targets (192 out of 192). For the 1:6 ratio, the system exhibited an over-spray rate of 37.5% (72 out of 192) where spraying occurred without detections. This rate decreased significantly at the 1:3 ratio, with only 8.3% (16 out of 192) instances of over-spraying. At the ratios of 1:2 and 1:1, there was 0% over-spray and 100% detection accuracy, indicating these configurations were highly efficient.

Table 4.2: Detection and spray performance in different camera-nozzle ratios in a 6-nozzle sprayer

Ratio	Target	Sprayed	Not Sprayed
1:6	Detected	192	0
	Not Detected	72	120
1:3	Detected	192	0
	Not Detected	16	176
1:2	Detected	192	0
	Not Detected	0	192
1:1	Detected	192	0
	Not Detected	0	192

Assuming successful detection of targets by machine vision, the ECU was able to deliver messages to spray on the detected objects at all times. The setback, however, was the increase in the number of times unnecessary spraying might take place at sections of the sprayer due to the nature of the algorithm in the ECU in creating S in between two

objects detected by one camera. It can also be noticed in the table that, when the ratio between the cameras and nozzles was 1:2, the performance of the ECU was ideal which means that no extra spray might be achieved while cutting the cost of mounting cameras to half and getting the same spot application performance when compared with a ratio of 1:1.

4.3.2 Field Test Scenario

In the fourth scenario, since the ratio (r) determined was 1:2, the total set of x -values Z consisted only of x_{min} , x_{max} , which meant that the probability of opening any nozzle unnecessarily was eliminated. Spray length measurements for a single detection were recorded at the three speeds using actuation or delay intervals of 10 ms, 40 ms, 100 ms, and 400 ms. The 10 ms delay provided the fastest response but resulted in insufficient spray lengths, though the 100 ms delay improved coverage, it remained inadequate at Speed 3. At 400 ms, spray lengths were sufficient across all speeds, ensuring consistent target coverage. Notably, this delay does not risk missing any protocol messages, as the machine vision system requires 422 ms to generate messages for single or multiple detections of a single instance. Our experiment used a delay time of 400 ms, as the machine vision system requires this time to complete detection after seeing the targets. During this delay, the nozzle remained open while continuously sending CAN messages after a target was selected.

Table 4.3: Different distributions and speeds, with the spray ground coverage

Distribution Type	Target Area Length (mm)	Speed 1	Speed 2	Speed 3
		Spray length (mm)		
Individual	110	345	700	1070
Intersection	110	345	700	1070
Sequential	1792	2082	2470	2760
Bulk	406	745	1010	1346
Long	550	785	1140	1520

This decision was made based on observations to have effective spray on weed in the wild blueberry cropping system which runs at low speeds like Speed 1. Table 4.3 summarizes the results of running the UTV three times at each speed while spraying on the targets of different distributions. At Speed 1, the individual and intersection targets were sprayed for 345 mm due to single machine vision detection – giving an equal buffer spraying at both sides of the target of 117 mm. It was observed that the buffer surrounding the target was created because of the combined effect of angled nozzles and ECU time delay which created the buffer before and after the target, respectively. At the other three distribution types when multiple machine vision detections took place on the go due to the enlarged size of the target, the entire spray time at a single detection of 345 mm was the buffer divided equally before and after the cluster of the target.

When the targets were arranged in sequence, all of them were sprayed with buffer spraying surrounding each target. More importantly, the successful sequential spraying was a demonstration of the ability of the ECU to continue getting information from the machine vision system while being busy sending CAN messages to spray, which was the result of separating the algorithm into two different electronic entities. Similarly at Speeds 2 and 3,

spraying hit 100% of the targets while creating buffer spraying surrounding each target. However, as the speed increased, the area of buffer spraying increased because of the fixed delay time of 400 ms regardless of the speed of the vehicle. Given that the pumping system on the UTV was running independently at a constant flow rate (approximately 275.79 kPa), this meant that the same volume of liquid was delivered over extended areas leading to possible ineffective spraying. Therefore, in actual field implementation, both the delay time of the ECU and the related pressure of the pumping system need to be adjusted as well as adjusting the pressure according to the speed of the vehicle to achieve active spraying.

Nevertheless, the ECU was able to manage the communication between the machine vision system and the spraying mechanism at every distribution of the target and at any speed with identical performance when running the experiment several times at the same speed. As of the possible problem of ineffective spraying at increasing speeds, the delay time can be reset for the application conditions of the sprayer to which the ECU would be mounted, as in typical situations, sprayers used for certain crops run at pre-determined constant forward speeds. Alternatively, the ECU can be upgraded so that it would receive the vehicle speed via the Engine-ECU over the CAN network.

The success of the ECU in controlling and managing the relationship between the cameras and nozzles at all scenarios, including field deployment can be attributed to the mapping of the detection spatial across the horizontal access of the FOV in the multi-camera. This was able to overcome one of the challenges outlined by Al-Mallahi et al. (2023) whose system, although was able to layout the foundation of communication via UART and CAN was limited to scenarios of one camera per nozzle. The ECU, on the other

hand, handles the multi-camera situation assuming that all the cameras are managed by one machine vision system. While in the scenarios tested throughout this research work machine vision systems managing up to 6 cameras were available, it is highly likely that in wider booms that can extend to up to 36 m, there will be multiple machine vision systems running simultaneously to process images of bigger number of cameras due to the image processing capacity of a single machine vision system. In this new situation, new developments in communication methods would be needed to enable ECUs to handle multiple machine vision systems running multiple cameras. Another possible limitation of the ECU is its lack of compliance with ISOBUS, which limits its interoperability with sprayer systems from different manufacturers. Including ISOBUS in the architecture of the ECU could provide interfacing via the VT screen of the tractor, exchanging data from other ECUs of the sprayer such as speed, which will eventually enhance the usability when running the sprayer at variable speeds.

4.4 CONCLUSION

The ECU, which consists of two different electronic entities, was able to simultaneously communicate with machine vision and implement bus. By minimizing the amount of information sent from the machine vision to the location of insects at the horizontal axis perpendicular to the direction of the travel of the tractor, the data needed to open and close nozzles were successfully transferred over CAN. Testing at different scenarios indicated that all pests within the FOV of any of the cameras were targeted using the algorithms in the ECU even if this resulted in occasional opening of nozzles where pests did not exist. This apparent setback is compromised by the fact that pests are sprayed

without fail regardless of their size of distribution within the FOV, while experiments demonstrate that the 1:2 ratio does not exhibit this issue.

The most important findings of this study are (1) The ability of the ECU to communicate simultaneously with both machine vision systems and the implement bus, demonstrating its capability to operate in real-time, (2) the effectiveness of the algorithm in targeting pests across different scenarios, even with occasional over-spraying, and (3) its flexibility to integrate with varying camera-to-nozzle ratios (1:2 to 1:6) across different machine vision systems and nozzle control units. The four different scenarios under which the ECU was tested were on two different commercial nozzle control units and three different machine vision systems as well as machine vision emulators. While the ECU currently communicates via the implement bus, it can be enhanced in the future by converting it to an ISOBUS-compatible ECU with a unique address. This conversion would simplify its camera and nozzle ratio setup through the VT, ensuring interoperability with other ISOBUS-compliant systems and allowing integration into existing agricultural machinery.

CHAPTER 5: DEVELOPMENT OF ISOBUS-COMPLIANT MVN FOR HYBRID COMMUNICATION

5.1 OVERVIEW

This chapter explores the design, development, and evaluation of an ISOBUS-compliant MVN for real-time spot spraying. The MVN addresses the growing complexity of integrating multiple machine vision systems required for wide boom sprayers. While consolidating data from multiple machine vision systems to multiple ECUs can resolve some challenges, it also introduces issues such as increased bus load, deployment complexity, and the need for additional ECUs as the boom expands. To overcome these limitations, the MVN is designed as a single-node solution that ensures individual nozzle control by implementing a hybrid communication framework. Protocol messages are transmitted through an Ethernet-based TCP/IP channel and converted to CAN for communication on the implement bus. Additionally, ISOBUS compatibility is integrated into the MVN, enhancing interoperability among agricultural equipment from different manufacturers by incorporating features such as the VT for operator control and the TC for data management.

5.2 ISOBUS ECU DESIGN AND IMPLEMENTATION

5.2.1 Hardware of MVN

The MVN depicted in Figure 5.1 consisted of an electronic entity for synchronized and simultaneous management of two different communication protocols: Ethernet and CAN. The ECU was implemented using a Single Board Computer (SBC) (Raspberry Pi 4B, Raspberry Pi, Milton, Cambridge, UK), powered by an ARM Cortex-A72 processor.

The SBC was chosen for the ECU platform because of its Ethernet interface and the ability to add CAN interfaces. The SBC was crowned with a 2-Channel CAN bus expansion HAT (Waveshare, Shenzhen, China) that supported CAN2.0. Raspbian, as its operating system, supported the necessary multithreading to manage concurrent processes. The ethernet of the SBC was connected to a router (Asus AC1750, Taipei, Taiwan) and received protocol data from multiple vision systems to make a fully functional node MVN. The two-channel isolated CAN bus interface ensured communication with ISOBUS networks. The first channel, i.e., CAN 0, was connected to the implement bus of the sprayer (Case IH Patriot 3340, CASE International, Wisconsin, US) to read speed data coming from the tractor bus through the TECU to the sprayer implement bus. The second channel of the CAN HAT, CAN 1, communicated with another implement bus for the Pentair rate controller (Hypro ProStop-E ISOBUS System, Pentair plc, London, UK), which controlled 60 nozzles deployed parallelly with the original spraying boom and valve by the Raven rate controller (Raven Industries Inc., South Dakota, US) of the CASE IH. The ECU was powered by a DC-to-DC voltage converter (CPT, Currents Logic Group Limited, Shenzhen, China), which received 12 V from the tractor and supplied 5 V to the SBC.

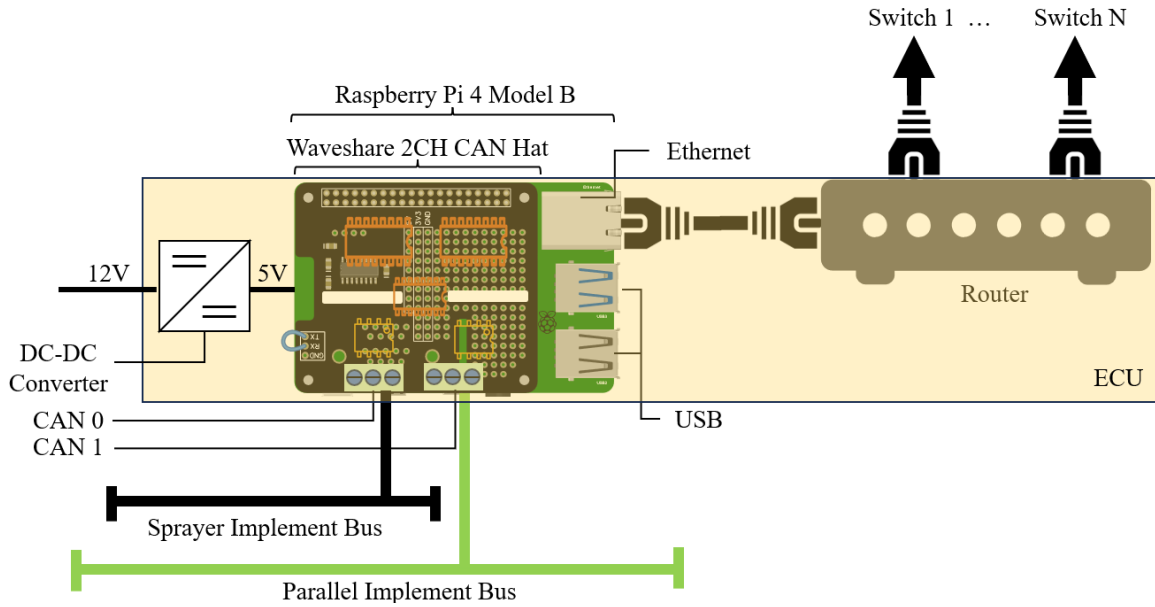


Figure 5.1: MVN hardware consisting of SBC (Raspberry Pi) and two-channel CAN HAT, CAN 1 communicates with parallel implement bus, CAN 0 receives speed data from the sprayer

5.2.2 Software of ECU

In the system flow diagram detailed in Figure 5.2, the system works in four stages: Initialization, Queue, Thread 1: to create nozzle control information, and Thread 2: to create and send CAN frame. At the initialization stage, the ECU sets itself up as a server by taking a fixed server port and Internet Protocol (IP) address within the router IP address class. All machine vision computers are assigned IP addresses as clients through the Dynamic Host Configuration Protocol (DHCP) by the router. The server continuously accepts new client connections at any time and always listens for incoming connections on the same IP address class. After any successful detection, the machine vision computers (i.e. clients) broadcast protocol messages on the Ethernet network and the ECU acting as a server receives all the messages via the router. Afterwards, the CAN network is configured to handle CAN bus communication, ensuring that all parameters are set for network

communication. The MVN memory storage also gets initialized to keep certain numbers of CAN frames as a temporary record. Utilizing the AgIsoStack++ library, the MVN registers itself on the ISOBUS network using a manufacturer ID of $0 \times 1C$, which corresponds to a registered but inactive manufacturer listed under the AEF. In case $0 \times 1C$ is unavailable, the system tries IDs $0 \times 1D$, $0 \times 1E$, or $0 \times 1F$ as alternatives. NAME is a 64-bit identifier that uniquely distinguishes a control function within the network parameters (ISO 11783-5, 2022); in this case, it is specifically defined as an ISOBUS Section Control (SC) function which manages individual implement sections such as nozzle sections on a sprayer. These sections were controlled by individual cameras for precise spraying operations.

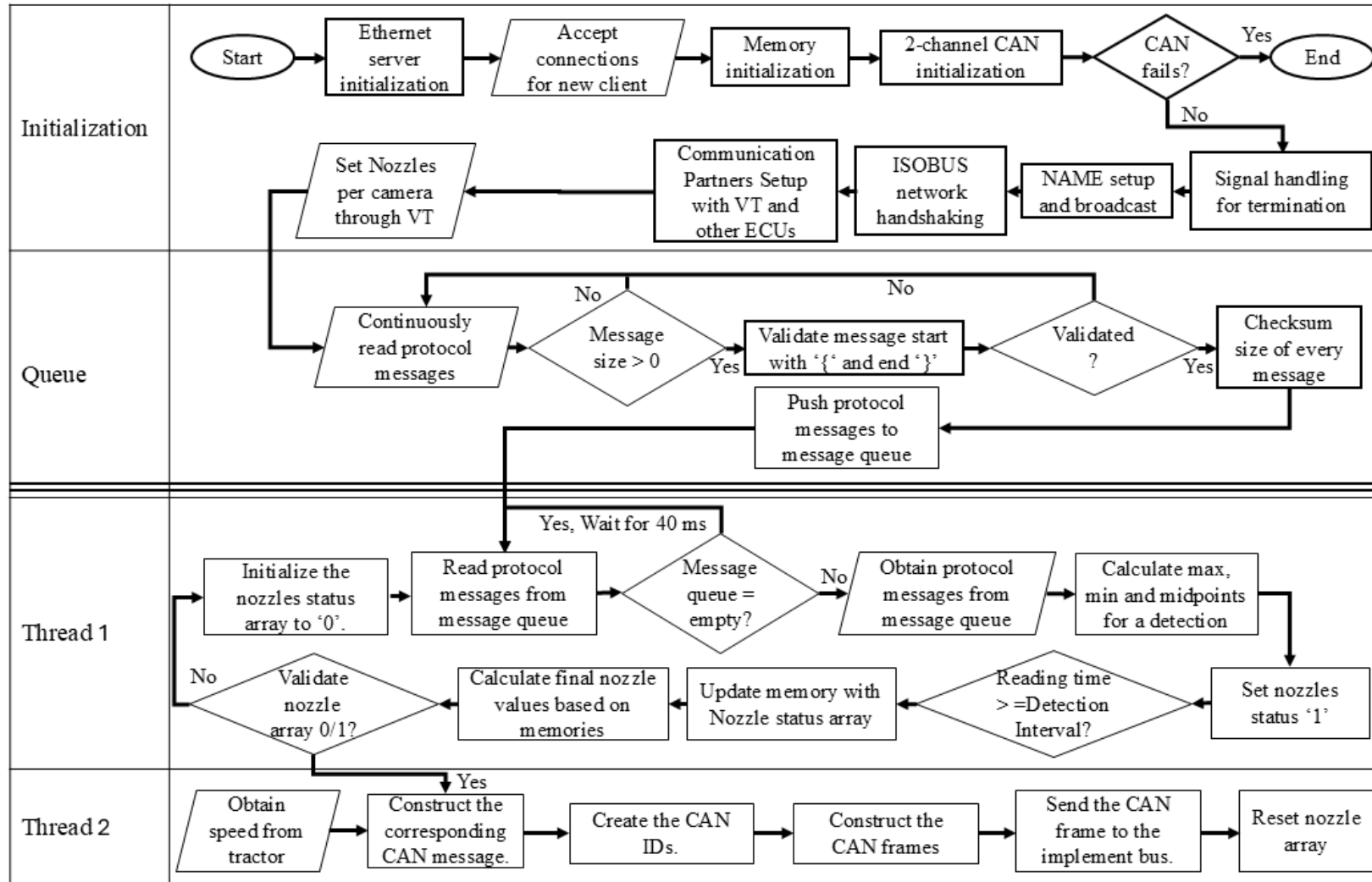


Figure 5.2: Flow diagram of the MVN including the thread control for protocol messages and CAN messages

Following signal handling, the system broadcasts the MVN NAME, facilitating ISOBUS network handshaking and establishing communication partnerships with the VT and other ECUs. A user interface for the VT (Figure 5.3) designed using the demo version of ISO-Designer v5.6.1 (Jetter AG, Ludwigsburg, Germany) allows the operator to directly adjust nozzles per camera. After successful handshaking, messages with source or destination IDs made the VT screen visible, enabling the operator to control camera and nozzle ratios through the ISOBUS-compatible VT.

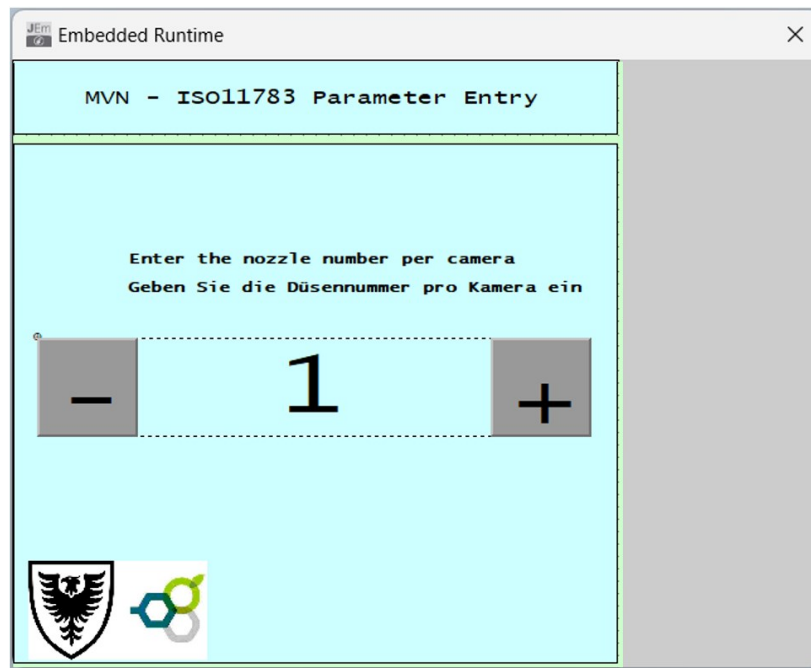


Figure 5.3: Custom user interface for VT designed to enter the number of nozzles controlled by one camera

The Queue stage continuously waits for 42-character fixed protocol messages from any of the clients after the foundational setup is complete. These messages contain information from the cameras of the machine vision system, including Camera ID, Pest ID, pest location in the FOV of the camera, total FOV width, time of detection, and detection completion time. An example protocol message looks as follows:

{01,B,-0216,+0243,1000,1,623,850,684,951,0250} which was developed initially by Motalab & Al-Mallahi (2024). However, a checksum mechanism was additionally implemented in the algorithm to address the low fault tolerance of the Ethernet protocol by verifying the start and end of the message ("{" and "}") and calculating its length. The checksum gets recalculated and compared with the transmitted checksum to confirm that no errors have occurred during transmission. Upon receiving a complete message, all the protocol messages are immediately pushed into a queue.

Thread 1 stage continuously monitors the queue for new messages (Figure 5.4). These messages are processed following the First In First Out (FIFO) principle. Every 40 ms, each message in the queue would be processed to build a nozzle array (A), which governs which nozzle to open across the boom sprayer.

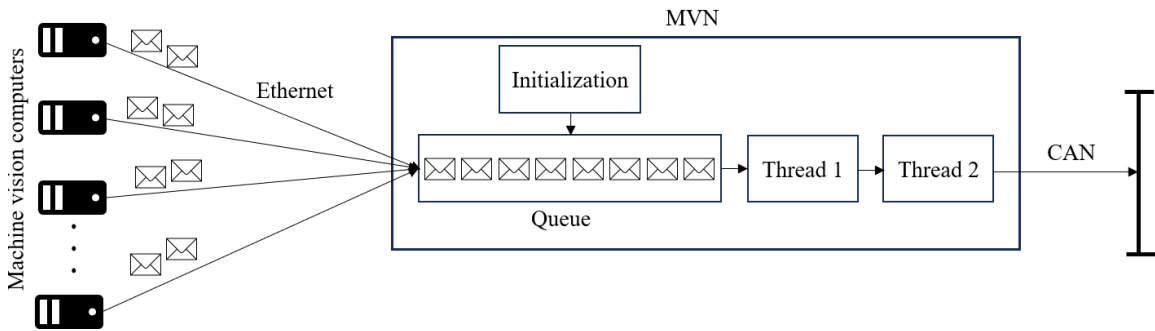


Figure 5.4: MVN queue generation for protocol messages received for machine vision computer, following FIFO

Thread 2 reads and validates the nozzle array and includes them in the memory. In this research work, the MVN was programmed to control up to 64 nozzles of a Pentair rate controller. Since each byte in the CAN data frame controls two nozzles (Pentair HYPRO™, 2019), Equation 5.1 was constructed so that,

$$b_k = (A[2k] \times 10) + (A[2k - 1] \times 160), k = \{1, 2, \dots, 32\} \quad (\text{Eq. 5.1})$$

where b , A , and k represent one byte in the CAN data frame in decimal value, nozzle array, and nozzle index, respectively. Afterwards, Thread 2 creates 4 CAN IDs based on Equation 5.2 starting from the hexadecimal value of 0x18BB961C,

$$G_d = 0x18BB961C + (d \times 0x100), \quad d = \{1, 2, 3, 4\} \quad (\text{Eq. 5.2})$$

where G and d represent the CAN ID and its order, respectively. These four CAN IDs with their data are formatted into CAN frames which get broadcast over the ISOBUS, ensuring seamless communication within the network.

Thread 2 includes an additional feature to adjust the nozzle actuation time based on the tractor speed to ensure that a nozzle would cover the same spraying area and density regardless of speed. To identify the tractor speed, it was required to get the appropriate PGN from the CAN network, as the PGN represents a specific function of the CAN frame. In ISOBUS-compatible tractors, speed data could be found in several PGNs: the Ground-based Speed and Distance (PGN 0xFE49, e.g., CAN ID $0 \times 18FE49FE$), the Wheel-based Speed and Distance (PGN 0xFE48, e.g., CAN ID $0 \times 18FE48FE$), and GNSS-based Vehicle Direction/Speed (PGN 0xFEE8, e.g., CAN ID $0 \times 18FEE81C$), etc. Among these, PGN 0xFE49 was selected to obtain the speed data, as it was the most commonly available on agricultural tractors. The speed data was found in the first and second quadrants of the CAN data and was converted by multiplying by 0.001 per bit to obtain the speed in m/s. When this PGN was received on channel CAN 0 of the CAN expansion HAT, the ECU converted the message to speed data. As a nozzle opening time of 400 ms was found to be

appropriate for optimal spraying at a speed of 6.44 kph (Motalab & Al-Mallahi, 2024), Equation 5.3 was derived to calculate the nozzle opening time,

$$t = C \left(\frac{1}{v} \right), \quad (\text{Eq. 5.3})$$

where t and v are the nozzle opening time in ms and the speed of the sprayer in kph, whereas C is a coefficient equal to 2576 ms.kph. Finally, the program incorporated signal handling for smooth termination and confirmed that all processes were cleanly shut down upon program exit.

5.2.3 Lab Apparatus and Scenarios

To evaluate its performance, the time latency of the MVN was evaluated using an internal program that processed data via Ethernet and measured the interval for reading protocol messages at 40 ms to assess data throughput. After receiving protocol messages from different clients, MVN pushed them to a queue where it was expected that all messages would be stored within 40 ms. The computational efficiency of MVN was tested by timing the processing speed of the onboard algorithm until it sent actuation control commands to CAN. To ensure proper CAN frames were generated, an oscilloscope (DS1102E, Rigol Technology Limited, Beijing, China) was used to observe the signal waveforms from the MVN to assess the signal density and communication timing. The impact of the MVN on the total busload of the ISOBUS network was analyzed using a USB CAN adapter (PCAN-USB, PEAK-System Technik GmbH, Darmstadt, Germany) and its associated software (PCAN-View, V.5.3.0.942, PEAK-System Technik GmbH,

Darmstadt, Germany) focusing on busload variations during normal and peak data transmission phases.

Three ISOBUS networks were set up to test the MVN representing different sprayer manufacturers but with unified communication. After the industry-wide adaptation of ISOBUS, manufacturers developed VT for general acceptance across manufacturers and AEF named it Universal Terminal (UT). The first setup (Figure 5.5a) involved an ISOBUS network controlled by a RAVEN UT (CR7, Raven Industries Inc., South Dakota, US). The second setup (Figure 5.5b) involved a custom-made static sprayer with a Raven rate controller and a VT (AFS-Pro 700, Raven Industries Inc., South Dakota, US). The third setup (Figure 5.5c) used a John Deere 4640 UT, specially designed for older John Deere tractors and mixed fleets. Each device operated on a CAN bus system set to a 250 kbps communication speed, adhering to ISOBUS standards to ensure generalization.

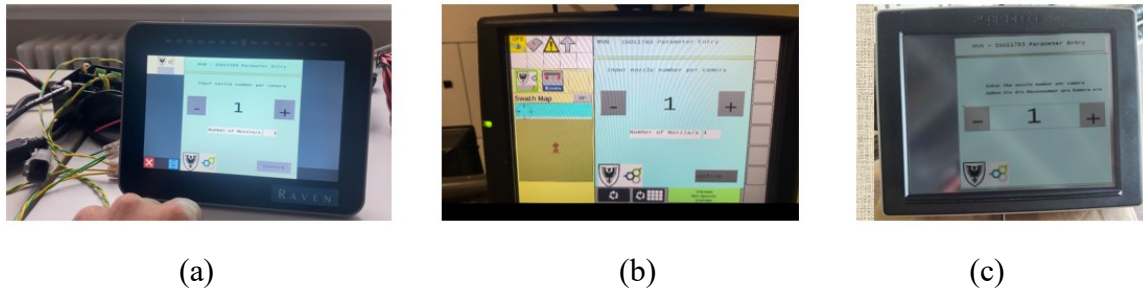


Figure 5.5: Screen view while MVN connected with three VT across different manufacturers: (a) RAVEN CR7 UT, (b) Raven AFS-Pro 700 VT, and (c) John Deere 4640 UT

5.2.4 Field Apparatus and Scenarios

The first field testing involved a full-size boom sprayer (Patriot 3240, Case IH, Wisconsin, USA) with a separate functional spraying system, including two tanks and pumps (Shurflo 2088, Pentair plc, London, UK). This setup was mounted with an AFS Pro-

700 VT, the Pentair rate controller, and 60 Pentair rotating valves (Hypro ProStop-E Single, Pentair plc, London, UK) with nozzles (3D90, Syngenta, Cambridge, UK) positioned parallel to the original boom sprayer at a 55° angle spraying backward with the travel direction. Figure 5.6 provides a visualization of the components of all the setups in terms of their connections on the communication buses. The MVN was tested using 8 machine vision computers (Nuvo-7160GC, Neousys Technology Inc., New Taipei City, Taiwan), each configured to send protocol messages with four different camera IDs, simulating the operation of four connected cameras detecting targets and communicating as actual machine vision systems. In total, the 8 machine vision computers transmitted the equivalent of 30 camera messages simultaneously over the Ethernet network, replicating a full-scale machine vision setup for testing purposes. The MVN generated the CAN frames and transmitted them to the parallel implement bus, i.e., the Pentair system via the CAN 1 channel. Simultaneously, the MVN received speed data from the original implement bus of the sprayer via the CAN 0 channel, enabling it to adjust the nozzle opening duration accordingly.

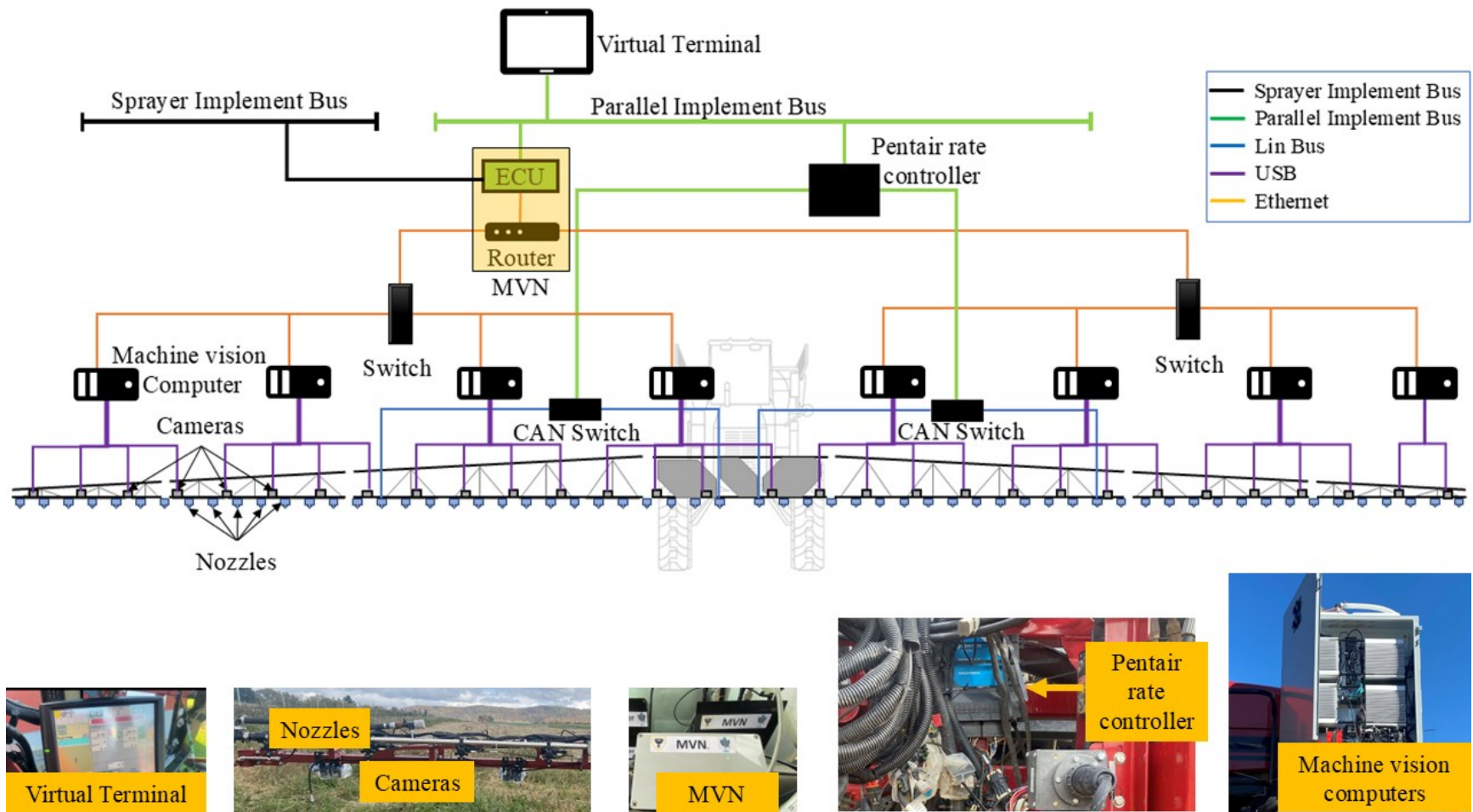


Figure 5.6: Drawing of the CAN-compatible spraying system for the Patriot 3240, MVN mounted and integrated into a Pentair spraying system, controlling 60 nozzles individually

In the second field test scenario, a complete machine vision system to detect weed called hair fescue (Hennessy et al., 2021) was comprised of six OAK-D cameras mounted 0.5 m above the ground. This setup controlled individual nozzles mounted on a UTV equipped with a Pentair spraying system featuring 12 nozzles (Figure 5.7). The angled nozzles sprayed backward similar to the boom sprayer setup to enable timely targeting of the weeds. For field experiments, multiple colour printouts of 3 photos of hair fescue tufts (Figure 5.8) were placed in clear sheet protectors (28.4 cm x 23.5 cm Standard Clear Sheet Protector, Staples, Canada) as target weeds in real-time.

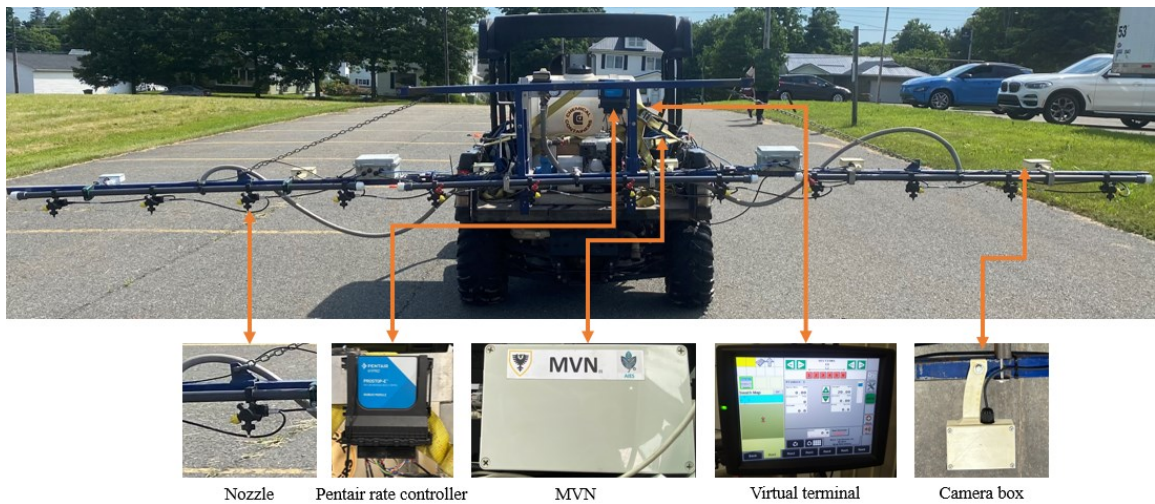


Figure 5.7: MVN mounted on UTV, equipped with Pentair spraying system, controlling 12 nozzles through a machine vision system comprising 6 cameras

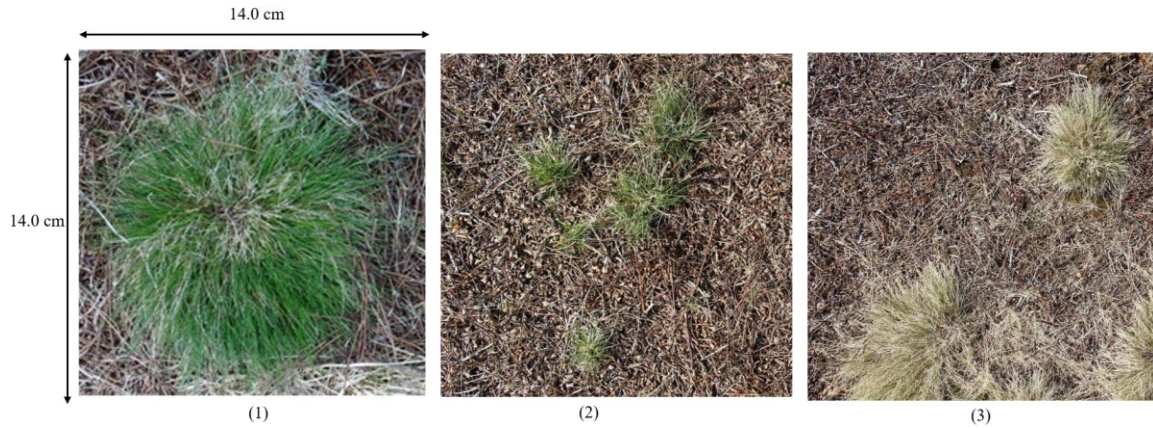


Figure 5.8: Three different images of Hair Fescue for field experimental detection with UTV setup

Using this configuration, experiments were conducted to explore various target distribution patterns simulating common weed distributions in agricultural fields. These patterns included individual targets, intersections (objects located between two cameras FOV), sequential activations (nozzles were activated one after another), wide/bulk distributions (clusters of targets), and elongated targets (aligned with the direction of the UTV), as shown in Figure 5.9.

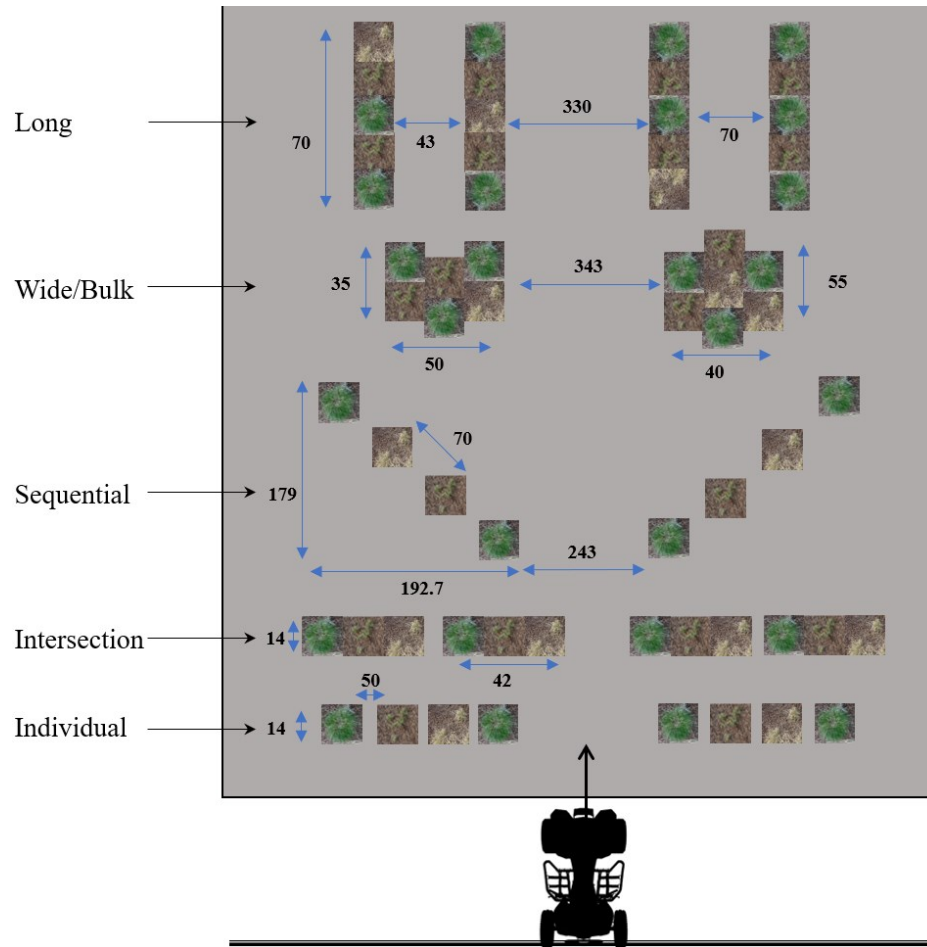


Figure 5.9: Target distribution on the ground, showing distances in cm, for the MVN field test

The experiment took place in an open testing area at the Dalhousie Agricultural Campus (Truro, Nova Scotia, Canada) and involved three different speeds: Speed 1 (3.22 kph), Speed 2 (6.44 kph), and Speed 3 (9.66 kph). These speeds represented typical operational ranges for UTV across blueberry terrain allowing us to evaluate the MVN functionalities in establishing successful communication between the machine vision system and the ISOBUS to hit the target accurately.

5.3 RESULT AND DISCUSSION

5.3.1 ECU Algorithm Performance

The MVN time latency was evaluated across three phases focusing on its ability to handle high frequency data and ensure timely responses in precision spraying tasks. During the Ethernet communication phase, 30 protocol messages were processed within 40 ms demonstrating the capacity of the system to handle multiple simultaneous data streams from 8 computers without significant latency. Here queue management played a crucial role in maintaining real-time data flow.

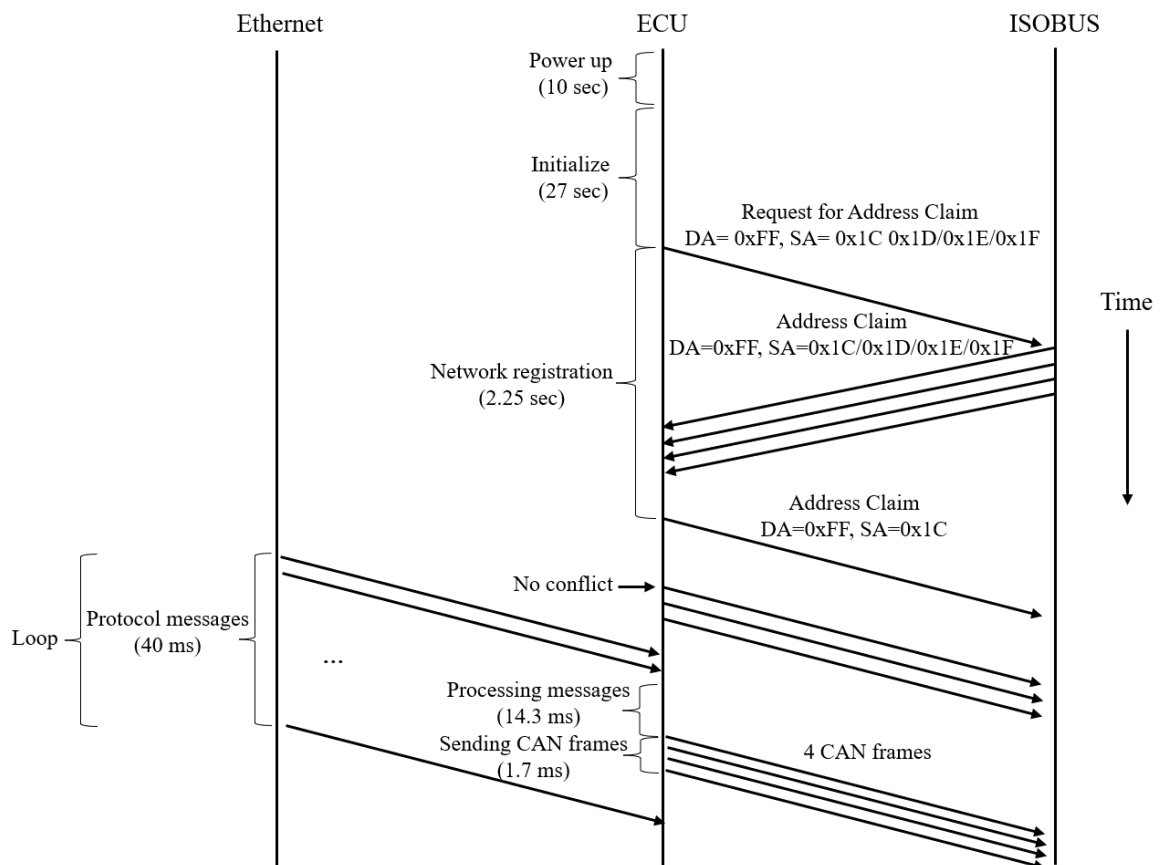


Figure 5.10: MVN timeline performance showing Ethernet communication, message processing, and CAN frame transmission

In the second phase, the MVN successfully read and processed all protocol messages queued within the 40 ms window demonstrating that the memory resources were sufficient to handle bursts of incoming data as depicted in Figure 5.10. In the third phase, the overall processing time was evaluated from receiving the protocol messages to generating and transmitting CAN frames. The MVN took 14.3 ms to process the protocol data into a 60-nozzle array and an additional 1.7 ms to create and send four CAN frames to the network. The total time of 16 ms for the complete operation ensured that the system remained responsive and stayed well within the targeted 40 ms window. This time was further optimized using the message queue, threaded programs, and memory management.

The oscilloscope waveform in Figure 5.11 illustrates the CAN signal voltage level generated by the MVN. The signal alternates between the dominant voltage level of 3.5 V and the recessive voltage level of 2.5 V. The interval between successive pulses is measured at approximately 4.4 μ s corresponding to a frequency of 69.4 kHz, highlighting the high frequency and dense signal transmission. This consistent timing demonstrates the ability of MVN to efficiently generate and transmit CAN frames, enabling faster data communication. The observed waveform reflects the capability of the MVN to handle higher data throughput with stable and precise signal generation, which is key for real-time applications.

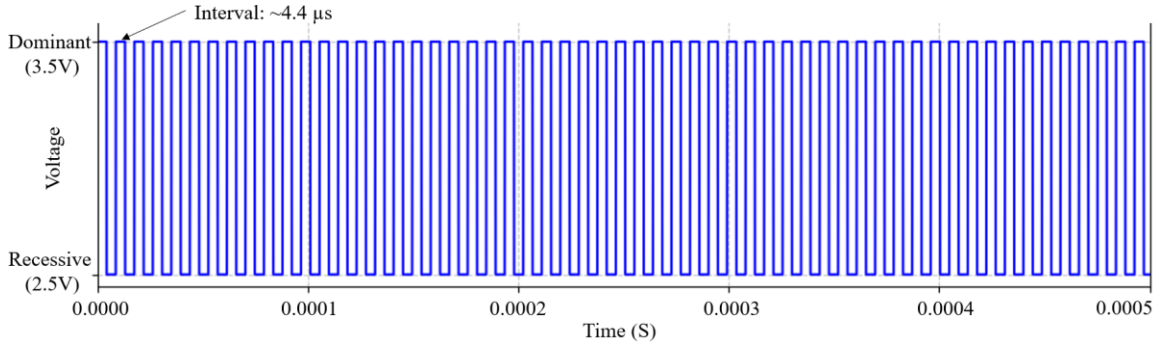


Figure 5.11: Oscilloscope signals of CAN frame transmission the MVN

When the MVN was tested across three different ISOBUS VT/UT setups, it was consistently connected and displayed successfully. Table 5.1 summarizes the time it took for each VT/UT to display the interactive screen. These results confirmed that the MVN could connect and display successfully across different VT/UT systems, with varying times for the display to pop up depending on the VT/UT, confirming its compatibility with ISOBUS.

Table 5.1: Time taken for MVN to display on various VT/UT across different setups

Setup VT/UT	With implement?	Displayed on VT?	Time to display (Sec.)
Raven CR7	No	Yes	58
Raven AFS PRO700	Yes	Yes	51.5
John Deere 4640	No	Yes	70

5.3.2 Busload Analysis

The CAN busload performance evaluation and comparison of the algorithms depending on the frequency and increased CAN frames to control a higher number of nozzles are shown in Figure 5.12. In this figure, ISOBUS handshaking messages were excluded to ensure a consistent basis for comparison focusing solely on actuation CAN

frames over 10 min. When sending one CAN ID every 400 ms the average busload was 0.15 %, which increased to 1.47 % when the CAN ID was sent every 40 ms.

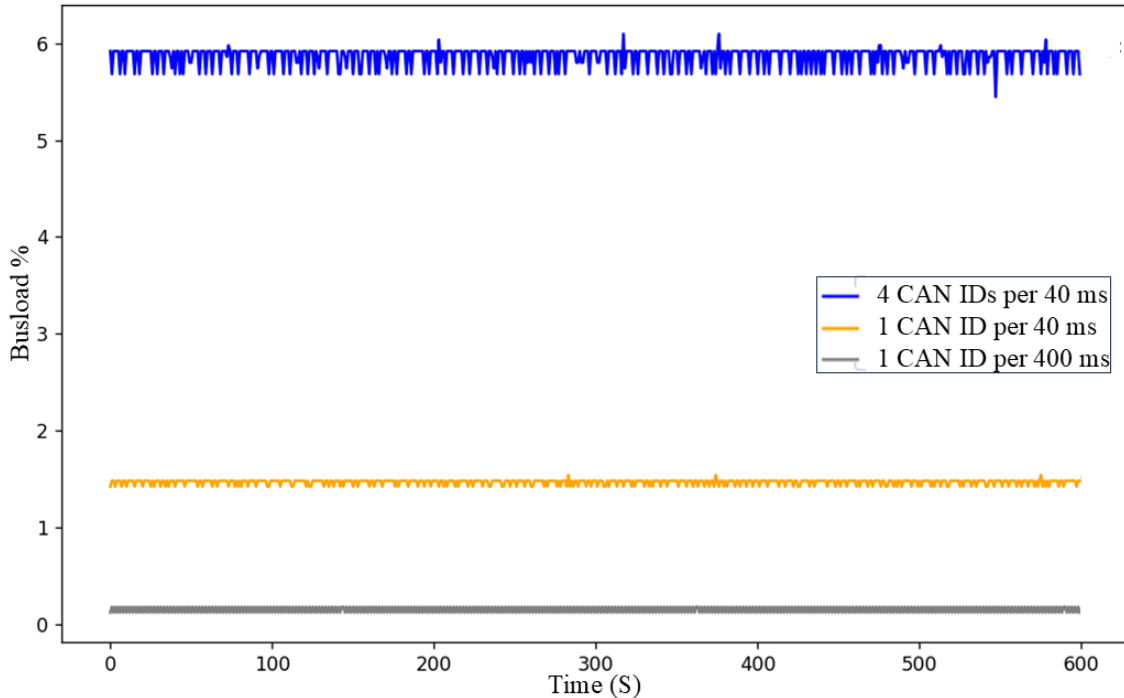


Figure 5.12: MVN busload performance comparison at different numbers of CAN frames and their frequency

The highest busload was observed when the algorithm generated four CAN IDs within 40 ms to manage the control of 60 nozzles. This configuration resulted in a significantly higher busload of 5.86 % indicating the increased traffic on the CAN bus due to the higher quantity of CAN frames required to control a greater number of nozzles. This signified the possible minimum busload added to the network to control up to 64 nozzles, highlighting the trade-off between message frequency and busload.

The graphs in Figure 5.13 represent the busload performance for 10-min evaluation of the two different spraying systems tested in this research work. The 60-nozzle system on the boom sprayer showed a busload that peaked at the initialization at approximately 25

% and before dropping to approximately 22 % at steady state. While the baseline busload was measured at 16.1 % at steady state due to all components broadcasting on the network, integrating the MVN added 5.86 %. The MVN successfully controlled all nozzles processing 450,000 protocol messages that were randomly generated from the 8 machine vision computers and transmitted over Ethernet. It handled a minimum of 30 protocol messages within every 40 ms interval achieving a 100 % success rate in real-time nozzle control.

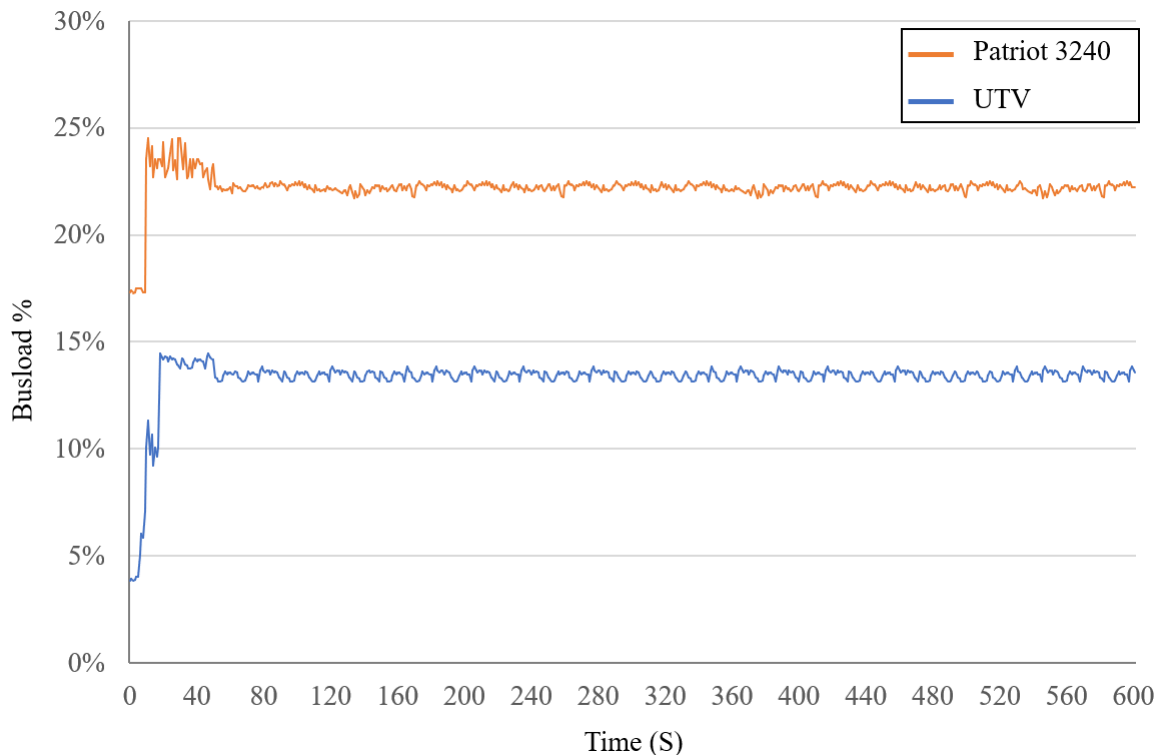


Figure 5.13: ISOBUS load performance during a 10-min evaluation of the two different spray systems, on Patriot 3240, and the UTV

On the other hand, the busload of the 12-nozzle system on the UTV, where the Pentair rate controller and VT initially occupied 7.44 % of the busload. Adding the MVN increased the busload to 13.30 %. Also in this experiment, the MVN successfully controlled the

sprayer, responding to 6 protocol messages within 40 ms with a 100 % success rate. For both cases, the implement busload remained within the acceptable 45 % limit.

5.3.3 Field Implementation Analysis

Table 5.2 summarizes the results of running the UTV three times at each speed while spraying on targets with different distributions. In the final field experiment, the MVN adjusted the nozzle opening time based on UTV speed, ensuring consistent spray length across all speeds. The goal was to maintain uniform spray coverage regardless of vehicle speed by varying the nozzle opening time. At Speed 1, for both individual and intersection targets, a buffer spray of approximately 28.76 cm was applied on each side. This buffer remained consistent at higher speeds, with nozzle opening time reduced for Speed 2 and Speed 3. Despite this reduction, the spray length remained the same for individual and intersection targets across all speeds, demonstrating the success of MVN in adjusting for speed changes.

Table 5.2: Unified spraying areas at different distributions of objects and different speeds

Distribution Type	Target Area Length (cm)	Speed 1	Speed 2	Speed 3
		Spray length (cm)		
Individual	14	71.52	71.52	71.52
Intersection	14	71.52	71.52	71.52
Sequential	179	329	329	329
Bulk	35	95	95	95
Long	70	200	200	200

For larger target distributions, such as sequential, bulk, and long, the MVN dynamically adjusted the nozzle opening time to maintain consistent spray lengths across

all speeds. This confirmed the ability of the algorithm to control nozzle timing and maintain uniform coverage.

While the dynamic nozzle adjustment improved spot spraying precision, it led to a fixed spray length, potentially causing slightly higher spray coverage than desired. Additionally, spray density varied inversely with speed. Slower speeds resulted in denser spray, while faster speeds resulted in less dense spray. This variation presents a potential drawback to achieving consistent spray density across different speeds, even when the nozzle opening time is adjusted. Future improvements could focus on addressing this issue by controlling the pressure and flow rate on the boom, ensuring uniform spray density regardless of speed. However, compared to a uniform distribution approach this method significantly reduced overall spray usage.

5.4 CONCLUSION

The novel ISOBUS-compliant MVN introduced in this study was able to integrate multiple machine vision systems to wide boom sprayers, enabling individual nozzle control for real-time spot spraying on different targets through hybrid communication. The MVN was capable of communicating with both the implement bus and machine vision systems, efficiently managing high-frequency protocol messages with minimal latency. This was achieved by incorporating a client-server threaded program, along with checksum verification and message queuing. The ability to dynamically adjust nozzle opening times based on sprayer speed ensured consistent spray coverage, reducing overspray and optimizing resource use. The MVN maintained a high but uniform busload distribution, staying within the standard busload threshold. The key findings highlight the capability of

the MVN to handle a minimum of 30 messages within 40 ms via the Ethernet protocol used in the system processes to control 60 individual nozzles. The ability of MVN to adapt to real-time speed variations optimized spray usage and ensured coverage of all detected targets.

The compliance of MVN with ISOBUS systems across various VTs demonstrated its versatility and adaptability in different setups, highlighting its potential for widespread adoption in PA. Future improvements could focus on further field trials in actual spraying using pesticides for the final evaluation of performance on wide boom sprayers. The MVN offers a scalable solution for PA, capable of converting real-time spot spraying of pesticides on wide boom sprayers based on machine vision into reality.

CHAPTER 6: DEVELOPMENT AND INTEGRATION OF A PARALLEL CONTROLLER AREA NETWORK BUS FOR SPOT SPRAYING

6.1 OVERVIEW

This chapter presents two essential ECUs: 1. CAN filter, and 2. data logger for integrating additional communication and capturing components into sprayer systems. The CAN filter ECU reduces busload by selectively forwarding only essential CAN messages, such as GNSS position and ground speed, to the implement bus. The data logger ECU captures all CAN bus communications, enabling verification and analysis of sprayer activities. The integration of machine vision technology, involving 30 cameras, eight computers, and hydraulic systems including diaphragm and roller pumps, introduces significant power challenges. Due to these high-power demands, the existing power infrastructure was upgraded with a secondary alternator and battery pack to ensure reliable operation under maximum load conditions. The chapter concludes by outlining a comprehensive architecture for seamless operation for machine vision-based spot spraying.

6.2 CAN FILTER AND DATA LOGGER ECU DEVELOPMENT

The CAN filter ECU is responsible for filtering critical information, such as speed and geographic coordinates, from the sprayer default implement bus and transmitting this filtered data to the parallel implement bus, specifically the Pentair system. By enabling real-time data transfer, the CAN filter ECU ensures that the sprayer can access and utilize vital operational parameters for accurate spraying. On the other hand, the data logger ECU captures all CAN messages from the Pentair ISOBUS system and stores them in a structured database. This provides a reliable record of operational data, enabling post-field

analysis and contributing valuable insights into the long-term impact of precision application in pest management.

The implementation of these ECUs marks a significant step forward in the development of a comprehensive machine vision-based spot spraying system. By bridging the communication gap between the existing sprayer CAN bus and the parallel Pentair ISOBUS network, the CAN filter ECU transfers essential operational data flawlessly. Simultaneously, the data logger ECU provides the necessary infrastructure for data analysis and future research, enabling continuous improvement of precision spraying technologies.

6.2.1 Hardware of the ECUs

The CAN filter and data logger ECUs as shown in Figure 6.1, consist of an integrated electronic system capable of synchronized and simultaneous management of the CAN communication protocol.

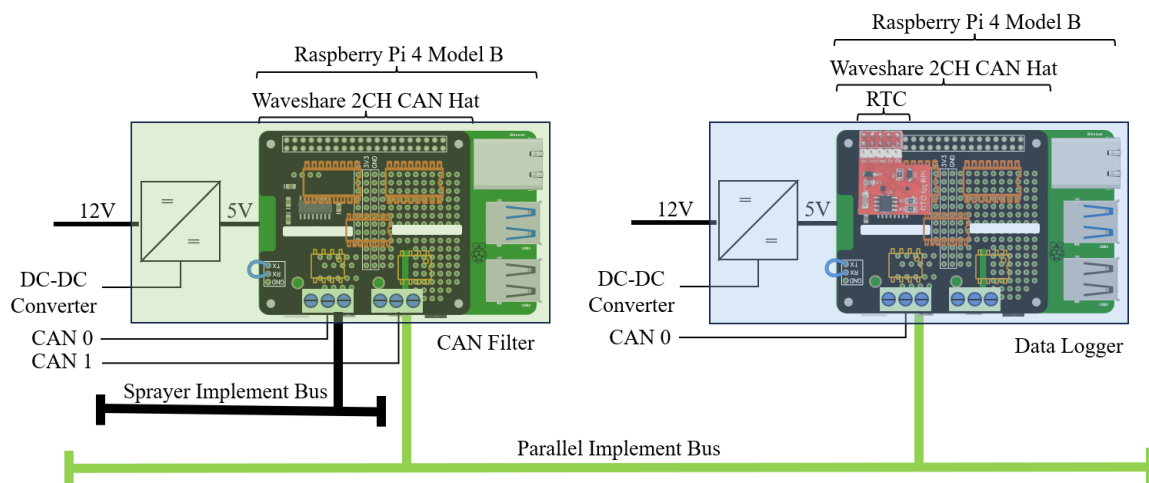


Figure 6.1: Two ECUs CAN filter and data logger, both using RPi4 and 2 channel CAN expansion hat. CAN filter connected with both busses to exchange information between them. Data logger acquiring all the CAN data from the Pentair system.

The ECUs are implemented on an RPi 4B platform, powered by an ARM Cortex-A72 processor. The RPi is equipped with a 2-Channel CAN bus expansion HAT (Waveshare, Shenzhen, China), which provides a dual isolated CAN bus interface that supports CAN2.0 communication, facilitating reliable connectivity with ISOBUS networks. For both ECUs, the hardware configuration remains almost the same, with specific functional distinctions in channel usage. The CAN filter ECU utilizes both channels CAN0 and CAN1 of the CAN HAT. CAN0 is connected to the implement bus of the boom sprayer filter specific data elements such as speed and georeferenced information, some of them are transmitted from the tractor bus through the TECU to the sprayer default implement bus. The filtered data is then communicated to the Pentair rate controller i.e. parallel implement bus via the second channel CAN1, thus it can maintain instant data transmission. In contrast, the data logger ECU reads all CAN messages through its CAN0 channel exclusively from the Pentair ISOBUS system and stores these messages in a local database for future research and analysis. A Real Time Clock (RTC) expansion module (Seeed Technology Co. Ltd. Shenzhen, China) powered by a DS1307 chip (Maxim Integrated Products, Inc., California, US), is integrated with this ECU to provide accurate timekeeping, as the RPi4 lacks an onboard RTC. This ensures that the data logger captures CAN messages and every entry in the database is stamped with the timestamp for the reliability of data tracking. Both ECUs are powered by a 12V to 5V DC-to-DC converter which converts the 12V supply from tractor to 5V, meeting the power requirements of the RPi.

6.2.2 Software for the ECUs

In the software for the CAN filter ECU, both CAN0 and CAN1 channels are activated initially to establish connections with the relevant buses. The software uses a predefined code dictionary to identify which PGNs to filter from CAN0 and relay to CAN1, providing flexibility to adjust filtering by adding or removing PGNs without modifying the main software. For our setup, the software is configured to discard all incoming CAN messages from CAN0 except those listed in the dictionary, ensuring that only the specified PGNs are retained and sent to CAN1. The key PGNs filtered and transferred include ground-based speed and distance (65097 or 0xFE49, e.g., CAN ID 18FE49FE), wheel-based speed and distance (65096 or 0xFE48, e.g., CAN ID 18FE48FE), GNSS based vehicle direction/speed (65256 or 0xFEE8, e.g., CAN ID 18FEE81C), vehicle position (65267 or 0xFE3, e.g., CAN ID 18FEF3F0), time and date (65254 or 0xFEE6, e.g., CAN ID 18FEE626), precise GNSS data (61184 or 0xEF00, e.g., CAN ID 14EF1CCD), and additional precise GNSS data (44032 or 0xAC00, e.g., CAN ID 0CAC1C13). As soon as the software detects specified PGNs on CAN0 and redirects them to CAN1 in real-time, ensuring unified data flow and robustness against source or destination ID changes, as PGNs remain consistent across different tractor models, preserving compatibility.

The data acquisition and logging methodology for CAN messages in this research involved setting up a structured system to capture and store all incoming messages from the Pentair CAN network on the sprayer. Initially, the software activates the CAN1 channel to establish a connection with the appropriate bus. Each incoming CAN message was received on the CAN1 channel, and key message parameters such as the timestamp, DLC CAN ID, and CAN data were captured. For data storage and retrieval, all CAN data was

logged into MySQL (Oracle Corporation, Texas, US), an open-source relational database management system. MySQL was selected for its scalability and flexibility, enabling future use of the data for comprehensive farm management applications. To facilitate database management, an additional open-source administration platform, phpMyAdmin, was implemented. This platform allowed easy access and monitoring of logged data, providing a user-friendly interface to query, review, and export data for further analysis.

6.2.3 Evaluation and Discussion

Our ECU setup on the boom sprayer includes the CAN filter and data logger, as illustrated in Figure 6.2, which details the architecture of the complete machine vision based spot application system. Alongside other ECUs, these two components are essential for enabling machine vision-based spot spraying. The primary role of the boom sprayer CAN network in this configuration is to supply necessary speed and location information, which is subsequently relayed to the Pentair system via the CAN filter ECU. Notably, the CAN filter and data logger ECUs do not possess ECU IDs, as they are designed to operate without registering on the implement bus network, in contrast to the other ECUs within the system. All ECU IDs do not resemble to physically separate units, for instance, in the Pentair system IDs 0x97 and 0x97 representing Segment 1 and Segment 2, both originate from CAN Node 1. Similarly, IDs 0x98 and 0x99 representing Segment 1 and Segment 2 originate from CAN Node 2.

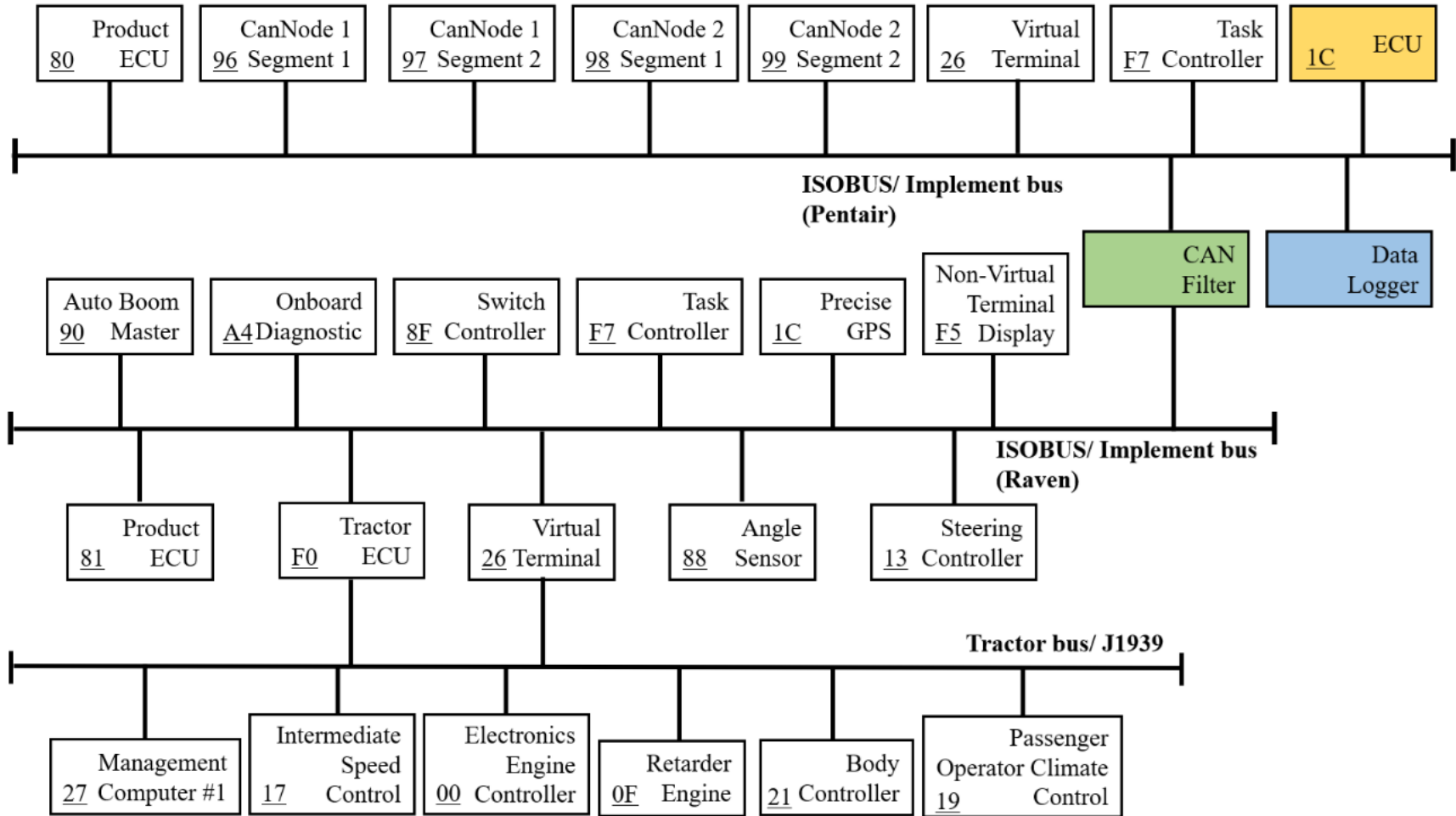


Figure 6.2: BUS connection of the ECUs on the Case IH Patriot 3240 CAN network for spot spraying

The CAN filter ECU functioning as an intermediary like the TECU connects the Raven and Pentair systems by filtering and transmitting 8 required PGNs (8 extended CAN frames), contributing only 3.81% busload to the 250 kbps ISOBUS of the Pentair system while bridging the two networks. This has been observed that ISOBUS-compatible MVN and the precise GNSS module, both assigned the ECU ID 0x1C, will not encounter message conflicts since each device is associated with a unique PGN, making their CAN IDs distinct. Additionally, as described in Chapter 6, at the start of the system this MVN initially attempts to claim the address 0x1C. If unsuccessful, it will sequentially attempt alternative IDs: 0x1D, then 0x1E, and finally 0x1F if previous attempts fail. The data logger module underwent rigorous lab testing with emulators generating extended CAN messages at a 95% busload, successfully capturing all messages from the network. Upon deployment on the boom sprayer (Figure 6.3), the data logger recorded a total of 3.27 GB of CAN data from the Pentair network for the summers of 2023 and 2024.

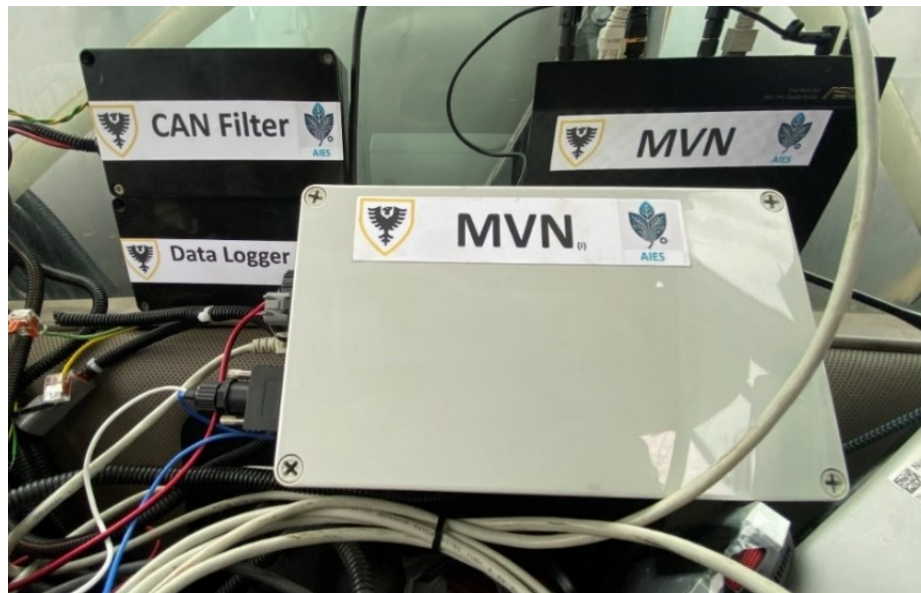


Figure 6.3: ISOBUS compatible ECU including a router (marked MVN), CAN filter and data logger deployed in the cabin of Patriot 3240

This extensive dataset is thoroughly managed using MySQL. However, accessing and processing this volume presented challenges; the RPi4 lacked the processing capacity for such a load, often resulting in system hang-ups or reboots. A standard computer was able to handle the data without issues. Notably, a successful attempt was made to store this data in a cloud-based MySQL database, suggesting that in the near future, real-time field data from this sprayer could be directly uploaded to the cloud for more accessible and scalable storage solutions.

6.3 COMPREHENSIVE COMMUNICATION ARCHITECTURE TOWARDS MACHINE VISION BASED SPOT APPLICATION

The complete communication architecture of this research for the integration of multiple machine vision towards spot application depicted in Figure 6.4 which is an enhancement of Figure 6.2, illustrates the comprehensive communication architecture for a machine vision-based spot spraying system implemented on the boom sprayer with a parallel 60-nozzle valve spraying system operating in parallel with the existing spraying system. This setup integrates three custom ECUs with 60 nozzle valves, controlled by a robust machine vision network.

In this setup, eight computers with 30 cameras are strategically placed to manage spot-specific spraying. Each camera monitors multiple nozzle sections, enabling targeted application across the field. The MVN acts as the central unit, coordinating nozzle control based on camera data, while integrating with the Pentair ISOBUS network. This system optimizes machine vision use and reduces costs by minimizing the number of cameras and computational resources needed for full coverage.

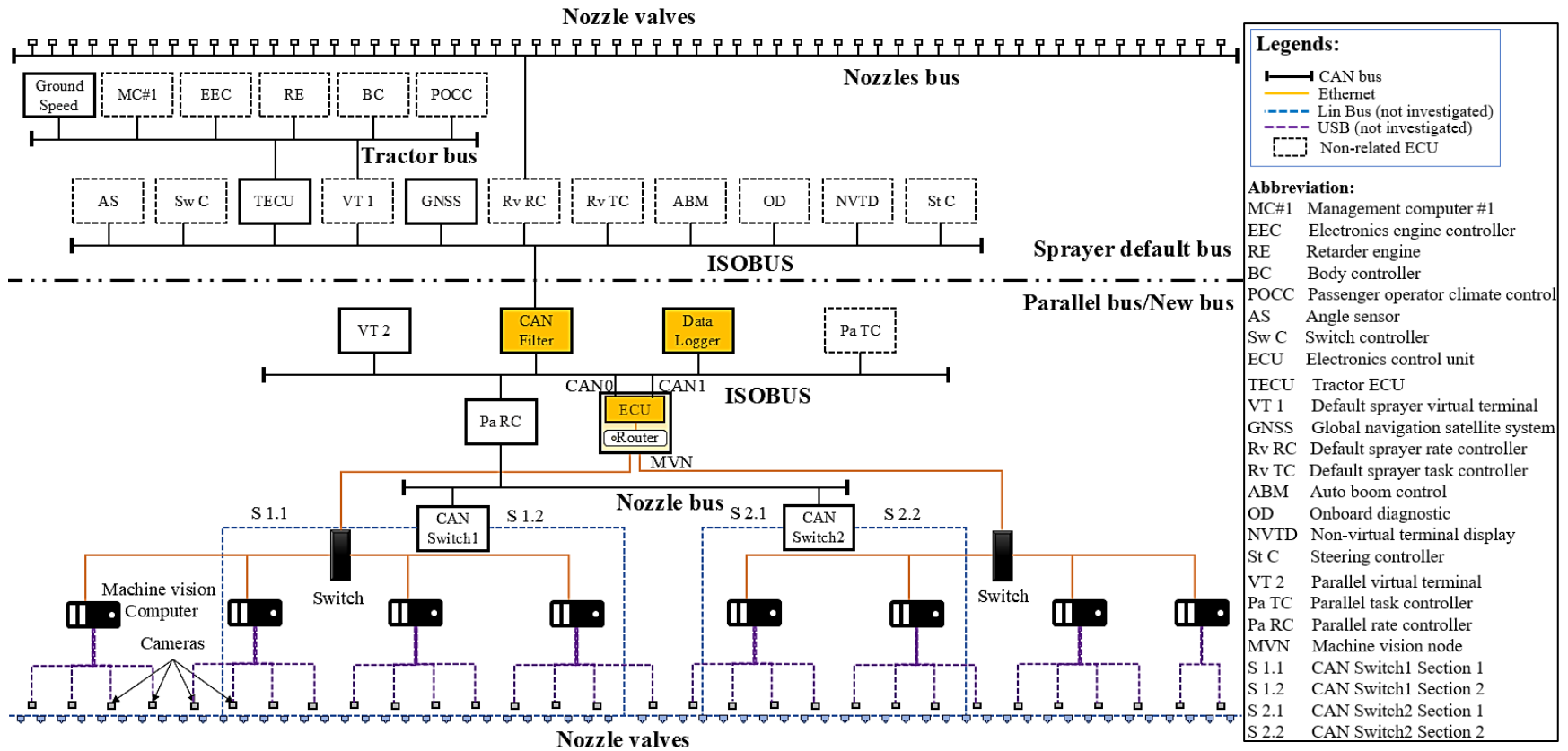


Figure 6.4: Overall network architecture for machine vision-based spot spraying

The network layout incorporates multiple communication buses, enabling uninterrupted data flow between components. The green lines represent the ISOBUS network of the Raven system, while the Pentair ISOBUS network is shown in parallel. Ethernet lines connect the machine vision components, allowing high-speed data exchange between computers and cameras. Additionally, USB connections facilitate device integration on the computers, while LIN buses connect each nozzle control segment with the CAN Nodes. These CAN Nodes are essential for maintaining communication integrity, as they allow the synchronized control of nozzle valves along the boom, ensuring timely activation based on the detected target.

Overall, this architecture not only supports machine vision-based spot spraying but also provides a scalable framework to accommodate future upgrades in PA technology. The data logger ECU captures and stores all message traffic on the Pentair system, enabling post-field analysis, while the CAN filter ECU facilitates the transfer of critical vehicle data (such as speed and location) between the Raven and Pentair networks, ensuring coordinated and spraying operations.

6.4 INVESTIGATION OF ELECTRICAL REQUIREMENTS ASSOCIATED WITH MOUNTING SPOT APPLICATION SYSTEM

To achieve spot spraying compatibility, the detection and spraying mechanisms can be scaled to cover full booms by integrating the Pentair ISOBUS system with 60 Hypro nozzle valves in parallel with the boom sprayer. In addition to leveraging advancements in detection and communication components, the next steps involve enabling real-time spraying through modifications to the pumping and nozzle systems. This setup also

requires additional components such as computers, multiple cameras, and several pumps to support a machine vision-based spot spraying system. Given these added requirements, the existing power system of the boom sprayer may not be sufficient. Therefore, a detailed power calculation is essential to assess and ensure adequate power availability.

6.4.1 Power Requirements of ISOBUS system

In this section, the power requirements have been analyzed for the Pentair system. Various calculations and observations were made on multiple components, including nozzle valves, product controllers, VT, and associated sensors. A multimeter (HT118A, Kaiweets Technology Limited, Hong Kong, China) whose range is less than 10 A was used to measure the voltage drop and current consumption across various system components on several setups, helping to understand power needs under different operational scenarios.

Initially, all relevant components within each system were identified, allowing for specific power contribution measurements of each unit. The power consumption of individual components was measured using the multimeter placed between the battery and the series line. An incremental approach was used, adding or removing components to isolate their current draw. Maximum current and voltage values were applied to calculate peak power consumption under full load, providing a detailed understanding of the power needs for both sprayer systems during operation.

It has been observed that upon activation of the Pentair spraying system, all Pentair nozzle valves are immediately powered, establishing a baseline current consumption. The current demand of the system increases linearly with each additional nozzle valve

connected via the CAN node. When the nozzle valves are activated, a small spike in current occurs. After the activation, the current level quickly returns to the baseline. The current spike ranges between 0.11 A and 0.13 A were observed during nozzle activation. A current spike of 1.95 A was observed when turning off the nozzles. The average current during normal operation was 1.77 A. The maximum current increase when shutting down the system was 0.18 A increase.

Additionally, upon initiating the full system an instantaneous surge in current was measured. Specifically, the current spike at startup for all components, excluding the nozzles was calculated as the difference between the maximum startup current of 2.82 A and the normal operating current without a nozzle valve load of 1.21 A, yielding a starting surge of 1.61 A. Similarly, during the process of turning off all nozzles, a current increase was recorded over multiple iterations. The maximum observed current increase for deactivation was calculated at 0.19 A, derived from the difference between the peak current spike of 1.95 A. Table 6.1 below summarizes the maximum current and power consumption across key components of the Pentair spraying system. In total, the system exhibits a maximum of 2.82 A, equivalent power consumption of 33.84 W under full load, without nozzle valves.

Table 6.1: Maximum current and power consumption for key components of the Pentair system

Consumption measurement	Product Controller	VT	CAN Node	System loss	Total
Max. Current (A)	1.23	0.74	0.59	0.26	2.82
Max. Power (W)	14.76	8.88	7.08	3.12	33.84

For a 60-nozzle Pentair setup on the sprayer, the power requirements increase due to the additional components and the parallel structure needed to support the full nozzle array. This configuration comprises one Hypro ISOBUS Rate Controller, a VT, two CAN Node modules, and 60 individual nozzle valves. Since the system requires extra CAN Node modules to manage 60 nozzles, each CAN Node consumes 7.08 W, resulting in a combined consumption of 14.16 W. Additionally, the system aspects slight power losses i.e. 4.9 W during signal transmission. The main power draw comes from the 60 ProStop-E nozzles themselves. Based on the analysis from a 12-nozzle system, each nozzle valve draws approximately 0.53 A at 12 V when in full operation. Extrapolating this to a 60-nozzle setup, the nozzles collectively draw around 31.80 A or approximately 381.6 W of power solely for nozzle operation when all are activated simultaneously. Summing these values gives the estimated total consumption for the 60-nozzle Pentair setup approximately 35.36 A on a 12 V line, equivalent to 424.2 W of power. This setup assumes that all nozzles are open simultaneously, reflecting the maximum power scenario. Now, the power requirements need to calculate for the machine vision cameras, computers and pumps to estimate the total power needed for the complete setup.

6.4.2 Power Requirements for Machine Vision and Hydraulics Components

For a successful spot-specific sprayer with ISOBUS-compatible spraying implements, the integration of a machine vision detection system and a hydraulics system is essential. The machine vision system comprises a combination of high-resolution cameras and computers, while the hydraulics system primarily includes pumps, flow control devices, and pressure sensors. Compared to the ISOBUS spraying system, these

components demand a substantial power supply, particularly due to the number of computers and pumps required for comprehensive operation.

When deploying multiple cameras, the cumulative power requirements increase significantly. Following the field deployment methodology of Chapter 5, where each camera controls two nozzles for optimized coverage, a minimum setup of 30 cameras is necessary to manage 60 nozzles. Each computer in this setup is capable of controlling up to 4 cameras, leading to a total requirement of 8 industrial computers (IPC) (Nuvo-7160GC, Neosys Technology Inc., New Taipei City, Taiwan) to handle the machine vision system. Four computers are mounted within a customized box, with two IPC boxes placed on each side of the sprayer. Each box is designated for mounting IPCs and holds four IPCs (Nuvo-7160GC, Neosys Technology Inc., New Taipei City, Taiwan), a six-port switch (Xelity 6TX, Murrelektronik Inc., Georgia, US), and fifteen external video capture cards (HCA26P, Kuhaimi Electronics Co., Shenzhen, China). Additionally, to maintain adequate pressure across different sections of the boom, a total of nine pumps are required. Two types of pumps are used: six diaphragm pumps (5059-1311-D011, Pentair plc, London, UK) and three roller pumps (4001N-E2H, Pentair plc, London, UK).

To enable spot-specific spraying, the integrated ISOBUS-compatible setup requires a machine vision detection system and a hydraulics system to manage real-time nozzle control. The machine vision system consists of camera boxes that each include an RGB camera, a microcontroller, a servo motor, and a 12-5 V DC-DC power converter. Each camera box operates at a peak current of 0.32 A at 12 V. Given the configuration of 30 camera boxes in this setup, the cumulative peak power demand of these components is

significant. In addition to the cameras, eight computers are required to handle the data from the cameras. Each computer draws up to 20.2 A during high-load operations, such as startup and intensive image processing for spot detection.

Meanwhile, a 150-litre auxiliary water tank mounted on each side of the sprayer connected with pumps for hydraulic flow. Each diaphragm pump is capable of drawing up to 14 A, and each roller pump can also draw up to 27 A under peak conditions (Pentair HYPRO, 2024). The total power requirement for all six diaphragm pumps is 1,008 W, and for all three roller pumps combined, the total power requirement amounts to 972 W. Altogether, the nine pumps require 1,980 W to operate at peak performance. The following table (Table 6.2) summarizes the peak current and power requirements for each component in the setup. The total peak power requirement for this machine vision and hydraulics setup is approximately 4,043.4 W.

Table 6.2: Peak current and power requirements for machine vision components and pumps

Component	Peak Current per Unit (A)	Number of Units	Total Peak Current (A)	Power (W)
Camera Boxes	0.32	30	9.6	115.2
Computers	20.2	8	161.6	1939.2
Diaphragm Pumps	14	6	84	1,008
Roller Pumps	27	3	81	972
Total			336.2	4034.4

Here, it is important to note that the six diaphragm pumps are not expected to run continuously at peak power. Once the boom pressure reaches the required level, these pumps will turn off to maintain efficient power use. Similarly, the roller pumps may not

need to always operate at full capacity, as they will adjust based on the specific application demands of the sprayer. This setup helps optimize power consumption and reduces unnecessary energy use during operation. To support this level of additional power on the boom sprayer, a separate power source is necessary. An additional dynamo, coupled with a battery bank, will ensure a continuous power supply during field operations, facilitating the uninterrupted performance of the machine vision and hydraulics systems.

6.4.3 Power Source and Modifications

The default alternator in the boom sprayer provides sufficient power to operate all existing components and parallel implements with some additional capacity for a few more ECUs as add-ons. However, the machine vision system and hydraulic pumps require significantly more power, necessitating a secondary power source. A suitable option is an additional alternator (A0014962PA, Leece-Neville, Ohio, US) rated at 14 V, 320 A (operating at 13.8 V, 320 A) was selected, delivering up to 4,416 W sufficient for high-power demands. The additional alternator was mounted alongside the default unit (Figure 6.5), requiring repositioning to optimize RPM transfer. The added alternator powers a dedicated battery pack, independent of the main system.

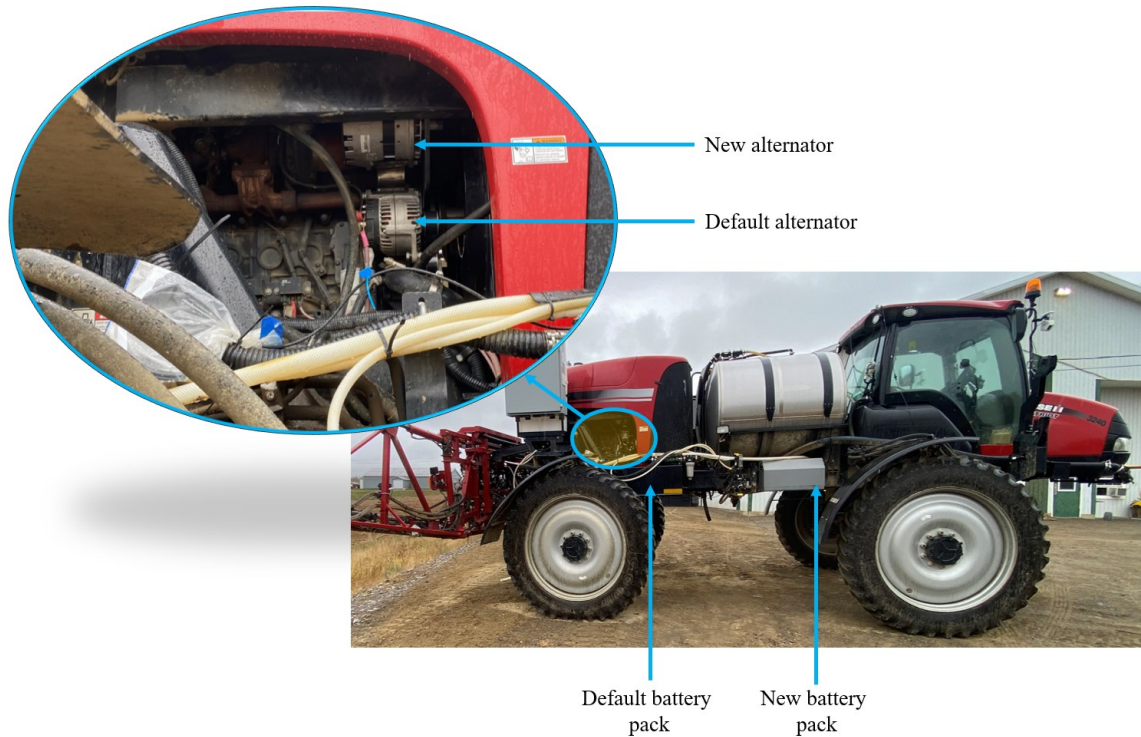


Figure 6.5: Integration of new alternator and battery pack with boom sprayer for enhanced power supply

Both the default and newly installed power sources are essential for managing the machine vision-based spot application system. The parallel implement is powered by the default source, sharing the same ground. All ECUs controlling this implement also rely on the default power source, drawing 424.2 W (35.36 A at 12 V) via the sprayer's in-cabin three-pin power connector. Meanwhile, the machine vision and pump systems, requiring 4,034.4 W (336.2 A at 12 V), are powered exclusively by the new alternator and battery setup, ensuring a stable and independent supply.

6.5 CONCLUSION

The integration of additional ECUs and an enhanced power system in the boom sprayer advances PA by enabling continuous data exchange and reliable post-field analysis. The CAN filter and data logger ECUs bridge communication between the sprayer default implement bus and the parallel implement network, ensuring accurate machine vision-based spot spraying. Addressing the power demands of advanced agricultural systems, the redesign included a secondary alternator and battery pack to support the machine vision system, hydraulic components, and additional ECUs. These modifications ensure reliable operation under full load conditions. Overall, this work demonstrates the feasibility of integrating advanced technologies into existing agricultural equipment, offering scalable solutions for modern farming.

CHAPTER 7: FUTURE WORKS AND CONCLUSION

7.1 OVERVIEW

This chapter explores the future directions and concluding insights derived from the research on the development of machine vision-based spot spraying systems. A complete evaluation methodology required for the system to be proven under actual spot application scenarios is outlined. The advancements in ISOBUS are highlighted, focusing on the need for better compatibility, data management, and the shift to Ethernet-based networks to support high-speed, data-intensive applications like machine vision. Challenges and opportunities in implementing ISOBUS-compatible networks are discussed. Recommendations for future research include exploring scalable and modular system designs, adopting advanced communication protocols like Ethernet-based ISOBUS, and testing these technologies under real-world conditions.

7.2 Methodology for Machine Vision-Based Spot Application Evaluation of Liquid Spraying

The communication system has been successfully developed, and field tests have demonstrated the integration of sensors and actuators. However, the technology still needs to be validated through actual machine vision-based spot spray field trials. Currently, no standard procedure exists for evaluating machine vision-based spot spraying. The closest evaluation procedure standard is ASABE S573.1 (ASABE S573, 2024), designed to assess the application accuracy of granular materials in variable-rate applicators for fertilizer distribution. This standard is customized here to address the unique characteristics of real-time camera-guided liquid application, particularly in detecting insects and applying

insecticide. The primary objective is to evaluate spatial accuracy, actuation timing, and application efficiency under both controlled and field conditions. Emphasis is placed on measuring actuation delay, nozzle swath coverage, and rates of false or missed applications.

7.2.1 System Components and Configuration

The proposed spot application system comprises a machine vision unit mounted on a boom sprayer to detect insect in real time. The MVN processes visual data and sends actuation commands via a hybrid communication network, synchronizing detection, control, and spray. The hydraulic system includes electromechanical nozzles, a flow controller, and a boom pressure ECU to regulate spray pressure alongside the pump. Evaluation is conducted at a constant ground speed along a predefined test strip to ensure repeatable and measurable system performance.

7.2.2 Test Environment and Anomaly Layout

A 1-hectare test field will be selected to simulate real-world conditions. Artificial anomalies, representing CPB, will be placed at known intervals across the field. Management zones will be established, approximately 20 in total, based on expected variability in real CPB density. Only zones containing targets will be used for assessment. To evaluate spray detection and coverage, water-sensitive paper (WSP) will be placed at selected target locations as shown in a hypothetical management zone map below Figure 7.1.

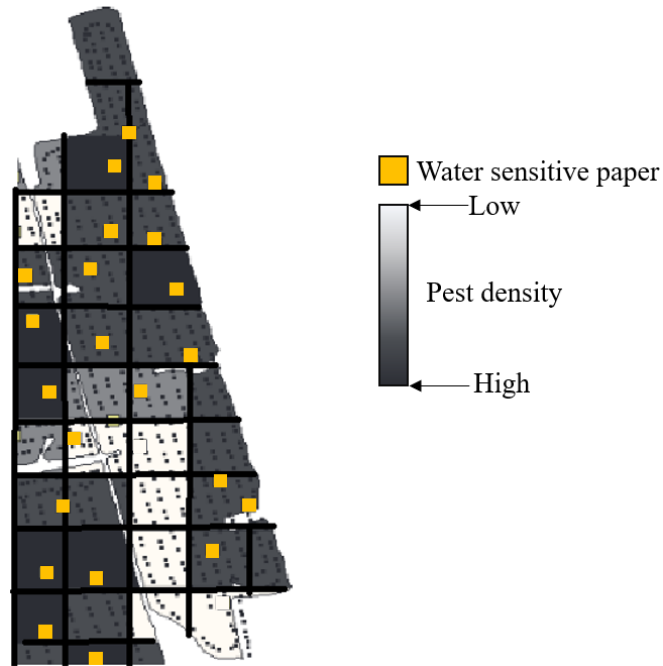


Figure 7.1: Hypothetical management map considering real pest density with artificial pest on water-sensitive paper

The zones without CPB targets will not include WSP deployment. In conjunction, dyed water in the sprayer allows for visual confirmation of spray coverage patterns. Sample collection pans will be placed at key points to quantify droplet deposition.

7.2.3 Evaluation of Latency and Spatial Accuracy

To evaluate application performance under different field speeds, five ground speeds will be tested: 3, 5, 10, 15, and 25 kph, representing a spectrum from below normal to maximum operating conditions. For each speed, the system's base application quantity will be estimated under uniform pressure conditions.

The application material required will be calculated in two ways: uniform-rate application, where full-field broadcast at a constant rate, and management zone application that is based on CPB density per zone (like a prescription map). These estimated quantities

will then be compared with the actual application volume delivered during real-time, vision-based spot spraying. Evaluation will be conducted from three perspectives:

1. Machine Vision Detection: The system logs detection events with GNSS coordinates and timestamps, enabling the generation of detection maps for each tested speed. These maps are used to assess the consistency and accuracy of detection under varying speeds.
2. MVN Actuation Timing: The MVN operates with a fixed spray actuation duration of 400 ms, triggered every 40 ms. This timing remains constant across all field tests and is used to correlate nozzle activity with detection locations.
3. Nozzle and Hydraulic Performance: Based on actuation signals and travel speed, five spray maps will be constructed to evaluate swath width, coverage uniformity, and deviations from target zones. Manual inspection of dyed spray patterns—both before and after WSP collection—will help validate real-world hit accuracy.

The evaluation will further consider key metrics like Hit rate for the percentage of CPB targets correctly sprayed, Miss rate for the percentage of identified targets not sprayed, and Over-application rate for the areas sprayed where no targets were detected. Each of these metrics will be statistically analyzed across the five speeds to determine system consistency and responsiveness.

On the other hand, data gathered from WSP analysis, actuation logs, and GNSS coordinates will be used to generate a. Heatmaps of spray deposition relative to detected

targets, and b. Detection vs. Spray Coverage Plots, comparing prescribed and actual application locations. This methodology serves as a step toward creating a formal standard for evaluating intelligent, camera-guided sprayers and contributes to the larger vision of developing a standardized, ISOBUS-compatible, precision boom sprayer capable of real-time spot application via hybrid communication networks.

7.3 POTENTIAL DEVELOPMENTS IN ISOBUS TECHNOLOGY

As ISOBUS technology becomes increasingly integral to modern agriculture, future advancements are likely to focus on improving compatibility and data management across diverse agricultural systems. One anticipated development is compatibility across a broader range of equipment, allowing farmers to integrate legacy machinery with cutting-edge precision technology (Sharipov et al., 2023). As machine vision and AI evolve, ISOBUS must support real-time data exchange between sensors, ECUs, and controllers (Cutini et al., 2023; László et al., 2021).

The advancements in ISOBUS technology are primarily geared toward enhancing data transfer speed and system compatibility across agricultural machinery (Smart & Brill, 2019). Current research focuses on enhancing ISOBUS by integrating high-speed communication protocols, such as CAN FD (Lundh, 2024; Potter et al., 2025) and Ethernet-based solutions (Keil, 2023). While current standards support control functions and data communication over a CAN-based network, there is an ongoing shift to Ethernet-based networks to meet growing data demands (Allmendinger et al., 2022). This shift allows higher data throughput and improved support for technologies like machine vision, where high-speed image processing and analysis are crucial for real-time decision-making

(Oksanen et al., 2016; Suomi & Oksanen, 2015). Implementing Ethernet with Open Platform Communications Unified Architecture (OPC UA) middleware can support modular and plug-and-play compatibility across devices, as it offers object-oriented information modelling and allows data integration between disparate systems (Siponen et al., 2022). While Ethernet-based ISOBUS offers large data and higher transfer speeds, it also introduces challenges in terms of system compatibility and implementation complexity. The shift requires significant upgrades to existing infrastructure, which may not be feasible and retrofitted to existing agricultural machinery. Additionally, handling high volumes of data may also introduce latency and reliability concerns where in field robust performance is crucial (Oksanen et al., 2016; Suomi & Oksanen, 2015).

7.4 ENHANCED ISOBUS SECURITY USING OPC UA AND OPEN62541

Future research should develop scalable, modular systems with advanced protocols like CAN FD and improved ISOBUS standards for higher data loads. Energy-efficient processors and rugged electronics are crucial for field use. Testing high-speed ISOBUS and Ethernet networks in agriculture will validate performance, optimize latency, and enhance multi-task crop management.

As agricultural automation advances, secure machine-to-machine communication is becoming a critical focus (Smart & Brill, 2022). ISO 23870, currently under development, seeks to transition from CAN-based ISOBUS to an Ethernet-based architecture (1000BASE-T1 Type B Automotive Ethernet), incorporating a middleware layer for improved information modelling and cybersecurity (Peter Vlugt, 2023). The OPC UA is a promising candidate for this middleware, offering a robust security framework that

supports multiple transport layers without altering core functionality (OPC Foundation, 2024). Ensuring OPC UA security features on low-bandwidth CAN-based ISOBUS systems is challenging. To address this, researchers implemented OPC UA over ISOBUS using the SAE J1939 and Extended Transport Protocols for secure data transmission in agricultural vehicles. However, experiments showed encryption delays, with a single value taking ~50 ms and 10,000 values requiring 7.52 s, making real-time field operations impractical (Brodie & Oksanen, 2023). Brodie & Oksanen (2025) also proposed leveraging secure OPC UA channels during low-traffic periods for frequent rekeying, enabling encrypted CAN communication without increasing busload. This approach enhances security while maintaining ISOBUS compatibility.

As part of this research, a data logger module was tested for cloud connectivity and data storage, as shown in Figure 7.2. Over two cropping seasons, field data was stored in a local database with the capability for direct cloud transfer, which can occur live based on internet availability. The figure highlights the foundational elements for adopting OPC UA, where the required components are already in place, needing only integration. Establishing these connections will pave the way for future advancements, including farm management dashboards, FMIS integration, and remote service capabilities such as prescription map uploads and system diagnostics.

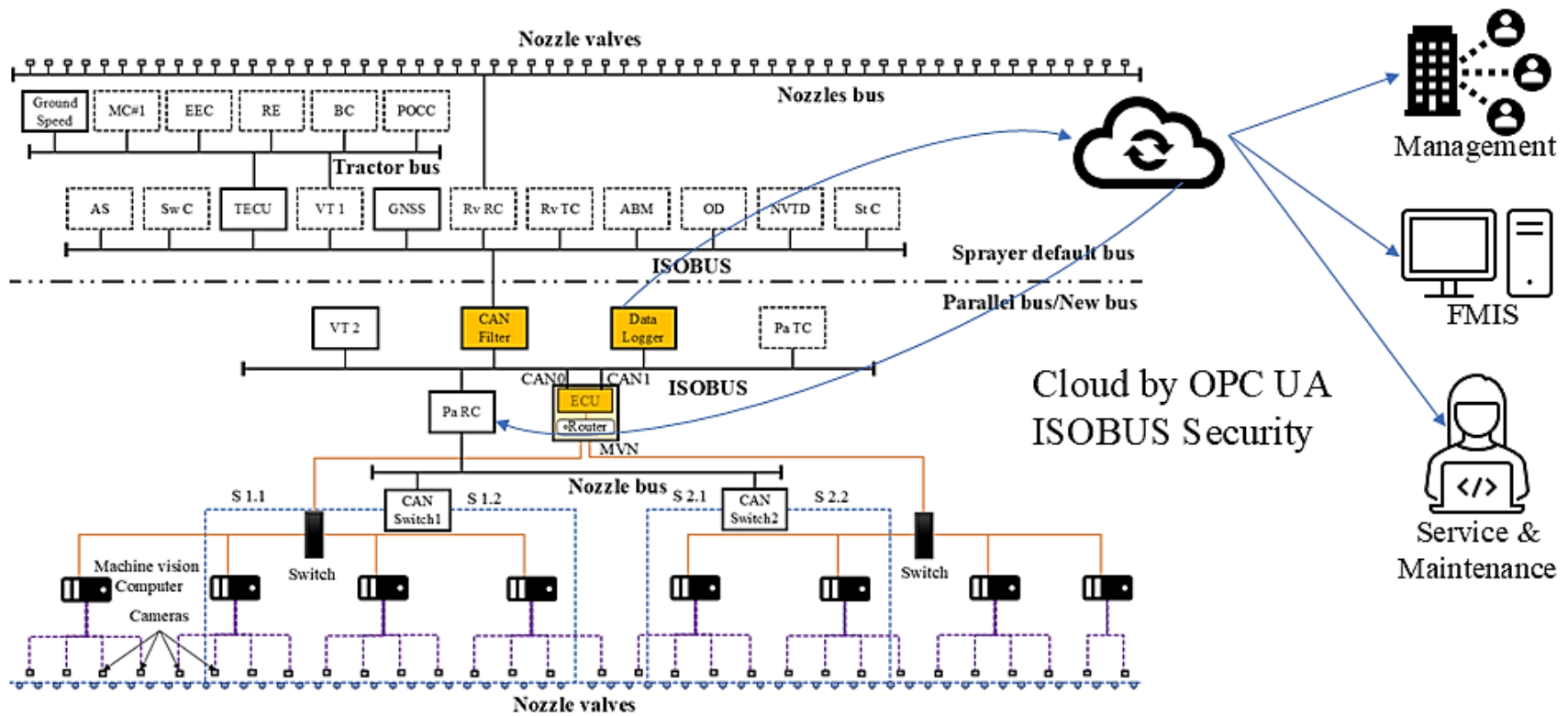


Figure 7.2: Future integration of ISOBUS and cloud through OPC UA for secure and scalable agricultural data management

To enable secure OPC UA implementation over ISO 11783, researchers modified the open62541 library, a lightweight, open-source OPC UA framework, to function with SAE J1939 and ISO 11783 protocols (Götz Görisch, 2023). Typically, open62541 relies on TCP/IP sockets, but this work modified key networking functions, including start, listen, stop, send, receive, and close, to operate over ISO 11783 instead of standard IP-based transport. The implementation was tested using the Basic256Sha256 security policy, which enforces signed and encrypted data transfer, ensuring message integrity and authentication (Barker, 2020; Pohlmann & Sikora, 2018). The results confirm that secure OPC UA communication is feasible over ISO 11783, allowing confidential yield data transfer and authentication of critical implement commands.

With increasing legislative mandates such as UN Regulation No. 155 and the ISO 24882 cybersecurity standard under development, securing agricultural vehicle networks will soon become a regulatory requirement rather than an option (UN Regulation, 2021). The transition to ISO 23870 (Ethernet-based ISOBUS) will further drive the adoption of high-speed, more secure data exchange, integrating AI-driven decision-making and cloud-based OPC UA solutions for remote monitoring and control (ISO/AWI 23870-3, 2024). Additionally, there is an opportunity to assess how the OPC UA publish-subscribe (PubSub) model over ISO 11783, which enables multicast data distribution compares to the client-server model currently used in ISOBUS setups (Siponen et al., 2022). While full-scale OPC UA adoption for real-time ISOBUS operations remains constrained by bandwidth limitations, this research provides a practical cybersecurity enhancement for current agricultural systems, ensuring safe and reliable communication across mixed-generation fleets.

7.5 SUMMARY AND CONCLUDING REMARKS

This research successfully developed and validated a PA boom sprayer system that integrates sensing and actuation technologies for real-time site-specific applications. A key achievement was the design of an ISOBUS-compliant ECU capable of interfacing with machine vision systems and diverse agricultural machinery. A key achievement was the design of an ISOBUS-compliant ECU capable of interfacing with machine vision systems and diverse agricultural machinery. Laboratory and field trials demonstrated the ability of the ECU to optimize spraying precision, significantly reducing chemical usage while maintaining high application accuracy. The compatibility of the ECU with the ISOBUS protocol provides interoperability across manufacturers, making it a scalable and flexible solution for diverse agricultural contexts. The findings of this research have important implications for both practice and policy. For practitioners, the technology provides an economically feasible pathway to retrofit existing equipment, making advanced precision spraying accessible to small and medium-sized farms. The reduction in chemical usage aligns with sustainable farming practices, supporting regulatory policies aimed at minimizing environmental impacts. Policymakers could use these insights to incentivize the adoption of PA technologies through subsidies or training programs, promoting sustainable resource use at a larger scale.

This study contributes to the advancement of PA by addressing critical gaps in spot-specific spraying technologies. Integrating an ISOBUS-compliant ECU into conventional spraying systems bridges the divide between modern sensing capabilities and conventional farming equipment. Moreover, the research highlights a scalable framework for integrating

machine vision, enhancing the adaptability of agricultural systems to varying field conditions. By prioritizing cost-efficiency and sustainability, this work offers a model for developing agricultural technologies that are both environmentally and economically viable. This empirical work lays the groundwork for future advancements in PA. Future research could focus on optimizing the performance of machine vision algorithms for real-time detection and exploring advanced communication protocols to enhance system responsiveness. Additionally, integrating emerging technologies like AI and high-speed wireless communication can further expand the capabilities of precision spraying systems. Continued interdisciplinary collaboration will be crucial in addressing the challenges of sustainable agriculture and ensuring the widespread adoption of these technologies.

In conclusion, this research provides a robust and adaptable solution for improving agricultural productivity while supporting environmental stewardship. By fostering a balance between technological innovation and practical implementation, the outcomes of this study contribute to a more sustainable and resilient agricultural future.

REFERENCES

- AEF. (2015). *ISOBUS in Functionalities* (180-1-D/EN 10/2015). https://www.aef-online.org/fileadmin/user_upload/Content/pdfs/AEF_handfan_EN.pdf
- AEF. (2024). *AEF members* [Dataset]. <https://www.aef-isobus-database.org/isobusdb/internal/compatibility/index.jsf>
- Alam, M., Alam, M. S., Roman, M., Tufail, M., Khan, M. U., & Khan, M. T. (2020). Real-Time Machine-Learning Based Crop/Weed Detection and Classification for Variable-Rate Spraying in Precision Agriculture. *2020 7th International Conference on Electrical and Electronics Engineering (ICEEE)*, 273–280. <https://doi.org/10.1109/ICEEE49618.2020.9102505>
- Allmendinger, A., Spaeth, M., Saile, M., Peteinatos, G. G., & Gerhards, R. (2022). Precision Chemical Weed Management Strategies: A Review and a Design of a New CNN-Based Modular Spot Sprayer. *Agronomy*, *12*(7), 1620. <https://doi.org/10.3390/agronomy12071620>
- Al-Mallahi, A., Natarajan, M., & Shirzadifar, A. (2023). Development of robust communication algorithm between machine vision and boom sprayer for spot application via ISO 11783. *Smart Agricultural Technology*, *4*, 100212. <https://doi.org/10.1016/j.atech.2023.100212>
- Anastasiou, E., Fountas, S., Voulgaraki, M., Psiroukis, V., Koutsiaras, M., Kriezi, O., Lazarou, E., Vatsanidou, A., Fu, L., Bartolo, F. D., Barreiro-Hurle, J., & Gómez-Barbero, M. (2023). Precision farming technologies for crop protection: A meta-analysis. *Smart Agricultural Technology*, *5*, 100323. <https://doi.org/10.1016/j.atech.2023.100323>
- ASABE. (2024). *Procedures for Evaluating Variable-Rate Granular Material Application Accuracy of Broadcast applicators* (ASABE S573.1). ASABE. <https://elibrary.asabe.org/pdfviewer.aspx?GUID=929E2AEE-B989-4060-BB82-B45AEC7C7996>
- Auernhammer, H., & Demmel, M. (2015). State of the Art and Future Requirements. In Q. Zhang, *Precision Agriculture Technology for Crop Farming* (1st ed., pp. 299–346). CRC Press. <https://doi.org/10.1201/b19336-10>
- Backman, J., Linkolehto, R., Koistinen, M., Nikander, J., Ronkainen, A., Kaivosoja, J., Suomi, P., & Pesonen, L. (2019). Cropinfra research data collection platform for ISO 11783 compatible and retrofit farm equipment. *Computers and Electronics in Agriculture*, *166*, 105008. <https://doi.org/10.1016/j.compag.2019.105008>
- Balafoutis, A., Beck, B., Fountas, S., Vangeyte, J., Wal, T., Soto, I., Gómez-Barbero, M., Barnes, A., & Eory, V. (2017). Precision Agriculture Technologies Positively

- Contributing to GHG Emissions Mitigation, Farm Productivity and Economics. *Sustainability*, 9(8), 1339. <https://doi.org/10.3390/su9081339>
- Barker, E. (2020). *Recommendation for key management: Part 1 - general* (NIST SP 800-57pt1r5; p. NIST SP 800-57pt1r5). National Institute of Standards and Technology. <https://doi.org/10.6028/NIST.SP.800-57pt1r5>
- Bob Blakely. (2023, September 12). *ONE SMART SPRAY from Fendt and Bosch BASF Wins CropLife IRON Showstopper Award at MAGIE 2023*. <https://news.agcocorp.com/2023-09-12-ONE-SMART-SPRAY-from-Fendt-and-Bosch-BASF-Wins-CropLife-IRON-Showstopper-Award-at-MAGIE-2023>
- Brodie, S., & Oksanen, T. (2023). OPC UA client-server connection over an ISO 11783 vehicle network. *At - Automatisierungstechnik*, 71(11), 916–927. <https://doi.org/10.1515/auto-2023-0030>
- Brodie, S., & Oksanen, T. (2025). Securing CAN-Based ISO 11783 communications in agricultural vehicles using OPC UA. *Computers and Electronics in Agriculture*, 231, 110047. <https://doi.org/10.1016/j.compag.2025.110047>
- BSI. (2016). *Road vehicles. Controller area network (CAN) Data link layer and physical signalling* (Under Review). BSI Standards Limited 2016. https://webstore.ansi.org/preview-pages/BSI/preview_30283340.pdf
- Campbell, C., Al-Mallahi, A., & Watson, W. (2022). Automatic imaging system mounted on boom sprayer for crop scouting using an off-the-shelf RGB camera. *Computers and Electronics in Agriculture*, 193, 106690. <https://doi.org/10.1016/j.compag.2022.106690>
- Campos, J., Llop, J., Gallart, M., García-Ruiz, F., Gras, A., Salcedo, R., & Gil, E. (2019). Development of canopy vigour maps using UAV for site-specific management during vineyard spraying process. *Precision Agriculture*, 20(6), 1136–1156. <https://doi.org/10.1007/s11119-019-09643-z>
- Case, P. (2019). Tech Talk: Tractor Implement Management. *Farmers Weekly*, 172(5), 17–17.
- Cavallo, D. P., Cefola, M., Pace, B., Logrieco, A. F., & Attolico, G. (2019). Non-destructive and contactless quality evaluation of table grapes by a computer vision system. *Computers and Electronics in Agriculture*, 156, 558–564. <https://doi.org/10.1016/j.compag.2018.12.019>
- Cena, G., Cibrario Bertolotti, I., Hu, T., & Valenzano, A. (2019). On a software-defined CAN controller for embedded systems. *Computer Standards & Interfaces*, 63, 43–51. <https://doi.org/10.1016/j.csi.2018.11.007>

- Cena, G., & Valenzano, A. (2000). New efficient communication services for ISO 11898 networks. *Computer Standards & Interfaces*, 22(1), 61–74. [https://doi.org/10.1016/S0920-5489\(99\)00027-6](https://doi.org/10.1016/S0920-5489(99)00027-6)
- Chincholi, H. (2009). Wireless Controller area network based cross channel data link. *2009 International Conference on Application of Information and Communication Technologies*, 1–5. <https://doi.org/10.1109/ICAICT.2009.5372553>
- CNH Industrial N.V. (2014). *PATRIOT® 40 SERIES SPRAYERS*. CNH Industrial N.V. https://assets.cnhindustrial.com/caseih/NAFTA/NAFTAASSETS/Products/Application-Equipment/Patriot-Series-Sprayers/Brochures/Patriot_40_Series_Brochure.pdf
- Cochran, K. A. (2024). Networking Fundamentals. In K. A. Cochran, *CompTIA A+ Certification Companion* (pp. 63–104). Apress. https://doi.org/10.1007/979-8-8688-0867-8_3
- Comer, D. (2004). Network processors: Programmable technology for building network systems. *The Internet Protocol Journal*, 7(4), 2–12.
- Cowley, J. (2013). Network Protocols. In J. Cowley, *Communications and Networking* (pp. 81–109). Springer London. https://doi.org/10.1007/978-1-4471-4357-4_6
- Cutini, M., Bisaglia, C., Brambilla, M., Bragaglio, A., Pallottino, F., Assirelli, A., Romano, E., Montagni, A., Leo, E., Pezzola, M., Maroni, C., & Menesatti, P. (2023). A Co-Simulation Virtual Reality Machinery Simulator for Advanced Precision Agriculture Applications. *Agriculture*, 13(8), 1603. <https://doi.org/10.3390/agriculture13081603>
- Dange, K. M., Bodile, R. M., & Srinivasa Varma, B. (2023). A Comprehensive Review on Agriculture-Based Pesticide Spraying Robot. In M. Pandit, M. K. Gaur, & S. Kumar (Eds.), *Artificial Intelligence and Sustainable Computing* (pp. 359–370). Springer Nature Singapore. https://doi.org/10.1007/978-981-99-1431-9_28
- Darif, I., Politowski, C., Boussaidi, G. E., & Kpodjedo, S. (2022). A Domain Specific Language for the ARINC 653 Specification. *2022 IEEE International Symposium on Software Reliability Engineering Workshops (ISSREW)*, 238–245. <https://doi.org/10.1109/ISSREW55968.2022.00073>
- Decotignie, J.-D. (2005). Ethernet-Based Real-Time and Industrial Communications. *Proceedings of the IEEE*, 93(6), 1102–1117. <https://doi.org/10.1109/JPROC.2005.849721>
- Deveau, J. S. T. (2015). New Generation of Precision Sprayers. *Acta Horticulturae*, 1085, 135–137. <https://doi.org/10.17660/ActaHortic.2015.1085.23>

- Dolly Y. Wu & Timothy A. Deutsch. (2019). *IMAGE SENSOR AND MODULE FOR AGRICULTURAL CROP IMPROVEMENT* (United States Patent Patent US010255670B1).
<https://patentimages.storage.googleapis.com/b6/98/79/c865efeb169cf5/US10255670.pdf>
- Doopalam, E., Badarch, L., Togooch, A., Tumenjargal, E., Ham, W., & Kook, K. H. (2014). Implementation of Wireless PGN Analyzer of ISOBUS. *Proceedings of the International Conference on Embedded Systems and Applications (ESA)*, 1–4. ProQuest Central.
- Dou, H., Zhai, C., Chen, L., Wang, S., & Wang, X. (2021). Field Variation Characteristics of Sprayer Boom Height Using a Newly Designed Boom Height Detection System. *IEEE Access*, 9, 17148–17160.
<https://doi.org/10.1109/ACCESS.2021.3053035>
- Esau, T., Zaman, Q., Groulx, D., Farooque, A., Schumann, A., & Chang, Y. (2018). Machine vision smart sprayer for spot-application of agrochemical in wild blueberry fields. *Precision Agriculture*, 19(4), 770–788.
<https://doi.org/10.1007/s11119-017-9557-y>
- Farooque, A. A., Hussain, N., Schumann, A. W., Abbas, F., Afzaal, H., McKenzie-Gopsill, A., Esau, T., Zaman, Q., & Wang, X. (2023). Field evaluation of a deep learning-based smart variable-rate sprayer for targeted application of agrochemicals. *Smart Agricultural Technology*, 3, 100073.
<https://doi.org/10.1016/j.atech.2022.100073>
- Felix, O. O. (2024). TCP/IP stack transport layer performance, privacy, and security issues. *World Journal of Advanced Engineering Technology and Sciences*, 11(2), 175–200. <https://doi.org/10.30574/wjaets.2024.11.2.0098>
- Fontein, R. L. H. (2023, June). *Investigating DNS Information Flow In Corporate Networks*. <http://essay.utwente.nl/95121/>
- Fountas, S., Sorensen, C. G., Tsiropoulos, Z., Cavalaris, C., Liakos, V., & Gemtos, T. (2015). Farm machinery management information system. *Computers and Electronics in Agriculture*, 110, 131–138.
<https://doi.org/10.1016/j.compag.2014.11.011>
- Götz Görisch. (2023). *Open62541* (Version 1.3.8) [Computer software].
<https://github.com/open62541/open62541/releases/tag/v1.3.8>
- Gulaiya, S., Singh, S., Kaur, R., Joshi, M., Gautam, K. K., Adhikari, A., Yadav, K., Goyal, S. K., Kumar, R., & Kakkar, P. H. (2025). A Review on Conservation Agriculture: Challenges, Opportunities and Pathways to Sustainable Farming.

Journal of Scientific Research and Reports, 31(1), 97–107.
<https://doi.org/10.9734/jsrr/2025/v31i12750>

H Asaei, A. A Jafari, & M Loghavi. (2016). Development and evaluation of a targeted orchard sprayer using machine vision technology. *Māshīn'hā-Yi Kishāvarzī*, 6(2), 362–375. <https://doi.org/10.22067/jam.v6i2.37220>

Harris, T. (2018). AEF takes on automation, machine-to-machine communication. *Western Farm Press*.

Hasan, M. Z., & Mohd Hanapi, Z. (2023). Efficient and Secured Mechanisms for Data Link in IoT WSNs: A Literature Review. *Electronics*, 12(2), 458.
<https://doi.org/10.3390/electronics12020458>

Hester, R. E. (Ed.). (2012). *Environmental impacts of modern agriculture*. Royal Soc. of Chemistry.

Ibrahim, I. M., Zeebaree, S. R. M., Yasin, H. M., Sadeeq, M. A. M., Shukur, H. M., & Alkhayyat, A. (2021). Hybrid Client/Server Peer to Peer Multitier Video Streaming. *2021 International Conference on Advanced Computer Applications (ACA)*, 84–89. <https://doi.org/10.1109/ACA52198.2021.9626808>

Insam, E. (2003). *TCP/IP embedded internet applications*. Elsevier.

ISO 11783-2. (2019). *Tractors and machinery for agriculture and forestry Serial control and communications data network Part 2: Physical layer* (ISO 11783-2:2019; Version 3). International Organization for Standardization.
<https://www.iso.org/standard/57556.html>

ISO 11783-3. (2018). *Tractors and machinery for agriculture and forestry Serial control and communications data network Part 3: Data link layer* (ISO 11783-3:2018; Version 4).

ISO 11783-5. (2022). *Tractors and machinery for agriculture and forestry: Serial control and communications data network. Part 5, Network management* (Third edition.). International Organization for Standardization.

ISO 11783-6. (2018). *Tractors and machinery for agriculture and forestry Serial control and communications data network Part 6: Virtual terminal* (ISO 11783-6:2018; Version 4). International Organization for Standardization.
<https://www.iso.org/standard/71173.html>

ISO 11783-7. (2022). *Tractors and machinery for agriculture and forestry Serial control and communications data network Part 7: Implement messages application layer* (ISO/TC 23/SC 19; Version 4). <https://www.iso.org/standard/78295.html>

- ISO 11783-9. (2012). *Tractors and machinery for agriculture and forestry Serial control and communications data network Part 9: Tractor ECU* (ISO 11783-9:2012; Version 2). International Organization for Standardization. <https://www.iso.org/standard/54390.html>
- ISO 11898-1:2024. (2017). *Road vehicles—Controller area network (CAN)Part 1: Data link layer and physical coding sublayer* (ISO 11783-1:2017; Version 2). International Organization for Standardization. <https://www.iso.org/standard/86384.html>
- ISO/AWI 23870-3. (2024, August 9). *ISO/AWI 23870-3 Mobile machinery—High speed interconnect (HSI) Part 3: Single communication channel coupling connector* [Standard]. ISO/AWI 23870-3 Mobile Machinery — High Speed Interconnect (HSI) Part 3: Single Communication Channel Coupling Connector. <https://www.iso.org/standard/87876.html>
- Jain, H. (2025). Data analytics enabled by the Internet of Things and artificial intelligence for the management of Earth's resources. In *Data Analytics and Artificial Intelligence for Earth Resource Management* (pp. 19–36). Elsevier. <https://doi.org/10.1016/B978-0-443-23595-5.00002-4>
- Janu, P. (2014). Analysis of CANaerospace Protocol Communication Quality in Aviation System. *Advances in Electrical and Computer Engineering*, 14(1), 81–86. <https://doi.org/10.4316/AECE.2014.01013>
- Jia, W., Zhang, L., Yan, M., & Xue, X. (2013). Current situation and development trend of boom sprayer. *Journal of Chinese Agricultural Mechanization*, 34(4), Article 4.
- Jin, H. (2025). Low-power Intelligent Wireless Sensor Network for Precision Agriculture Oriented Agricultural Greenhouse Management System. *IEEE Access*, 1–1. <https://doi.org/10.1109/ACCESS.2025.3542866>
- Johannes Feldhaus, Richard A. Humpal, & Dolly Y. Wu. (2022). *SPRAY PATTERN OF NOZZLE SYSTEMS* (United States Patent Patent US011235345B2). <https://patentimages.storage.googleapis.com/ba/c3/53/3ba166cdfef76ba/US11235345.pdf>
- Jung, T.-H., Cates, B., Choi, I.-K., Lee, S.-H., & Choi, J.-M. (2020). Multi-Camera-Based Person Recognition System for Autonomous Tractors. *Designs*, 4(4), 54. <https://doi.org/10.3390/designs4040054>
- Kay, J. A., Entzminger, R. A., & Mazur, D. C. (2014). Industrial Ethernet- overview and best practices. *Conference Record of 2014 Annual Pulp and Paper Industry Technical Conference*, 18–27. <https://doi.org/10.1109/PPIC.2014.6871144>

- Keil, R. (2023). Standardization of Electric Tractor / Implement Interfaces: Challenge and Opportunity. *Elektromechanische Antriebssysteme 2023; 9. Fachtagung (VDE OVE)*, 274–280.
- Kim, C. Y., & Lee, I. (2015). Design and Implementation of NMEA2000 Protocol Application for Marine Monitoring System. *Journal of the Korea Institute of Information and Communication Engineering*, 19(2), 317–322. <https://doi.org/10.6109/jkiice.2015.19.2.317>
- Kolluru, D. S., & Reddy, P. B. (2021). IP to IP Calling Through Socket Programming. *2021 Asian Conference on Innovation in Technology (ASIANCON)*, 1–7. <https://doi.org/10.1109/ASIANCON51346.2021.9544997>
- Kool, J., de Jonge, E., Nieuwenhuizen, A., & Braam, H. (2023). *Green on Green weed detection: Finding weeds in a soybean crop in Brazilian fields with the Rometron WEED-IT sensor: Intermediary report*. Wageningen Plant Research.
- Kozik, R., & Choraś, M. (2016). Solution to Data Imbalance Problem in Application Layer Anomaly Detection Systems. In F. Martínez-Álvarez, A. Troncoso, H. Quintián, & E. Corchado (Eds.), *Hybrid Artificial Intelligent Systems* (Vol. 9648, pp. 441–450). Springer International Publishing. https://doi.org/10.1007/978-3-319-32034-2_37
- Krill, T. (1994). An introduction to site specific management. *Agricult. Finance Seminar*.
- kvaser. (2023, November 16). SAE J1939 Introduction [Company]. *SAE J1939 Introduction*. <https://www.kvaser.com/about-can/higher-layer-protocols/j1939-introduction/>
- L. Tian, J. F. Reid, & J. W. Hummel. (1999). DEVELOPMENT OF A PRECISION SPRAYER FOR SITE-SPECIFIC WEED MANAGEMENT. *Transactions of the ASAE*, 42(4), 893–900. <https://doi.org/10.13031/2013.13269>
- Lafata, P., & Vodrazka, J. (2011). Application of passive optical network with optimized bus topology for local backbone data network. *Microwave and Optical Technology Letters*, 53(10), 2351–2355. <https://doi.org/10.1002/mop.26291>
- László, M., Gligorević, K., Dražić, M., & Oljača, M. (2021). Determination of main parameters of ISOBUS system based agricultural machinery management. *Poljoprivredna Tehnika*, 46(3), 40–48. <https://doi.org/10.5937/PoljTeh2103040M>
- Lundh, S. (2024). *Programming of Automotive Electronic Control Units Over CAN Bus*.
- Manuel López-Correa, J., Moreno, H., Sebastian Pérez, D., Bromberg, F., & Andújar, D. (2024). Towards a true conservation zero tillage system: “A proposed solution

- based on computer vision to herbicide resistance.” *Computers and Electronics in Agriculture*, 217, 108576. <https://doi.org/10.1016/j.compag.2023.108576>
- McBride, W. D., & Daberkow, S. G. (2003). Information and The Adoption of Precision Farming Technologies. *Journal of Agribusiness*, 21(1), Article 1. <https://doi.org/10.22004/ag.econ.14671>
- Motalab, M. B., & Al-Mallahi, A. (2024). Development of a flexible electronic control unit for seamless integration of machine vision to CAN-enabled boom sprayers for spot application technology. *Smart Agricultural Technology*, 9, 100618. <https://doi.org/10.1016/j.atech.2024.100618>
- Münzenmay, M., Tanimou, M., & Kurre, H. (2020). Digital Ecosystem Nevonex for Smart Agriculture. *ATZheavy Duty Worldwide*, 13(2), 44–49. <https://doi.org/10.1007/s41321-020-0086-7>
- Murkomen, T. (2024). Performance, privacy, and security issues of TCP/IP at the application layer: A comprehensive survey. *GSC Advanced Research and Reviews*, 18(3), 234–264. <https://doi.org/10.30574/gscarr.2024.18.3.0106>
- Neményi, M., Mesterházi, P. Á., Pecze, Zs., & Stépán, Zs. (2003). The role of GIS and GPS in precision farming. *Computers and Electronics in Agriculture*, 40(1–3), 45–55. [https://doi.org/10.1016/S0168-1699\(03\)00010-3](https://doi.org/10.1016/S0168-1699(03)00010-3)
- Nicolopoulou-Stamati, P., Maipas, S., Kotampasi, C., Stamatis, P., & Hens, L. (2016). Chemical Pesticides and Human Health: The Urgent Need for a New Concept in Agriculture. *Frontiers in Public Health*, 4. <https://doi.org/10.3389/fpubh.2016.00148>
- Nils Herterich, K. L. (2025). *Multi-objective neural architecture search for real-time weed detection on embedded systems*. https://doi.org/10.18420/GILJT2025_03
- Nowakowski, P., Żórawski, P., Cabaj, K., & Mazurczyk, W. (2021). Study of the Error Detection and Correction Scheme for Distributed Network Covert Channels. *Proceedings of the 16th International Conference on Availability, Reliability and Security*, 1–8. <https://doi.org/10.1145/3465481.3470087>
- Oksanen, T., Linkolehto, R., & Seilonen, I. (2016). Adapting an industrial automation protocol to remote monitoring of mobile agricultural machinery: A combine harvester with IoT. *IFAC-PapersOnLine*, 49(16), 127–131. <https://doi.org/10.1016/j.ifacol.2016.10.024>
- Olds College. (2024). *Smart Farm 2024 Impact Report*. https://www.oldscollege.ca/_media/smartfarmimpactreport_2024.pdf

- OPC Foundation. (2024, November 29). *OPC 10000-6: UA Part 6: Mappings*. OPC Foundation. <https://reference.opcfoundation.org/Core/Part6/v105/docs/>
- Palleja, T., & Landers, A. J. (2015). Real time canopy density estimation using ultrasonic envelope signals in the orchard and vineyard. *Computers and Electronics in Agriculture*, *115*, 108–117. <https://doi.org/10.1016/j.compag.2015.05.014>
- Pallottino, F., Antonucci, F., Costa, C., Bisaglia, C., Figorilli, S., & Menesatti, P. (2019). Optoelectronic proximal sensing vehicle-mounted technologies in precision agriculture: A review. *Computers and Electronics in Agriculture*, *162*, 859–873. <https://doi.org/10.1016/j.compag.2019.05.034>
- Pampattiwar, S., Kubal, Y., & Perez-Bolivar, C. (2025). *Multifunction vehicle lamp* (Patent 18/788,903).
- Pandeya, S., Gyawali, B. R., & Upadhaya, S. (2025). Factors Influencing Precision Agriculture Technology Adoption Among Small-Scale Farmers in Kentucky and Their Implications for Policy and Practice. *Agriculture*, *15*(2), 177. <https://doi.org/10.3390/agriculture15020177>
- Pandit, N. R., Adhikari, S., Vista, S. P., & Choudhary, D. (2025). Nitrogen Management Utilizing 4R Nutrient Stewardship: A Sustainable Strategy for Enhancing NUE, Reducing Maize Yield Gap and Increasing Farm Profitability. *Nitrogen*, *6*(1), 7. <https://doi.org/10.3390/nitrogen6010007>
- Paraforos, D. S., Sharipov, G. M., & Griepentrog, H. W. (2019). ISO 11783-compatible industrial sensor and control systems and related research: A review. *Computers and Electronics in Agriculture*, *163*, 104863. <https://doi.org/10.1016/j.compag.2019.104863>
- Paraforos, D. S., Vassiliadis, V., Kortenbruck, D., Stamkopoulos, K., Ziogas, V., Sapounas, A. A., & Griepentrog, H. W. (2017). Automating the process of importing data into an FMIS using information from tractor's CAN-Bus communication. *Advances in Animal Biosciences*, *8*(2), 650–655. <https://doi.org/10.1017/S2040470017000395>
- Patadia, C., Patel, A., Gandhi, M., Patel, S., Jagadeesh, N., & Thirupatthi, T. N. (2024). Advanced DHCP Strategies for Seamless Inter-Campus Connectivity in Educational Networks. *2024 8th International Conference on I-SMAC (IoT in Social, Mobile, Analytics and Cloud) (I-SMAC)*, 722–726. <https://doi.org/10.1109/I-SMAC61858.2024.10714632>
- Paustian, M., & Theuvsen, L. (2017). Adoption of precision agriculture technologies by German crop farmers. *Precision Agriculture*, *18*(5), 701–716. <https://doi.org/10.1007/s11119-016-9482-5>

- Pentair HYPRO. (2024, January 5). *SPRAY PUMPS PRODUCT CATALOG*. Pentair. <https://www.pentair.com/content/dam/extranet/web/nam/hypro/catalogs/hyp01-hypro-spray-pumps-cat.pdf>
- Pentair HYPRO™. (2019, March 1). *CanNode Operation Manual*. Pentair plc. <https://www.pentair.com/content/dam/extranet/web/nam/hypro/sell-sheets/pentair-hypro-prostop-e-can-node-sale-sheet.pdf>
- Peter van der Vlugt. (2023, October 6). The ISObus transformation. *Diesel Progress*, 29–31.
- Plotnikov, D. A., Muzhenko, A. S., & Lachin, V. I. (2023). A method of describing a modular information and measurement system based on the CANopen protocol, taking into account intermodule information links. *Global Nuclear Safety*, 48(3), 26–36. <https://doi.org/10.26583/gns-2023-03-03>
- Pohlmann, U., & Sikora, A. (2018). Practical security recommendations for building OPC UA applications. *Industrial Ethernet Book*, 106.
- Potter, J., Puetz, K., Malarkey, J. D., Lindner, D., Schroeder, W. L., Bailey, D., Kondekar, R., Koehler, J., Labitzke, S., Jakob, A., & others. (2025, January 21). *Systems, methods and controllers for secure communications*. Google Patents.
- Priyadarshi, P. T. R. N. (2024). *Understanding Computer Networks: A Comprehensive Overview of Types, Configurations, and the OSI Model*. <https://doi.org/10.48550/ARXIV.2403.11296>
- Radočaj, D., Šiljeg, A., Marinović, R., & Jurišić, M. (2023). State of Major Vegetation Indices in Precision Agriculture Studies Indexed in Web of Science: A Review. *Agriculture*, 13(3), 707. <https://doi.org/10.3390/agriculture13030707>
- Rahman, K., & Zhang, D. (2018). Effects of Fertilizer Broadcasting on the Excessive Use of Inorganic Fertilizers and Environmental Sustainability. *Sustainability*, 10(3), 759. <https://doi.org/10.3390/su10030759>
- Raj, S. M. (2018). Machine Vision based Agricultural Weed Detection and Smart Herbicide Spraying. *Indian Journal of Science and Technology*, 11(1), 1–5. <https://doi.org/10.17485/ijst/2018/v11i23/129124>
- Raven. (2019, August). *Raven Rate Control Module (RCM) Operation Manual*. Raven Industries, Inc. https://www.agspray.com/userdocs/documents/016-0171-637-e_-_rcm_operation_manual.pdf?srsltid=AfmBOooLszCOv1Aonmle6dKgwjsee3E8-jZ8Hk2Ru9cN1juz9Vu_P098
- Raven Industries. (2014). *AutoBoom Calibration and Operation Manual*. Raven Industries.

- https://ravenindustries.mcoutput.com/assets/Content/Resources/PDF_Manuals/016-0130-062-G%20-%20AutoBoom%20Calibration%20and%20Operation%20Manual.pdf
- Raven Industries. (2016). *AccuBoom Universal Installation Manual*. Raven Industries. https://ravenindustries.mcoutput.com/assets/Content/Resources/PDF_Manuals/016-1001-073-B%20-%20AccuBoom%20Universal%20Installation%20Manual.pdf
- Reuss, H.-C. (1993). *Extended Frame Format—A New Option of the CAN Protocol* (HAI/AN 92 002; p. 9). https://www.mi.fu-berlin.de/inf/groups/ag-tech/projects/ScatterWeb/moduleComponents/CanBus_CAN2.pdf
- Rogers, M., Weigand, P., Happa, J., & Rasmussen, K. (2022). Detecting CAN Attacks on J1939 and NMEA 2000 Networks. *IEEE Transactions on Dependable and Secure Computing*, 1–15. <https://doi.org/10.1109/TDSC.2022.3182481>
- Rooney, T., & Dooley, M. (2021). *IP address management*. John Wiley & Sons.
- SAE. (2020). *Vehicle Application Layer Truck Bus Control and Communications Network Committee* (p. 32). SAE International. https://doi.org/10.4271/J1939/71_202002
- Salim, F., Darr, M., Covington, B., & Powell, L. (2016). The Performance of Farm Tractors as Reported by CAN-BUS Messages. *2016 ASABE International Meeting*, 1. <https://doi.org/10.13031/aim.20162461746>
- Sanchez, P. R., & Zhang, H. (2023). Precision spraying using variable time delays and vision-based velocity estimation. *Smart Agricultural Technology*, 5, 100253. <https://doi.org/10.1016/j.atech.2023.100253>
- Sean Mitchell, Nicholas Bannon, & Alfons Weersink. (2020). *PRECISION AGRICULTURE IN CANADA 2019 Precision Agriculture Dealership Services Surveys*. https://ageconsearch.umn.edu/record/303877/files/OABA_CAAR_report.pdf
- Serrano, J., Amaral, A., Shahidian, S., Silva, J. M. D., Moral, F. J., & Escribano, C. (2024). Technological Upgrade of a Vicon RS-EDW Spreader: Development of a Microcontroller for Variable Rate Application. *AgriEngineering*, 6(2), 1436–1449. <https://doi.org/10.3390/agriengineering6020082>
- Shannon, D. K., Clay, D., & Kitchen, N. R. (Eds.). (2018). *Precision agriculture basics*. American Society of Agronomy, Inc. : Crop Science Society of America : Soil Science Society of America : ACSESS Publications.
- Sharipov, G. M., Heiß, A., Bresilla, T., Nieuwenhuizen, A. T., Hemming, J., Van Evert, F. K., Baron, S., Benrais, A., Avgoustakis, I., Mylonas, N., Fountas, S., Vasilaros,

- P., Karagiannis, P., Vidal, J., & Paraforos, D. S. (2023). Smart implements by leveraging ISOBUS: Development and evaluation of field applications. *Smart Agricultural Technology*, 6, 100341. <https://doi.org/10.1016/j.atech.2023.100341>
- Sharipov, G. M., Heiß, A., Eshkabilov, S. L., Griepentrog, H. W., & Paraforos, D. S. (2021). Variable rate application accuracy of a centrifugal disc spreader using ISO 11783 communication data and granule motion modeling. *Computers and Electronics in Agriculture*, 182, 106006. <https://doi.org/10.1016/j.compag.2021.106006>
- Sheikh, A. F. (2024). Networking Fundamentals. In A. F. Sheikh, *CompTIA Linux+ Certification Companion* (pp. 215–243). Apress. https://doi.org/10.1007/979-8-8688-0128-0_12
- Siponen, M., Seilonen, I., Brodie, S., & Oksanen, T. (2022). Next Generation Task Controller for agricultural Machinery using OPC Unified architecture. *Computers and Electronics in Agriculture*, 203, 107475. <https://doi.org/10.1016/j.compag.2022.107475>
- Smart, D., & Brill, V. (2019). High Speed ISOBUS, an AEF Project for next generation Ag networking. In VDI Wissensforum GmbH (Ed.), *LAND.TECHNIK AgEng 2019* (pp. 91–106). VDI Verlag. <https://doi.org/10.51202/9783181023617-91>
- Smart, D., & Brill, V. (2022). AEF – High Speed ISOBUS – Technology Readiness for a Next Generation Network. In VDI Wissensforum GmbH (Ed.), *LAND.TECHNIK 2022* (pp. 551–558). VDI Verlag. <https://doi.org/10.51202/9783181023952-551>
- Soepeno, R. A. A. P. (2023). *Comprehensive Network Analysis Through a Single Main Network Architecture*.
- Sommer, J., Gunreben, S., Feller, F., Kohn, M., Mifdaoui, A., Sass, D., & Scharf, J. (2010). Ethernet – A Survey on its Fields of Application. *IEEE Communications Surveys & Tutorials*, 12(2), 263–284. <https://doi.org/10.1109/SURV.2010.021110.00086>
- Staff, A. (2022). See & Spray™ Select by John Deere. *Resource Magazine*, 29(3), 7–8.
- Stafford, J. V. (2000). Implementing Precision Agriculture in the 21st Century. *Journal of Agricultural Engineering Research*, 76(3), Article 3. <https://doi.org/10.1006/jaer.2000.0577>
- Stein, A., & Boysen, J. (2025). Organic Computing for Intelligent Agricultural Technology: Perspective and Case Study. *Agricultural Engineering.Eu*, 80(1). <https://doi.org/10.15150/AE.2025.3331>

- Steve Corrigan. (2008). *Controller Area Network Physical Layer Requirements* (SLLA270–January 2008). Texas Instruments.
<https://www.ti.com/lit/an/slla270/slla270.pdf?ts=1711122628337>
- Stoll, G. P., Luck, J. D., Pitla, S. K., & Rohrer, R. A. (2021). Integration of Auxiliary Sensor Data to ISOBUS for Agricultural Machinery Data Collection. *Applied Engineering in Agriculture*, 37(1), 157–162. <https://doi.org/10.13031/aea.14152>
- Suomi, P., & Oksanen, T. (2015). Automatic working depth control for seed drill using ISO 11783 remote control messages. *Computers and Electronics in Agriculture*, 116, 30–35. <https://doi.org/10.1016/j.compag.2015.05.016>
- Tang, Y., Chen, C., Leite, A. C., & Xiong, Y. (2023). Editorial: Precision control technology and application in agricultural pest and disease control. *Frontiers in Plant Science*, 14, 1163839. <https://doi.org/10.3389/fpls.2023.1163839>
- Taylor, L. B. (2017, September 6). *John Deere Acquires ‘See & Spray’ Robotics Startup Blue River Technology for \$305m*. <https://medium.com/@dcvc/john-deere-acquires-blue-river-technology-for-305-million-bringing-full-stack-ai-to-agriculture-7ca8c25a5fe1>
- Terra, F. P., Nascimento, G. H. do, Duarte, G. A., & Drews-Jr, P. L. J. (2021). Autonomous Agricultural Sprayer using Machine Vision and Nozzle Control. *Journal of Intelligent & Robotic Systems*, 102(2), 38.
<https://doi.org/10.1007/s10846-021-01361-x>
- Tomsho, G. (2011). *Guide to Networking Essentials, 6th Edition* (6th ed.). Course Technology Press.
- UN Regulation. (2021). *Uniform provisions concerning the approval of vehicles with regards to cyber security and cyber security management system*. UN New York.
- Valle, S. S., & Kienzle, J. (2020). *Agriculture 4.0 – Agricultural robotics and automated equipment for sustainable crop production* (Publication ISSN 1020-4555; Integrated Crop Management Series, p. 40). Food and Agriculture Organization (FAO). <https://openknowledge.fao.org/server/api/core/bitstreams/14fc8bf7-fdeb-4c7c-a2ed-b2d59118a70b/content>
- Van Loon, J., Speratti, A., Gabarra, L., & Govaerts, B. (2018). Precision for Smallholder Farmers: A Small-Scale-Tailored Variable Rate Fertilizer Application Kit. *Agriculture (Basel)*, 8(4), Article 4. <https://doi.org/10.3390/agriculture8040048>
- Vogt, W. (2021, September 7). *BASF, Bosch make joint venture official*. <https://www.farmprogress.com/crops/basf-bosch-make-joint-venture-official>

- Voss, W. (2008). *A comprehensible guide to controller area network* (2nd ed.). Copperhill Media.
- Vurchio, P., Isitan, A., Zelenic, A., Ionescu, C., Sevillano, C., Cem, G., Vasileiou, K., Sulak, M., Kutlubay, R. Ç., & Alessandroni, V. (2024). *Digital Traineeship in Agriculture*.
- Walter, R. P., & Walter, E. P. (2016). *Data acquisition from HD vehicles using J1939 Can Bus*. SAE International.
- Wang, X., Liu, Y., Jiao, K., Liu, P., Luo, X., & Liu, T. (2024). Intrusion Device Detection in Fieldbus Networks Based on Channel-State Group Fingerprint. *IEEE Transactions on Information Forensics and Security*, *19*, 4012–4027. <https://doi.org/10.1109/TIFS.2024.3374596>
- Wei, Z., Xue, X., Salcedo, R., Zhang, Z., Gil, E., Sun, Y., Li, Q., Shen, J., He, Q., Dou, Q., & Zhang, Y. (2022). Key Technologies for an Orchard Variable-Rate Sprayer: Current Status and Future Prospects. *Agronomy*, *13*(1), 59. <https://doi.org/10.3390/agronomy13010059>
- Xiao, K., Ma, Y., & Gao, G. (2017). An intelligent precision orchard pesticide spray technique based on the depth-of-field extraction algorithm. *Computers and Electronics in Agriculture*, *133*, 30–36. <https://doi.org/10.1016/j.compag.2016.12.002>
- Ye, K., Hu, G., Tong, Z., Xu, Y., & Zheng, J. (2025). Key Intelligent Pesticide Prescription Spraying Technologies for the Control of Pests, Diseases, and Weeds: A Review. *Agriculture*, *15*(1), 81. <https://doi.org/10.3390/agriculture15010081>
- Yin, H., Cao, Y., Marelli, B., Zeng, X., Mason, A. J., & Cao, C. (2021). Soil Sensors and Plant Wearables for Smart and Precision Agriculture. *Advanced Materials*, *33*(20), 2007764. <https://doi.org/10.1002/adma.202007764>
- Yuki, S., Yasuda, H., Matsubayashi, T., & Ishizuka, H. (2013). Development of Tractor Automatic Controlled Boom Sprayer Using CAN-BUS. *IFAC Proceedings Volumes*, *46*(18), 264–269. <https://doi.org/10.3182/20130828-2-SF-3019.00021>
- Zeltwanger, H. (2000, March 6). *CAN Standard Review: Changes and Enhancements of the ISO 11898*. SAE 2000 World Congress. <https://doi.org/10.4271/2000-01-0143>
- Zhang, X., Shi, L., Jia, X., Seielstad, G., & Helgason, C. (2010). Zone mapping application for precision-farming: A decision support tool for variable rate application. *Precision Agriculture*, *11*(2), 103–114. <https://doi.org/10.1007/s11119-009-9130-4>

Zhou, M., Li, R., Shang, L., & Zhang, L. (2013). Design of a Transmission-Aware Fault-Tolerant CAN Network. In M. Pathan, G. Wei, & G. Fortino (Eds.), *Internet and Distributed Computing Systems* (Vol. 8223, pp. 351–361). Springer Berlin Heidelberg. https://doi.org/10.1007/978-3-642-41428-2_28